Schlumberger

Well Test Interpretation

© Schlumberger 2002

All rights reserved. No part of this book may be reproduced, stored in a retrieval system, or transcribed in any form or by any means, electronic or mechanical, including photocopying and recording, without prior written permission of the publisher.

SMP-7086-5

An asterisk (*) is used throughout this document to denote a mark of Schlumberger.

Contents

Introduction	1
Fundamentals of Transient Well Test Behavior	3
Diffusivity equation	3
Sidebar: Modeling radial flow to a well	4
Wellbore storage and skin effects	5
Background	5
Type curves	7
Changing wellbore storage	9
Control of Downhole Environment	13
Downhole shut-in techniques	13
Downhole flow rate measurement	16
Wellsite Validation	19
Interpretation Review	25
Interpretation methodology	25
Data processing	25
Flow regime identification	27
Sidebar: Derivative computation	28
Derivative computation	28
Use of type curves	41
Use of numerical simulation	42
Three stages of modeling	43
Model identification	43
Parameter estimation	44
Results verification	47
Use of downhole flow rate measurements	48
Description of the problem	48
Model identification	50
Parameter estimation	52
Model and parameter verification	54
Gas well testing	57
Specialized Test Types	65
Layered reservoir testing	65
Selective inflow performance	66
Transient layered testing	69
Interpretation of layered reservoir testing	70
Horizontal wells	74
Multiple-well testing	79
Interference testing	80
Pulse testing	82
Vertical interference testing	85
Measurements while perforating	88

	Impulse testing	91
	Closed-chamber DST	94
	Water injection wells	97
	Pumping wells	101
	Permanent monitoring	104
Press	ure Transient and System Analysis	105
Appe	ndix: Type Curve Library	107
Refer	rences	123

Introduction

From its modest beginnings as a rudimentary productivity test, well testing has progressed to become one of the most powerful tools for determining complex reservoir characteristics.

This fifth book in the Schlumberger Testing Services set summarizes the state of the art in well test interpretation. It emphasizes the need for both a controlled downhole environment and high-performance gauges, which have made well testing a powerful reservoir description tool.

Also addressed in this book are descriptive (or reservoir) well testing, the application of simultaneously recorded downhole rate and pressure measurements to well testing, and testing gas wells. The special kinds of well testing discussed include testing layered reservoirs and horizontal wells, multiple-well testing, vertical interference, and combined perforation and testing techniques. Testing low-energy wells, water injection wells and sucker-rod pumping wells is also outlined.

Fundamentals of Transient Well Test Behavior

A brief review of pressure transient analysis explains why advances in technology have had such a significant impact on well testing.

At the start of production, pressure in the wellbore drops sharply and fluid near the well expands and moves toward the area of lower pressure. This movement is retarded by friction against the pore walls and the fluid's own inertia and viscosity. As the fluid moves, however, it in turn creates a pressure imbalance that induces neighboring fluid to move toward the well. The process continues until the drop in pressure that was created by the start of production is dissipated throughout the reservoir.

The physical process occurring throughout the reservoir can be described by the diffusivity equation.

Diffusivity equation

To model a well test, the diffusivity equation is expressed in radial coordinates and assumes that the fluid flows to a cylinder (the well) that is normal to two parallel, impermeable planar barriers. To solve diffusivity equation, it is first necessary to establish the initial and boundary conditions, such as the initial pressure distribution that existed before the onset of flow and the extent of the reservoir .

The Sidebar on page 4 shows how the diffusivity equation and boundary conditions can be combined and solved throughout the reservoir to provide a simple model of the radial pressure distribution about a well subjected to an abrupt change in the production rate. Use of the same diffusivity equation, but with new boundary conditions, enables finding other solutions, such as in a closed cylindrical reservoir.

Solutions for reservoirs with regular, straight boundaries, such as those that are rectangular or polygonal in shape, and that have a well location on or off center can be obtained using the same equations as for the infinite reservoir case in the Sidebar. This is achieved by applying the principle of superposition in space of well images. The superposition approach enables analysts to model the effects that features such as faults and changes in reservoir size could have on the pressure response.

The solution of the diffusivity equation shown in the Sidebar indicates that a plot of pressure versus the log of time is a straight line. This relation provides an easy graphical procedure for interpretation. The slope of the portion of the curve forming a straight line is used for calculating permeability. Therefore, initially well tests were interpreted by plotting the observed pressure measurements on a semilog graph and then determining permeability estimates from the straight-line portion of the curve. Radial flow was assumed to occur in this portion of the transient.

Sidebar: Modeling radial flow to a well

Most of the fundamental theory of well testing considers the case of a well situated in a porous medium of infinite radial extent—the so-called infinite-acting radial model. This model is based on a series of equations that compose the diffusivity equation

$$\frac{\partial^2 p}{\partial^2 r} + \frac{1}{p} \left(\frac{\partial p}{\partial r} \right) = \frac{1}{\eta} \left(\frac{\partial p}{\partial t} \right),$$

where

p = formation pressure

r = radial distance to the center of the wellbore

t = time

= diffusivity constant k/c_t (k = permeability, = porosity, c_t = total compressibility, and = viscosity), and equations that model the reservoir boundary conditions:

■ Initial condition— pressure is the same all over the reservoir and is equal to the initial pressure:

$$p(r, t=0) = p_i$$

• Outer-boundary condition— pressure is equal to the initial pressure at infinity:

$$p(r,t) = p_i \text{ as } r \to \infty$$

■ Inner-boundary condition— from time zero onward the fluid is withdrawn at a constant rate:

$$q_s = \frac{2\pi kh}{\mu} \left(r \frac{\partial p}{\partial r} \right)_{r_{\text{out}}},$$

where

 q_s = sandface flow rate

kh = permeability-thickness product (flow capacity)

 r_w = wellbore radius.

The diffusivity equation solution in its approximate form is

$$p_D \Big(r_D t_D \Big) = 0.5 \Bigg(ln \frac{t_D}{r_D^2} + 0.080907 \Bigg),$$

where dimensionless time is

$$t_D = \frac{0.0002637 \, kt}{\mu \phi \, c_t \, r_w^2}$$

and dimensionless pressure is

$$p_D = 0.00708 \frac{kh}{q_s \mu} (p_i - p_{wf}),$$

where

 p_{wf} = wellbore flowing pressure when the dimensionless radial distance r_D = 1.

Figure 1 shows that the early-time data are distorted by wellbore storage and skin effects, concepts that are discussed in the following section. The late-time portion of the pressure transient is affected by interference from other wells or by boundary effects, such as those that occur when the pressure disturbance reaches the reservoir edges. If these disturbances overlap with the early-time effects they can completely mask the critical straight-line portion where radial flow occurs. In these cases, analysis with a straight-line fit is impossible.

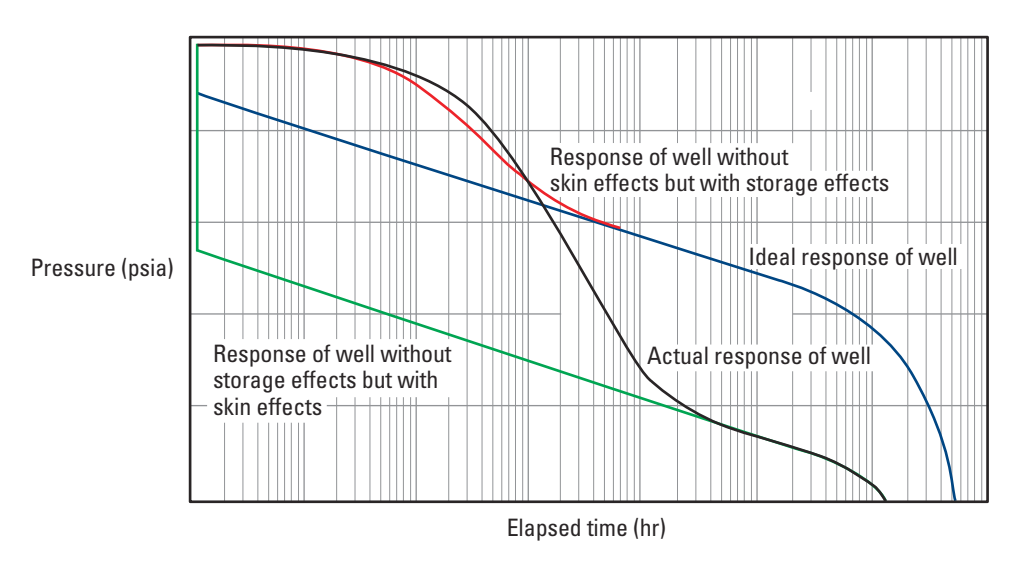


Figure 1. Wellbore storage and skin effects on the wellbore pressure response.

Wellbore storage and skin effects

Background

Wellbore storage effects are illustrated in Fig. 2. The term "skin" is brought into the computations to account for the drop in pressure that occurs across a localized zone near the well. Skin effects are caused by three main factors: flow convergence near the wellbore, visco-inertial flow velocity and the blocking of pores and fractures that occurs during drilling and production. Well testing provides a way of estimating the resulting extra pressure drop to analyze its impact on well productivity.

Traditional well tests had to be sufficiently long to overcome both wellbore storage and skin effects so that a straight line would plot. But even this approach presents drawbacks. More than one apparently straight line can appear, and analysts found it difficult to decide which to use. In addition, the choice of plotting scales may make some portions of the pressure response appear straight when, in reality, they are curved.

To overcome these difficulties, analysts developed other methods of analysis, and the era of type curves began.

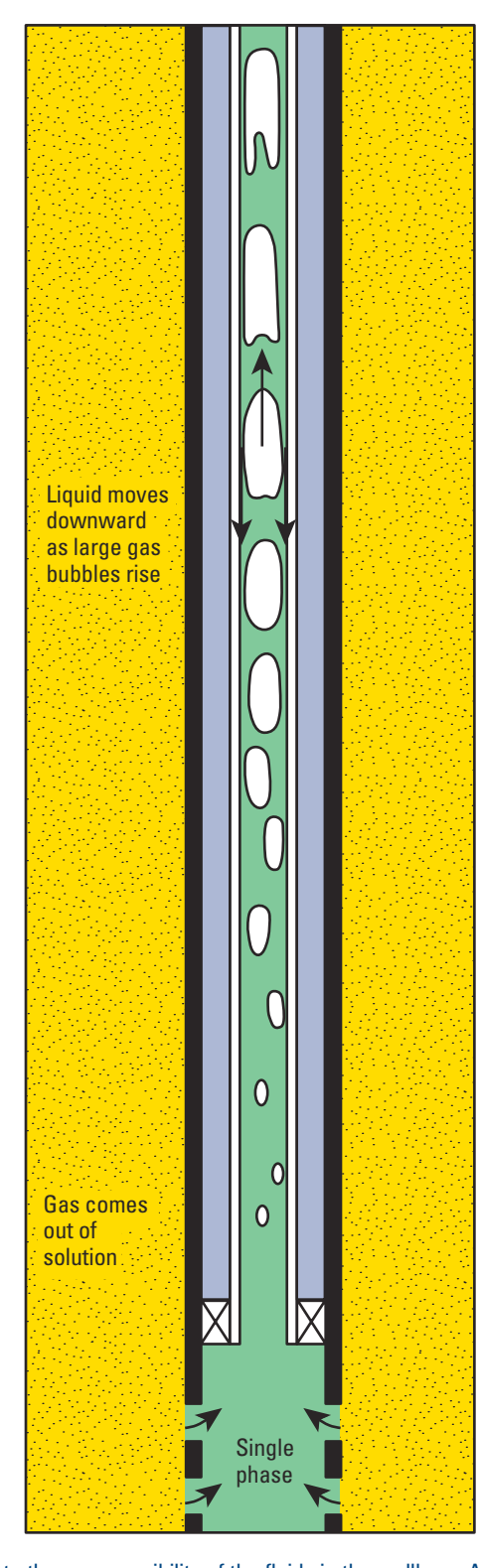


Figure 2. Wellbore storage effects are due to the compressibility of the fluids in the wellbore. Afterflow is induced after shutting in the well because flow from the reservoir does not stop immediately but continues at a slowly diminishing rate until the well pressure stabilizes. A further complication is the wellbore mechanics that drives fluids to segregate, which makes the wellbore storage variable with time.

Type curves

The infinite-acting radial flow equation derived in the Sidebar on page 4 can be written in terms of the wellbore storage coefficient C and skin factor s as follows (after Gringarten $et \ al.$, 1979):

$$p_{D} = 0.5 \left[\ln \left(\frac{t_{D}}{C_{D}} \right) + 0.80907 + \ln \left(C_{D} e^{2s} \right) \right], \tag{1}$$

where the dimensionless wellbore storage coefficient is

$$C_D = \frac{0.8937 \, C}{\phi h \, c_t \, r_w^2} \,. \tag{2}$$

The value of C is assumed to be constant, and it accounts for the compressibility of the well-bore fluid. The radial flow equation constitutes one of the basic mathematical models for modern well test analysis. The equation shows that the infinite-acting response of a well with constant wellbore storage and skin effects, when subjected to a single-step change in flow rate, can be described by three dimensionless terms: p_D , t_D/C_D and C_De^{2s} . The graphical representation of p_D and its derivative p_D (t_D/C_D) versus t_D/C_D on a log-log graph is one of the most widely used type curves. The derivative is computed with respect to the natural log of time ($\ln t$) and is representative of the slope of the pressure response on a semilog graph. It amplifies the effects that different formation characteristics have on the pressure transient response.

Figure 3 shows a set of type curves for different values of C_De^{2s} . At early time, all the curves merge into a unit-slope straight line corresponding to pure wellbore storage flow. At late time, all the derivative curves merge into a single horizontal line, representing pure radial flow. Distinctions in the shapes of the curve pairs, which are defined by the term C_De^{2s} , are more noticeable in the derivative curves.

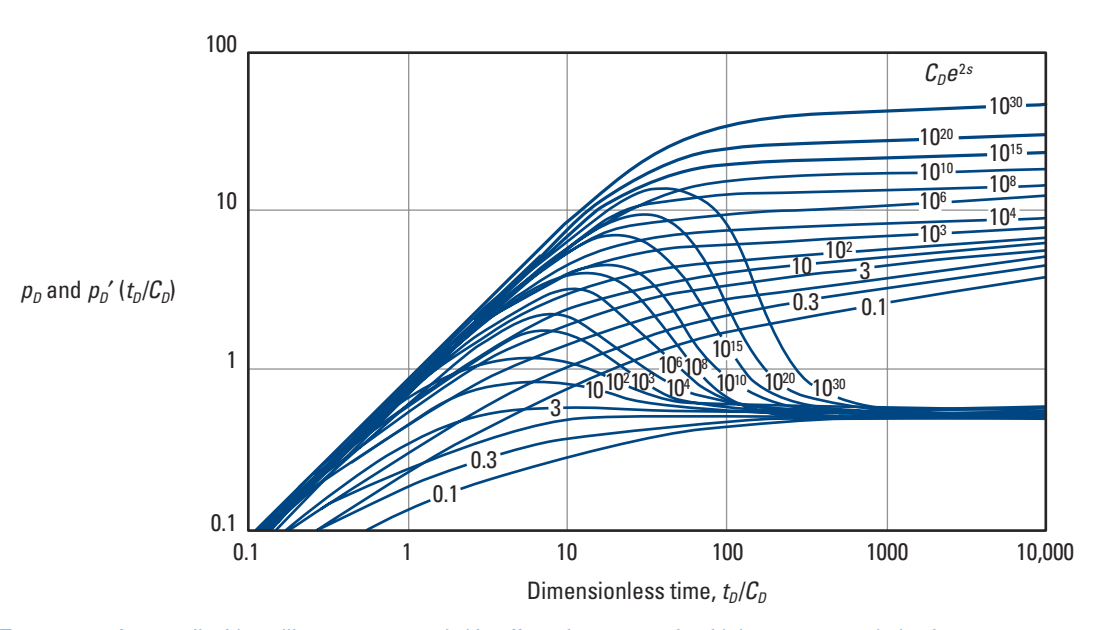


Figure 3. Type curves for a well with wellbore storage and skin effects in a reservoir with homogeneous behavior (Bourdet et al., 1983).

Test data are plotted in terms of the pressure change p and its derivative p t versus the elapsed time t and superimposed over the type curves. Once a match is found for both the pressure change and its derivative, the $C_D e^{2s}$ value of the matched curve pair, together with the translation of the axes of the data plot with respect to the type-curve axes, is used to calculate well and reservoir parameters. The permeability-thickness product is derived from the pressure match as

$$kh = 141.2 \, qB \, \mu \left(\frac{p_D}{\Delta p}\right)_M,\tag{3}$$

where

q = flow rate

B = formation volume factor

and the subscript M denotes a type-curve match.

The wellbore storage coefficient is derived from the time match as

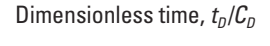
$$C = \left(\frac{0.000295 \, kh}{\mu}\right) \frac{\Delta t}{\left(\frac{t_D}{C_D}\right)_M}$$
 (44)d the

skin factor is from the C_De^{2s} curve:

$$s = 0.5 \ln \left[\frac{\left(C_D e^{2s} \right)_M}{C_D} \right]. \tag{5}$$

Figure 4 shows how type-curve matching is used to determine kh and the skin effect. In this example the test was terminated before the development of full radial flow. Application of the semilog plot technique to this data set would have provided erroneous results. The indication of radial flow by a flat trend in the pressure derivative and the easier identification of reservoir heterogeneities make the log-log plot of the pressure derivative a powerful tool for model identification. This application is discussed further in the "Interpretation Review" chapter.

Several sets of type curves have been published for different combinations of wellbore and formation characteristics. A library of the most commonly used type curves is in the Appendix to this book.



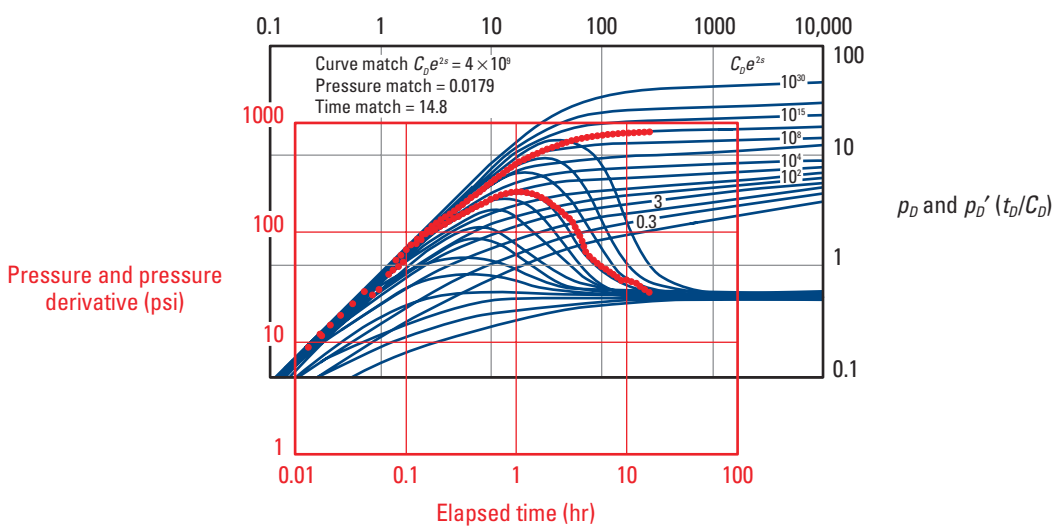


Figure 4. Type-curve matching of a data set that does not exhibit radial flow. The good match between the measured and theoretical data enables the computation of kh and s even though the test was ended before radial flow appeared (Bourdet et al., 1983).

Changing wellbore storage

The type-curve matching techniques described so far assume constant wellbore storage. However, it is not always operationally possible to keep the wellbore storage constant. Numerous circumstances cause change in wellbore storage, such as wellbore phase redistribution and increasing or decreasing storage associated with injection well testing. Figure 5 shows typical variations in wellbore storage during a conventional pressure buildup test with surface shut-in.

Downhole shut-in and combined downhole flow and pressure measurements reduce the effect of varying wellbore storage; but if the volume below the shut-in valve is compressible, downhole shut-in does not avoid the problem completely. Similarly, if the volume below the production logging tool is large or highly pressure dependent, the problem, although reduced, remains.

In these situations, adding a changing wellbore storage model to the reservoir model can improve type-curve matching. This storage model can be obtained using mathematical functions that exhibit characteristics representative of field data.

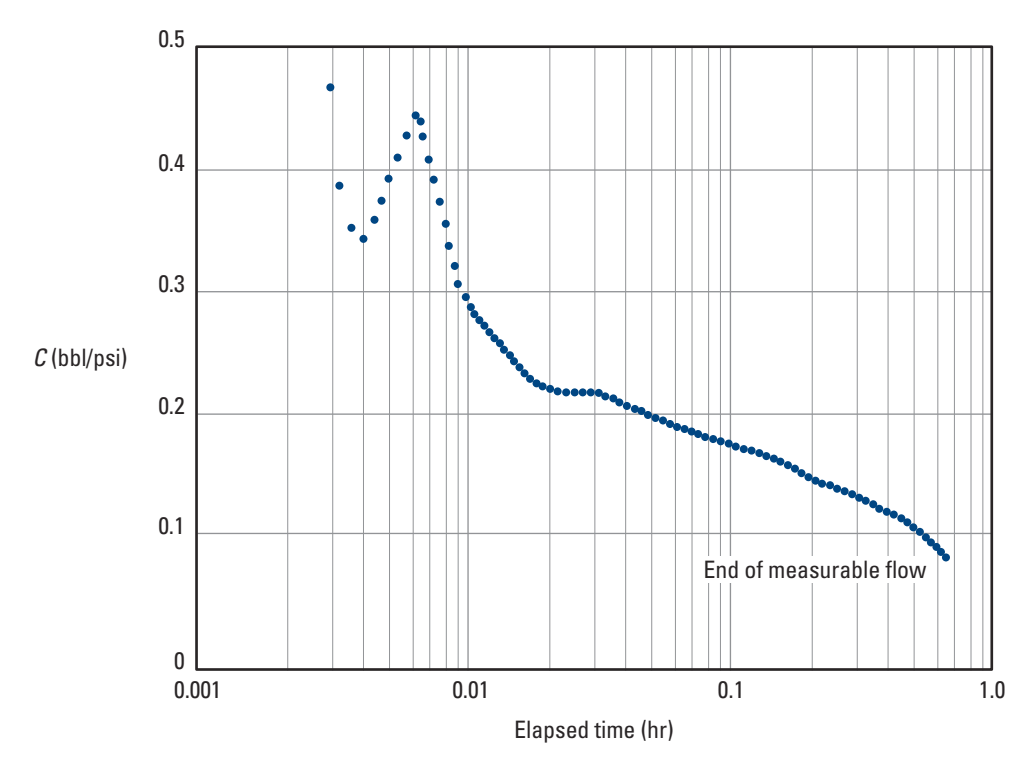


Figure 5. The wellbore storage coefficient can change during a buildup test that uses surface shut-in control.

Figure 6 shows an application of a variable wellbore storage model to a drillstem test (DST) data set. Log-log and Horner plots are shown for the extended buildup period along with the match using a homogeneous reservoir model with constant (Fig. 6a) and decreasing (Fig. 6b) wellbore storage. The data set is typical of the case in which the combined effects of changing wellbore storage and insufficient data complicate type-curve matching. The early-time data are severely distorted by decreasing wellbore storage effects, and the late-time data do not exhibit radial flow. Therefore, the match using a constant wellbore storage model in Fig. 6a does not convey sufficient confidence in the results. The match using a decreasing wellbore storage model in Fig. 6b shows the measured data in good agreement with the theoretical curves. This latter match resulted in a significantly lower value for $C_D e^{2s}$ with a corresponding lower value for the skin factor than the values calculated from the constant-storage match.

This example is representative of how the analysis of data sets affected by variable wellbore storage yields better results using type-curve matching that includes storage variations than a constant-storage analysis.

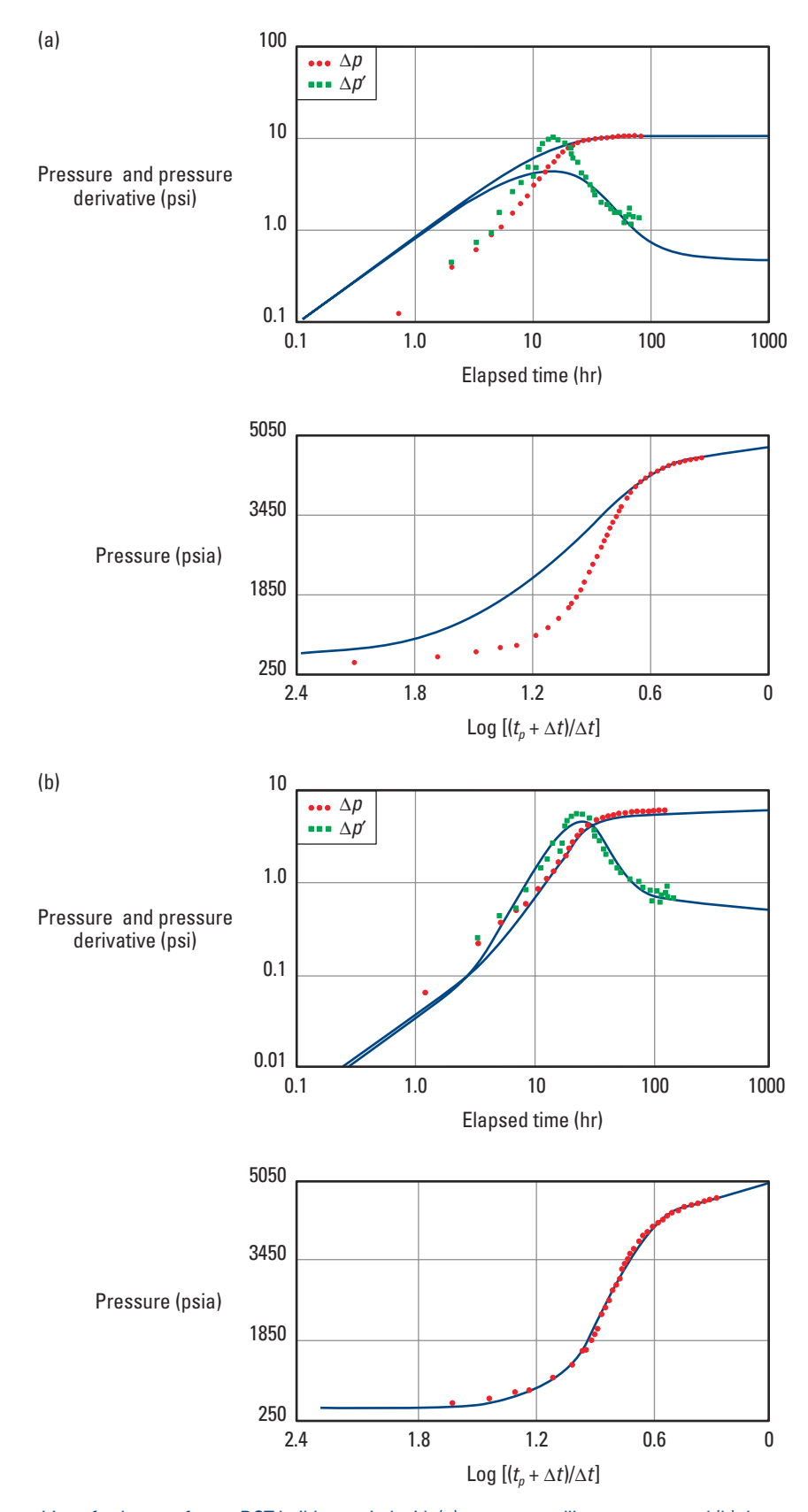


Figure 6. Type-curve matching of a data set from a DST buildup period with (a) constant wellbore storage and (b) decreasing wellbore storage models. The constant wellbore storage model yielded a skin factor of 8.7. The use of the decreasing wellbore storage model resulted in a skin factor of 2.9 (Hegeman *et al.*, 1993).

Control of Downhole Environment

Good control over well conditions improves the results obtained from well testing. Two important advances that have significantly improved control during well testing are downhole shut-in valves (described on page 71 of *Data Acquisition Services*, the fourth book in this set) and downhole flow measurements. These techniques have eliminated most of the drawbacks inherent in surface shut-in testing (large wellbore storage, long afterflow period and large variations of wellbore storage).

Another factor that has contributed to improved well testing practices is the advent of surface readout in real time. This enables the detection of problems that can be corrected to avoid data loss or improve data quality. Furthermore, surface readout reveals when sufficient data have been acquired to terminate the test, which optimizes rig time. Current surface data readout techniques are also described in *Data Acquisition Services*.

Downhole shut-in techniques

Downhole shut-in techniques play a critical role in modern well testing. The schematic diagram of a downhole shut-in valve in Fig. 7 shows how the pressure gauge monitors pressure in the well-bore chamber created beneath the closed valve.

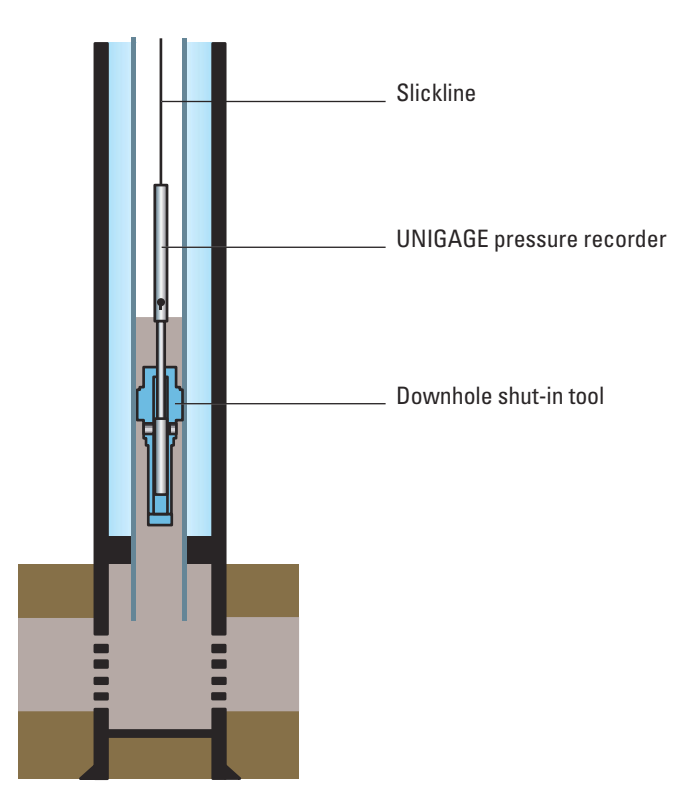


Figure 7. Downhole shut-in valve is used during pressure buildup tests to provide excellent downhole control.

The main advantages of using downhole shut-in are the minimization of both wellbore storage effects and the duration of the afterflow period. Figure 8 shows the comparative log-log plot of two well tests, one shut-in at the surface, the other shut-in downhole. In the surface shut-in test, wellbore storage masks the radial flow plateau for more than 100 hr. The plateau emerges clearly in the downhole shut-in data after just 1 hr into the transient.

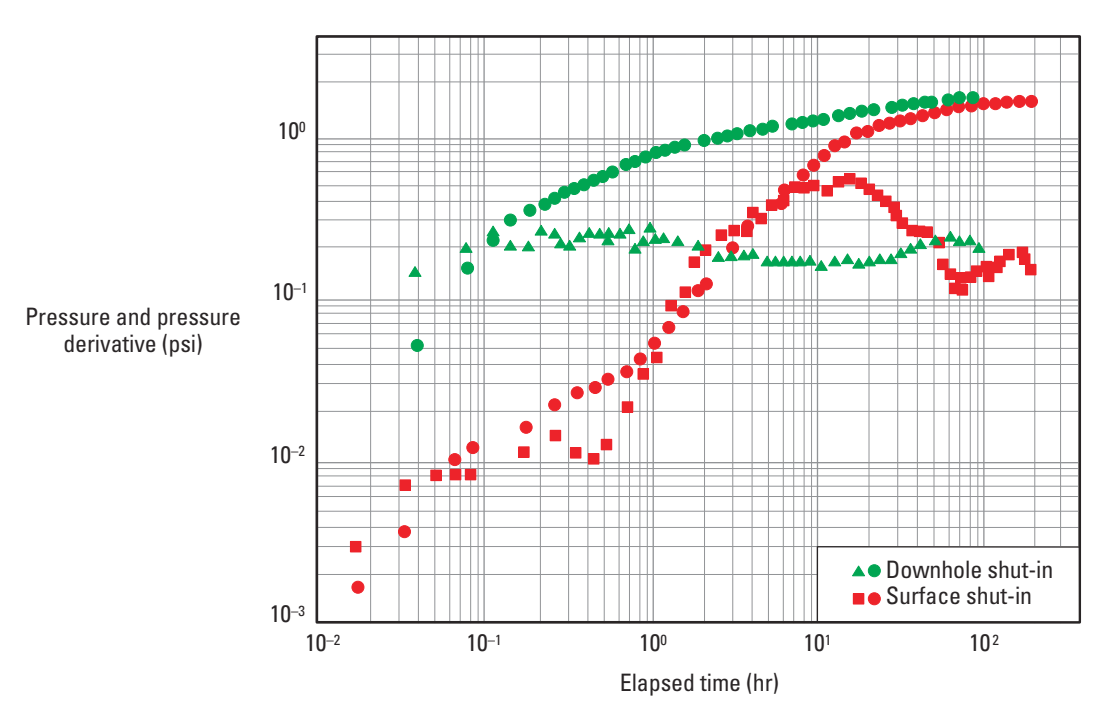


Figure 8. Log-log plot of two well tests shows wellbore storage reduction with downhole shut-in (Joseph and Ehlig-Economides, 1988).

When the downhole shut-in valve is closed, flow up the well is interrupted. Meanwhile, flow continues to enter the chamber below at an exponentially decreasing rate. Figure 9 shows a typical response during a buildup test using the downhole shut-in technique and also illustrates how flow into the well does not immediately cease after shut-in. Continued flow into the well undermines the assumptions made in the well testing solutions described on the Sidebar on page 4 and in the preceding "Fundamentals of Transient Well Test Behavior" chapter. These equations were derived assuming that flow stops immediately upon shut-in, which discounts the effects of fluid flow on the shape of the pressure transient curve. To overcome this dilemma, it is necessary to find a solution that accounts for flow rate effects.

Fortunately, the solution to the problem is relatively straightforward. The flow rate curve is first assumed to consist of a series of step changes. The pressure response of the reservoir at each step change on the curve is calculated using the standard equations described in the Sidebar on page 4. The computed pressure changes are then combined to obtain the complete pressure transient curve for the variable flow rate case. In mathematical terms, this process involves taking infinitely small flow steps that are summed through integration.

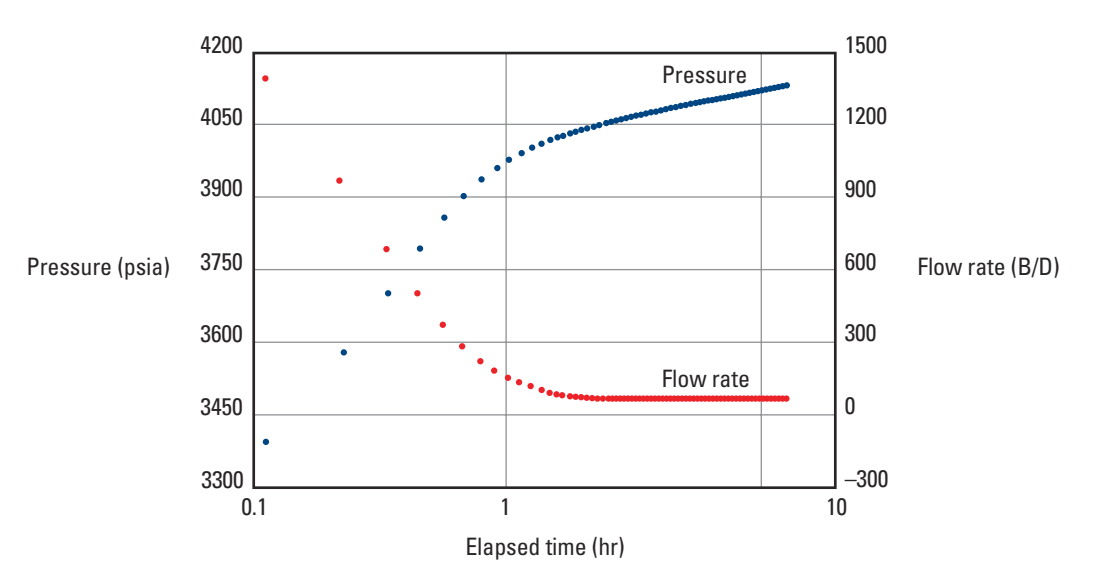


Figure 9. Pressure and flow rate variations that occur with the use of a downhole shut-in valve.

Downhole flow rate measurement

Simultaneous measurement of the flow rate and pressure downhole has been possible for some time with production logging tools (Fig. 10). However, the use of these measurements for transient analysis was introduced much later.

Downhole flow rate measurements are applicable to afterflow analysis, drawdown and injectivity tests, and layered reservoir testing (LRT). The continuously measured flow rate can be processed with the measured pressure to provide a response function that mimics the pressure that would have been measured using downhole shut-in. Except in gas wells, the measurable rates are of short duration; therefore, the real value of the sandface flow rate is observed while the well is flowing (see "Layered reservoir testing," page 65).

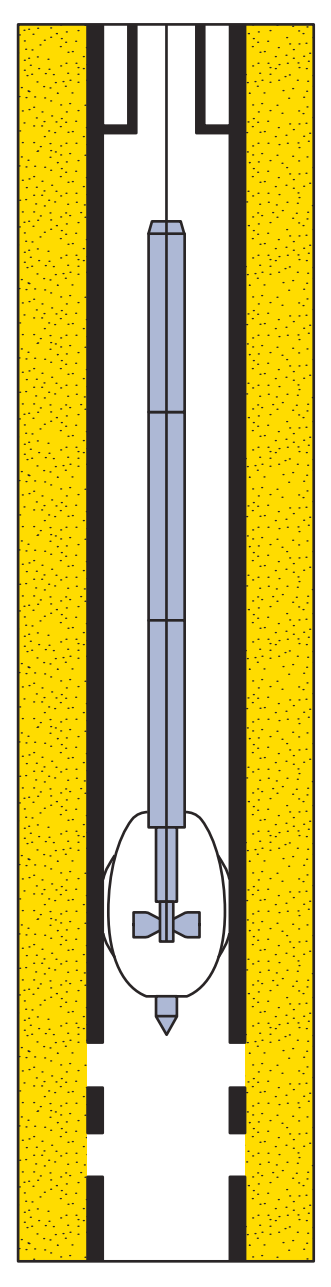


Figure 10. Schematic diagram of a production logging tool showing the flowmeter section at the top of the perforated interval in the well. This tool also simultaneously measures temperature, pressure and gradient.

16 Schlumberger

Figure 11 is an example of a plot of downhole flow measurements made during a drawdown test on an oil reservoir. It was thought that the well would not return to normal production without swabbing if a surface shut-in test was conducted. To avoid this problem, a surface choke valve was used to obtain a step change in the production rate while the downhole flow rate and pressure were measured using a production logging tool. These downhole measurements were analyzed using a technique that accounts for flow rate variations during the transient test, as subsequently discussed in "Use of downhole flow rate measurements" (page 48).

In many cases, particularly in thick or layered formations, only a small percentage of the perforated interval may be producing. This condition can result from blocked perforations or the presence of low-permeability layers. A conventional surface well test may incorrectly indicate that there are major skin effects caused by formation damage throughout the well. Downhole flow measurement enables measurement of the flow profile in a stabilized well for calculation of the skin effects caused by flow convergence. This technique makes it possible to infer the actual contribution of formation damage to the overall skin effect.

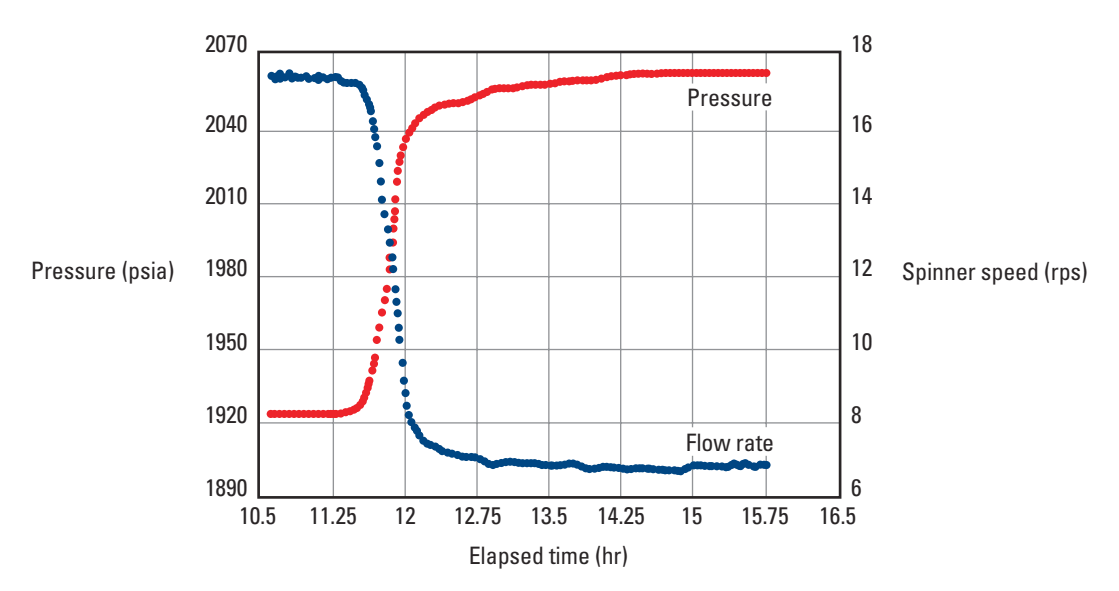


Figure 11. Plot of the bottomhole flow rate and pressure recorded during a drawdown test.

Wellsite Validation

Whether acquired through surface readout in real time or by downhole recorders, data must be validated at the wellsite. Validation ensures that the acquired data are of adequate quality to satisfy the test objectives. On-site validation also serves as a yardstick for measuring job success. When used with surface readout in real time, wellsite validation reveals when sufficient data have been acquired to terminate the test, thereby optimizing rig time.

Examining the acquired transient data in a log-log plot of the pressure change and its derivative versus elapsed time is the focus of wellsite validation. If the downhole flow rate and pressure are measured at the same time as the bottomhole pressure, the convolution derivative is also plotted. This technique is discussed in greater detail in "Use of downhole flow rate measurements" (page 46).

On-site validation can be complemented by a preliminary estimation of the formation parameters accomplished using specialized plots such as a generalized superposition or Horner plot (pressure data alone) or a sandface rate-convolution plot (downhole rate and pressure data). These plots are used for computing formation parameters such as kh, the near-wellbore value of s and the extrapolated pressure at infinite shut-in time p^* . The appropriate straight-line portion used in these specialized plots is the data subset that exhibits a flat trend in the derivative response (see "Flow regime identification," page 27).

Figure 12 illustrates the validation of a test conducted using a surface pressure readout configuration, followed by an early estimation of formation parameters. The validation plot at the top of the figure shows that infinite-acting radial flow was reached during the test. The superposition (or generalized Horner) plot shown on the bottom has the pressure plotted on the y-axis and the multirate (or superposition) time function on the x-axis. The selected straight-line portion (highlighted) corresponds to where the derivative is flat. Its intersection with the y-axis defines p^* , and kh and s can be calculated from the slope.

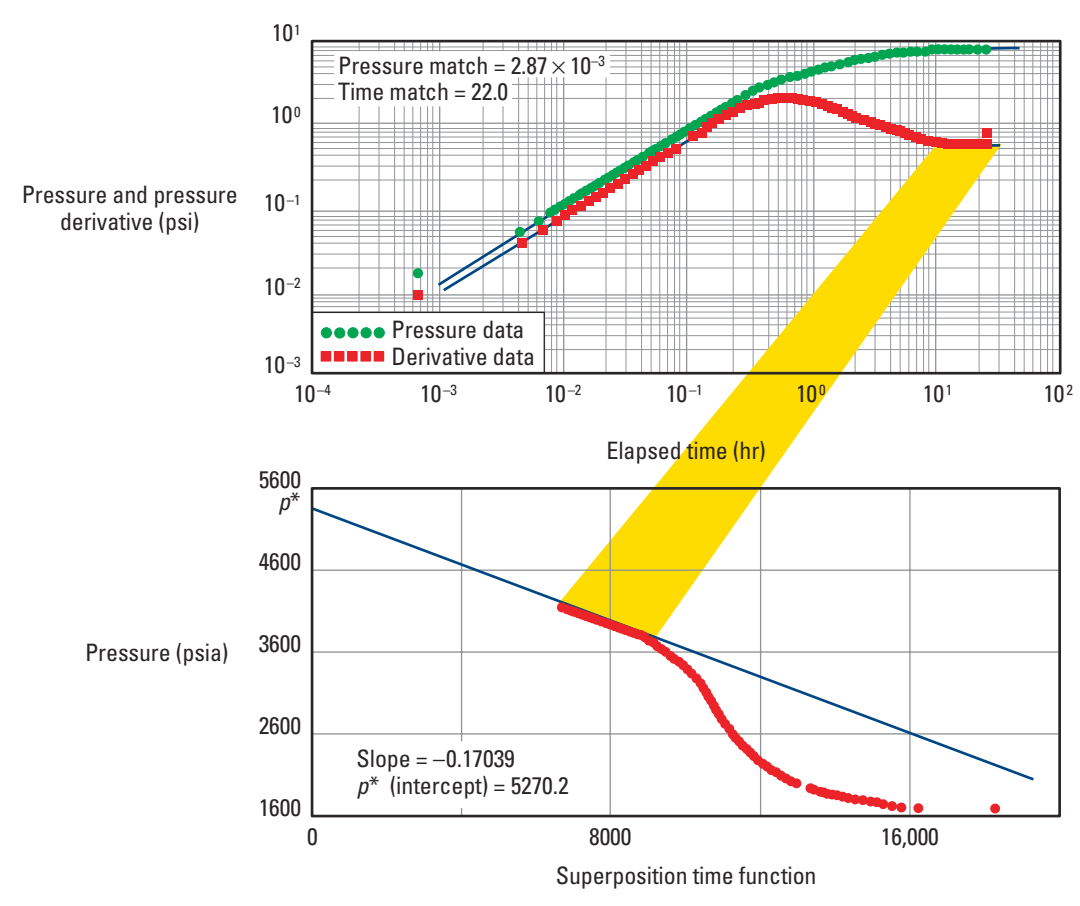


Figure 12. Test validation and early estimation of parameters using the log-log diagnostic plot (top) and generalized superposition plot (bottom).

20 Schlumberger

The log-log plot of an openhole DST in a gas well is shown in Fig. 13. The data were acquired with downhole memory recorders. The pressure derivative curve fails to exhibit the horizontal portion indicative of radial flow in the reservoir; therefore, kh and s must be determined from a type-curve match. If the data had been acquired with real-time surface readout or the DataLatch* system, which transmits data stored in downhole memory to the surface before terminating the test, the lack of straight-line formation could have been recognized and the transient test continued for a few more hours.

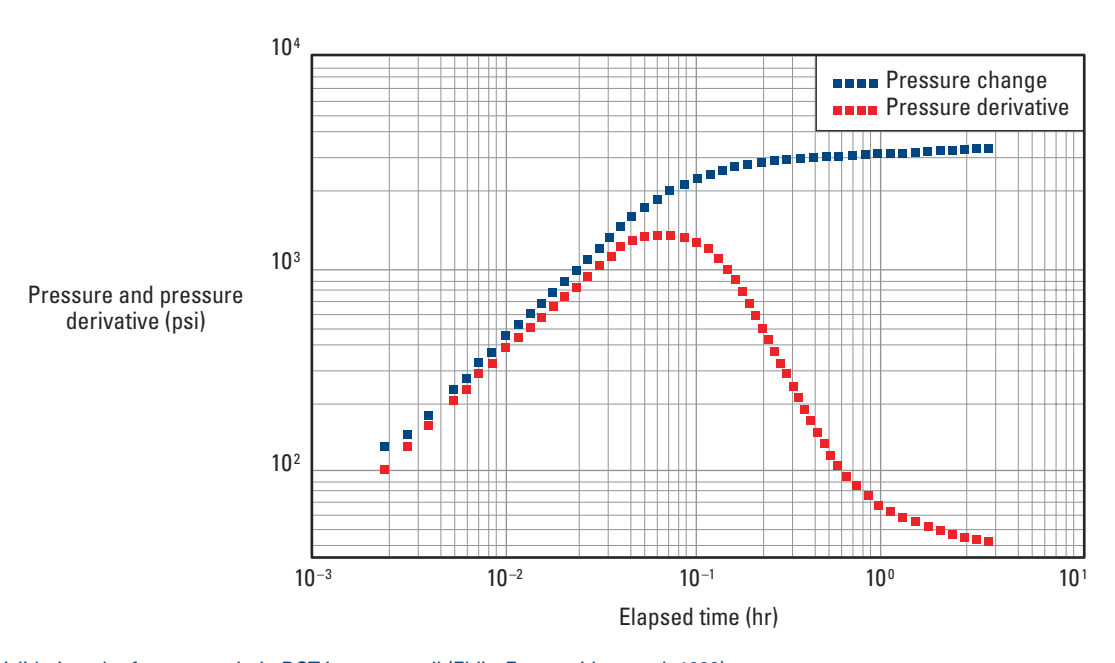


Figure 13. Validation plot for an openhole DST in a gas well (Ehlig-Economides et al., 1990).

Figure 14 shows the log-log plot of a drawdown test with transient downhole flow rate and pressure data. The plot also shows the convolution derivative curve. This curve accounts for flow rate variations during the transient, which cannot be interpreted using pressure data alone. It is particularly useful in this example because the changes in flow rate during the test resulted in a pressure derivative curve with a complete lack of character, precluding any estimation of the reservoir parameters. However, the convolution derivative contains enough information to enable parameter estimation. It also suggests that part of the tested interval was not open to flow. A flow profile run at the end of the test confirmed this hypothesis.

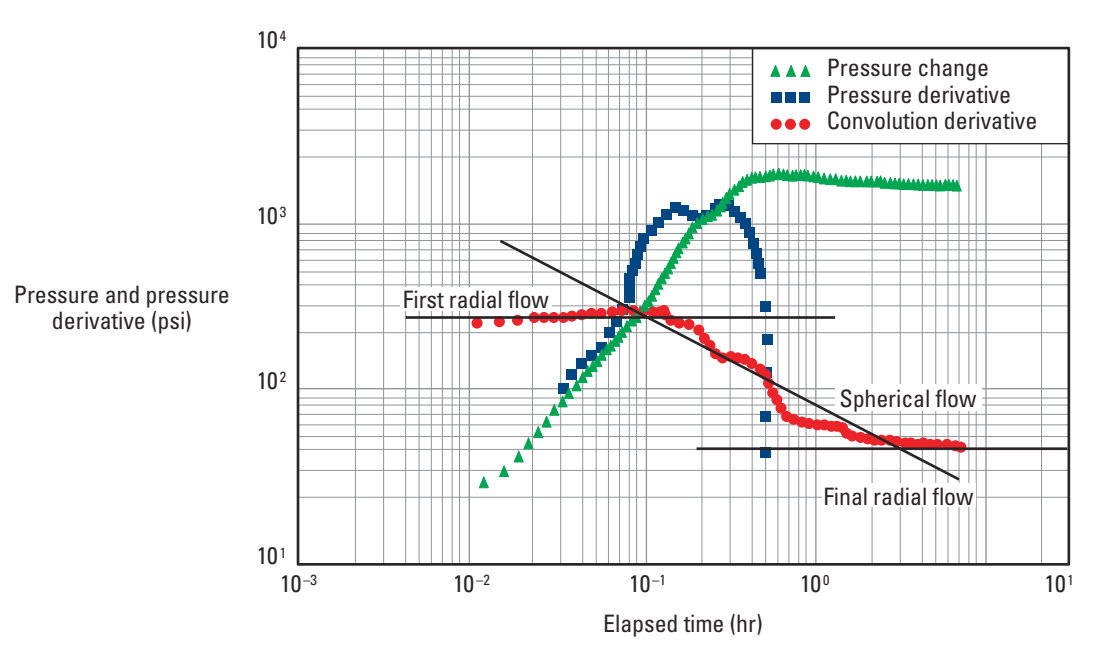


Figure 14. Validation plot for a drawdown test with transient rate and pressure data (Joseph and Ehlig-Economides, 1988).

Figure 15 shows a validation plot for a test dominated by outer-boundary effects. Like Fig. 14, this data set does not exhibit a flat portion in the derivative curve. However, the data are of excellent quality and can be interpreted by type-curve matching.

Complete analysis of these data types requires detailed modeling techniques. The best results are realized when the interpretation is conducted by an expert analyst, using sophisticated well testing software and accessing information from other disciplines (seismic, geology and petrophysics).

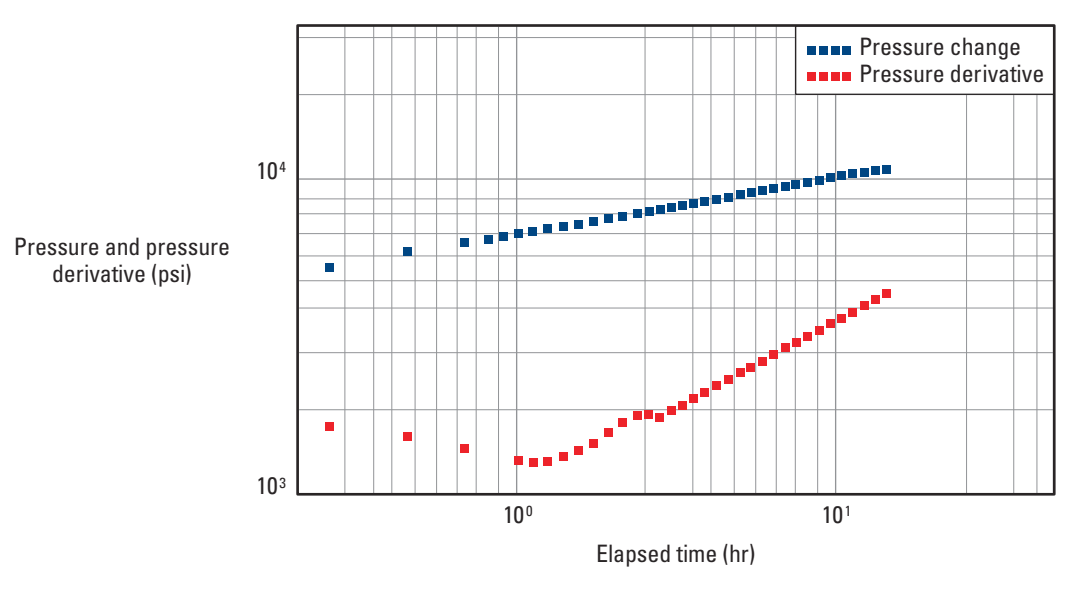


Figure 15. Validation plot for a reservoir limits test (Ehlig-Economides et al., 1990).

Interpretation Review

Comprehensive interpretation of acquired data is critical for efficient reservoir development and management because it quantifies the parameters that characterize the dynamic response of the reservoir.

This chapter reviews a rational approach to interpreting pressure transient tests. The different steps of modern interpretation methods are explained, including the techniques used when acquiring downhole rate and pressure data simultaneously. Also included is the interpretation of gas well testing, with an emphasis on the differences from liquid well testing.

Interpretation methodology

The objective of well test interpretation is to obtain the most self-consistent and correct results. This can be achieved by following a systematic approach. Figure 16 shows a logical task sequence that spans the entire spectrum of a well testing job. The focus here on the interpretation methodology builds on the information previously presented in this set to date: test design in *Introduction to Testing Services*, hardware selection in *Safety Systems* and *Well Testing Services*, data acquisition in *Data Acquisition Services* and validation in this book.

Data processing

Transient well tests are conducted as a series of dynamic events triggered by specified changes in the surface flow rate. During interpretation, it may be desirable to analyze just one particular event or all events simultaneously. In either case, the data must first be processed.

The first step in data processing is to split the entire data set into individual flow periods. The exact start and end of each flow period are specified. Because the sampling rate is usually high, each transient typically includes many more data points than are actually required. A high density of data is needed only for early-time transients. Therefore, special algorithms are usually employed to reduce the data set to a manageable size. Because of the nature of the pressure disturbance propagation, a logarithmic sampling rate is preferred.

The sequence of events should incorporate the recent flow rate history of the well with the surface flow rate changes observed during the test. This enables rigorous accounting for superposition effects. As stated previously, the shape of the pressure transient curve is affected by the production history of the reservoir. Each change in production rate generates a new pressure transient that passes into the reservoir and merges with the previous pressure effects. The pressure trends observed at the wellbore result from the superposition of all the pressure changes.

The next step is to transform the reduced data so that they display the same identifiable features, regardless of test type. A popular transformation is the pressure derivative in the Sidebar (page 28). Other useful transformations are the rate-normalized pressure, sandface rate-convolved time function and convolution derivative (see "Use of downhole flow rate measurements," page 48).

After the data are transformed, the task of identifying the flow regime begins.

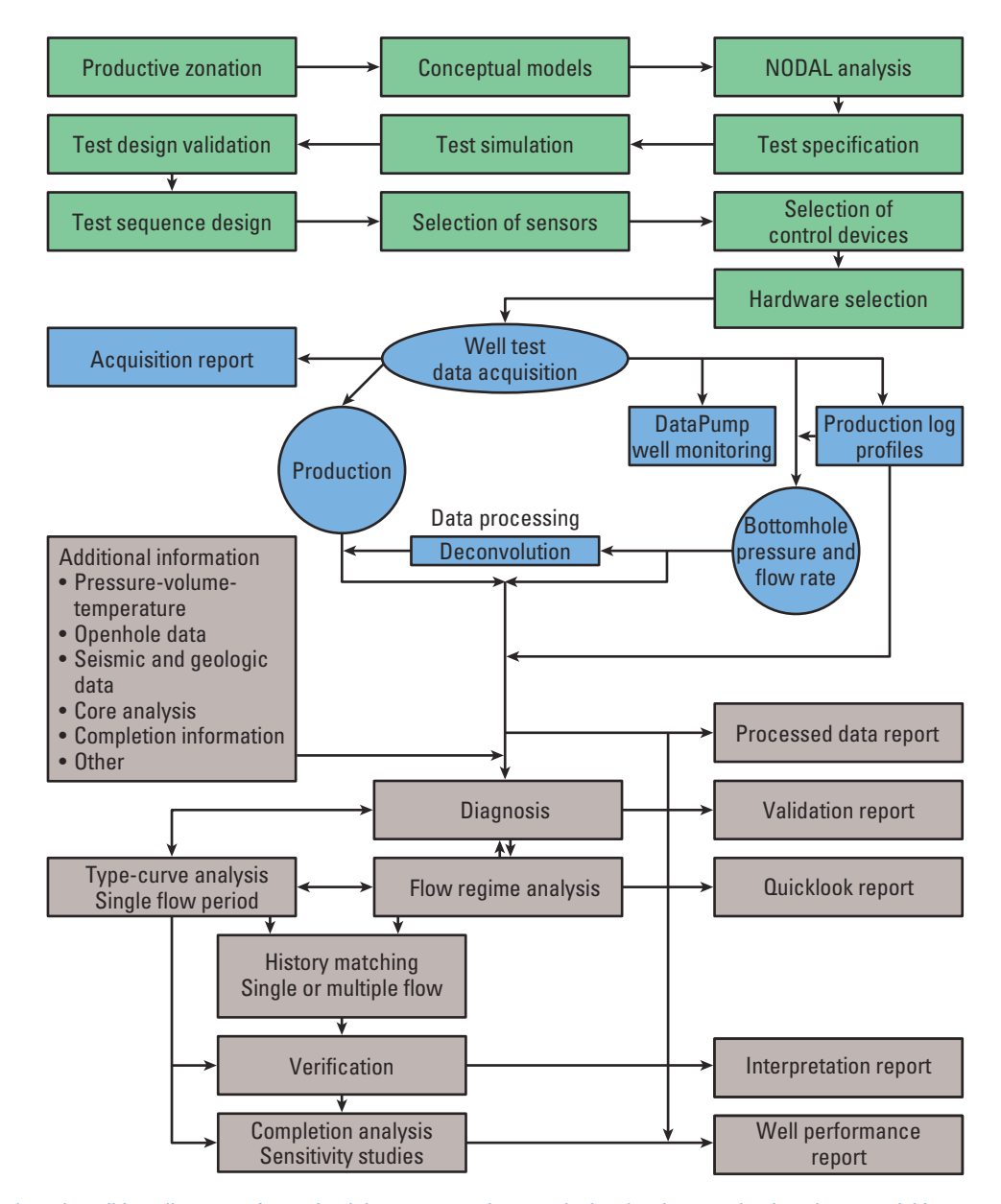


Figure 16. Flowchart describing all stages of a testing job, encompassing test design, hardware selection, data acquisition, data validation, interpretation and reporting of the results (Joseph and Ehlig-Economides, 1988).

Flow regime identification

Identifying flow regimes, which appear as characteristic patterns displayed by the pressure derivative data, is important because a regime is the geometry of the flow streamlines in the tested formation. Thus, for each flow regime identified, a set of well or reservoir parameters can be computed using only the portion of the transient data that exhibits the characteristic pattern behavior.

The eight flow regime patterns commonly observed in well test data are radial, spherical, linear, bilinear, compression/expansion, steady-state, dual-porosity or -permeability, and slope-doubling.

■ Flow Regime Identification tool

The popular Flow Regime Identification tool (Fig. 17) is used to differentiate the eight common subsurface flow regimes on log-log plots for their application in determining and understanding downhole and reservoir conditions. The tool template (SMP-4975) is included in the front of this book.

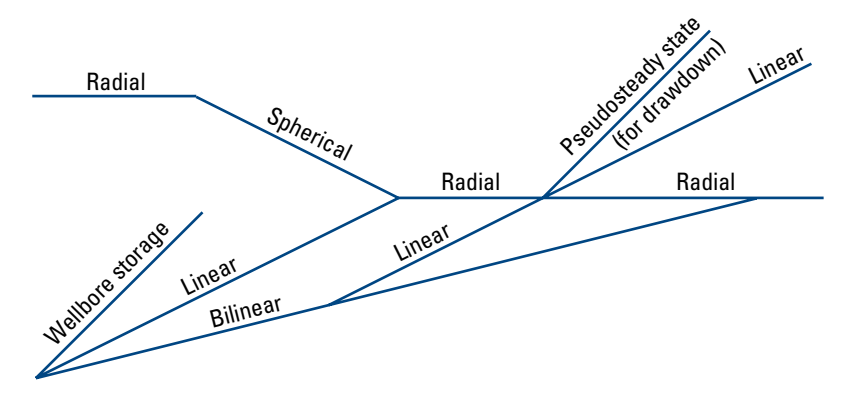


Figure 17. Flow Regime Identification tool.

Sidebar: Derivative computation

To compute the change in the pressure derivative $\ \ p$, the pressure change must be computed for the drawdown data

$$\Delta p = p_i - p_{wf} \Big(\Delta t \Big)$$

and for the buildup data

$$\Delta p = p_{ws} \left(\Delta t \right) - p_{wf} \left(t_p \right),$$

where

 p_i = initial formation pressure

 p_{wf} = bottomhole flowing pressure

 p_{ws} = bottomhole shut-in pressure

t = elapsed time since the start of the transient test

 t_p = duration of production time before shut-in, obtained by dividing the cumulative production before the buildup test by the last rate before shut-in.

For drawdown transient data, the pressure derivative is computed as the derivative of p with respect to the natural logarithm of the elapsed time interval $t_i = t_i - t_0$:

$$\frac{d\Delta p}{d\ln\left(\Delta t\right)} = \frac{p\left(t_{i+1}\right) - p\left(t_{i-1}\right)}{\ln\left(t_{i+1}\right) - \ln\left(t_{i-1}\right)},$$

where

 t_0 = start time for the transient data.

For buildup transient data, the preferred derivative computation is

$$\frac{d\Delta p}{d\tau} = \frac{p(t_{i+1}) - p(t_{i-1})}{\tau_{i+1} - \tau_{i-1}},$$

where

= superposition time, and

$$\tau_i = \ln \frac{t_p + \Delta t_i}{\Delta t_i}.$$

This computation is approximate. For more information on computational accuracy, see Bourdet $et\ al.$ (1984).

Radial flow

The most important flow regime for well test interpretation is radial flow, which is recognized as an extended constant or flat trend in the derivative. Radial flow geometry is described as flow streamlines converging to a circular cylinder (Fig. 18). In fully completed wells, the cylinder may represent the portion of the wellbore intersecting the entire formation (Fig. 18b). In partially penetrated formations or partially completed wells, the radial flow may be restricted in early time to only the section of the formation thickness where flow is directly into the wellbore (Fig. 18a). When a well is stimulated (Fig. 18c) or horizontally completed (Fig. 18e), the effective radius for the radial flow may be enlarged. Horizontal wells may also exhibit early-time radial flow in the vertical plane normal to the well (Fig. 18d). If the well is located near a barrier to flow, such as a fault, the pressure transient response may exhibit radial flow to the well, followed by radial flow to the well plus its image across the boundary (Fig. 18f).

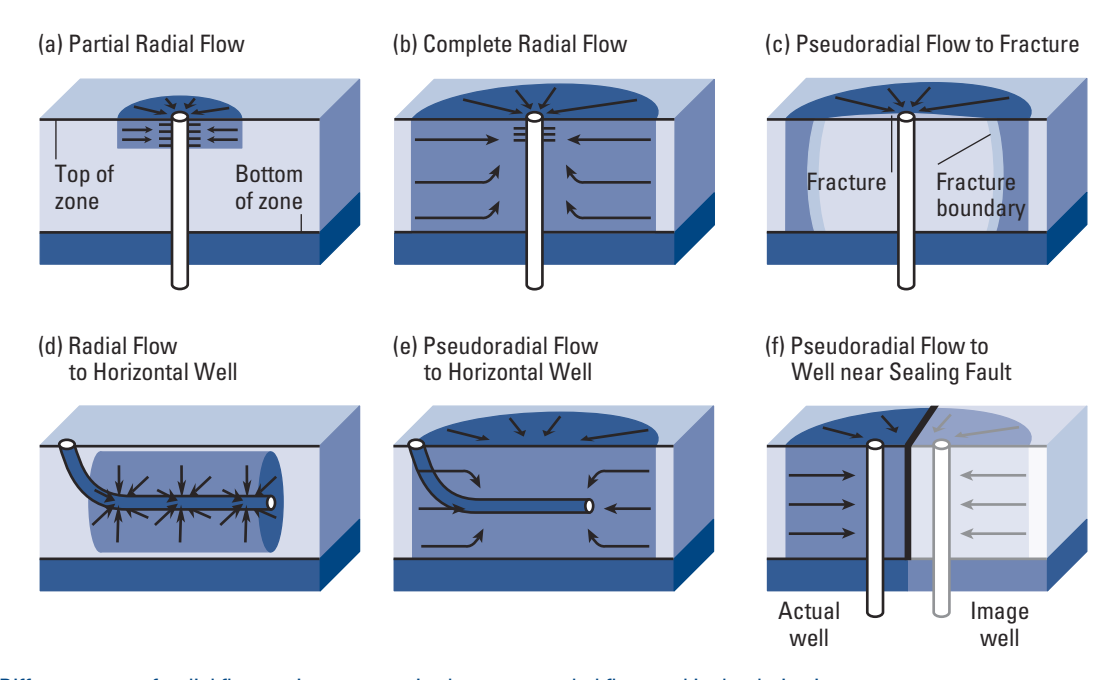


Figure 18. Different types of radial flow regimes, recognized as an extended flat trend in the derivative (Ehlig-Economides *et al.*, 1994).

Whenever radial flow occurs, the values for k and s can be determined; when radial flow occurs in late time, the extrapolated reservoir pressure p^* can also be computed. In Well A in Fig. 19, radial flow occurs in late time, so k, s and p^* can be quantified.

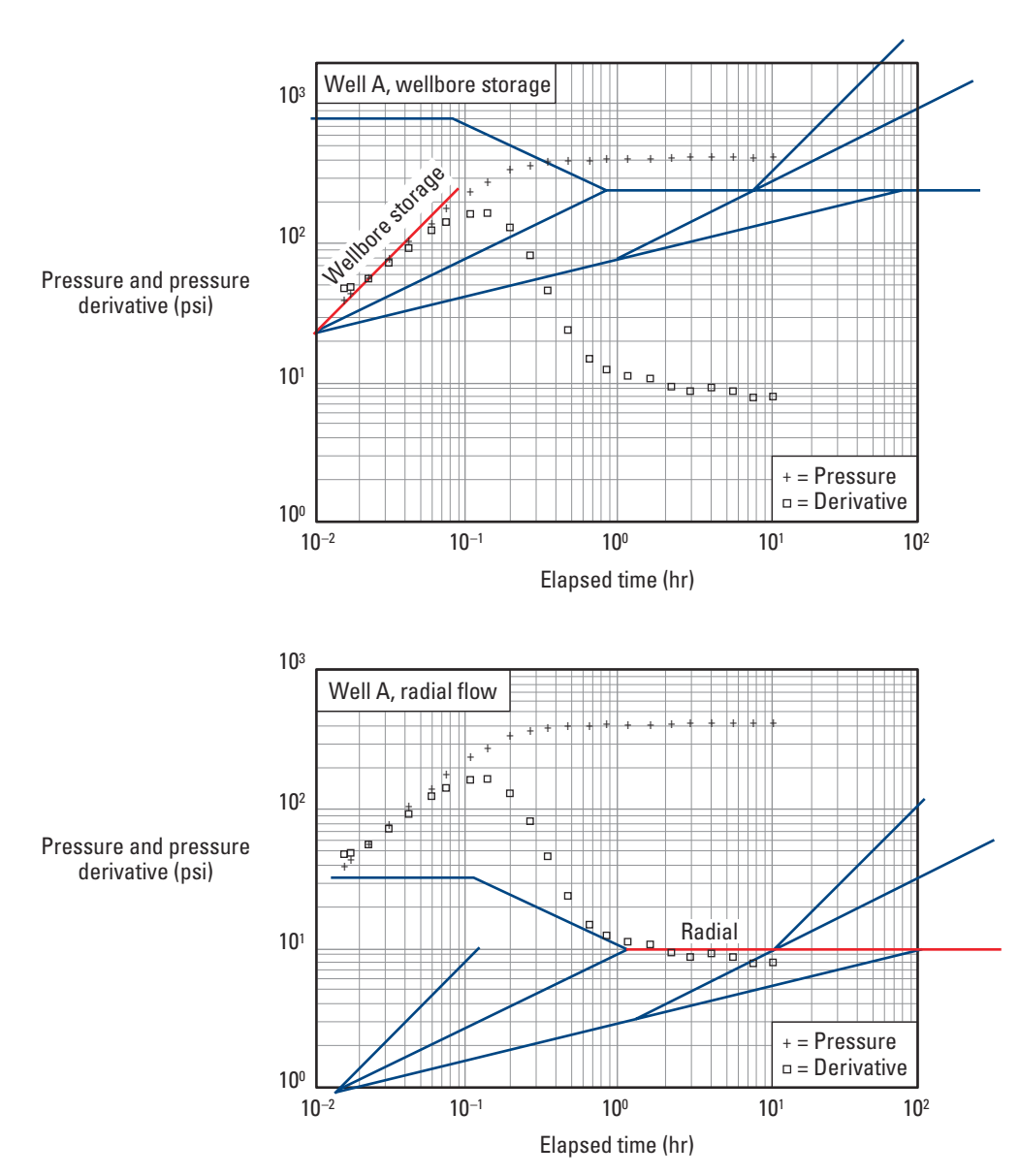


Figure 19. Radial flow occurring at late time. Values for the permeability, skin effect and extrapolated pressure to infinite shut-in can be computed (Ehlig-Economides *et al.*, 1994).

30 Schlumberger

Spherical flow

Spherical flow occurs when the flow streamlines converge to a point (Fig. 20). This flow regime occurs in partially completed wells (Fig. 20a) and partially penetrated formations (Fig. 20b). For the case of partial completion or partial penetration near the upper or lower bed boundary, the nearest impermeable bed imposes a hemispherical flow regime. Both spherical and hemispherical flow are seen on the derivative as a negative half-slope trend. Once the spherical permeability is determined from this pattern, it can be used with the horizontal permeability k_h quantified from a radial flow regime occurring in another portion of the data to determine the vertical permeability k_v .

The importance of k_v in predicting gas or water coning or horizontal well performance emphasizes the practical need for quantifying this parameter. A DST can be conducted when only a small portion of the formation has been drilled (or perforated) to potentially yield values for both k_v and k_h , which could be used to optimize the completion engineering or provide a rationale to drill a horizontal well.

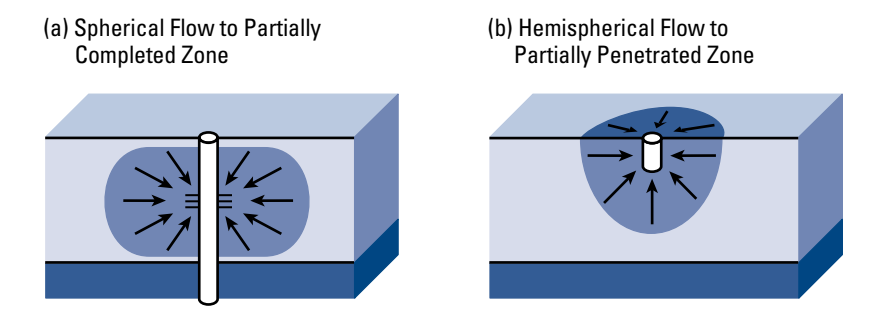


Figure 20. Spherical flow regime, which results from flow streamlines converging to a point (Ehlig-Economides et al., 1994).

Well B (Fig. 21) is an example of a DST from which the values of k_v and k_h were determined for the lower layer. These permeabilities were derived from the portion of the data exhibiting the spherical flow regime (negative half-slope) trend (red line in Fig. 21a). The reason why spherical flow occurred in early time is evident from the openhole log in Fig. 22, which shows only a few feet of perforations into the middle of the lower layer (Fig. 20a).

Negative half-slope behavior is commonly observed in well tests that indicate a high value of s. A complete analysis in these cases may provide the value of k_v and decompose the skin effect into components that indicate how much is due to the limited entry and how much to damage along the actively flowing interval. The treatable portion of the damage can then be determined and the cost effectiveness of damage removal and reperforating to improve the well productivity can be evaluated.

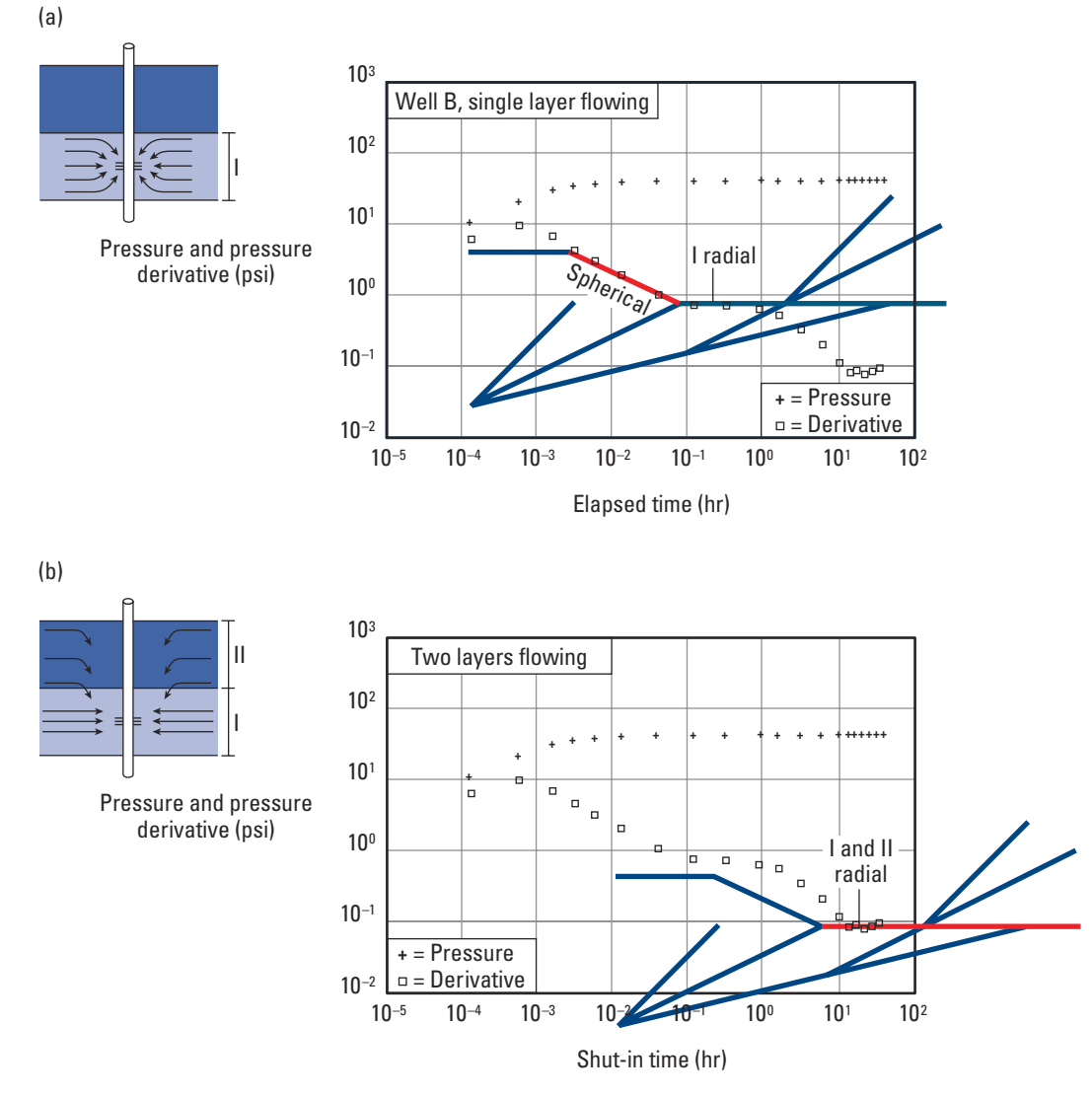


Figure 21. (a) Spherical flow regime in the lower layer is indicated by the negative half-slope trend (red line), followed by late-time radial flow. (b) Following a transition period, radial flow is from the combined two layers (Ehlig-Economides *et al.*, 1994).

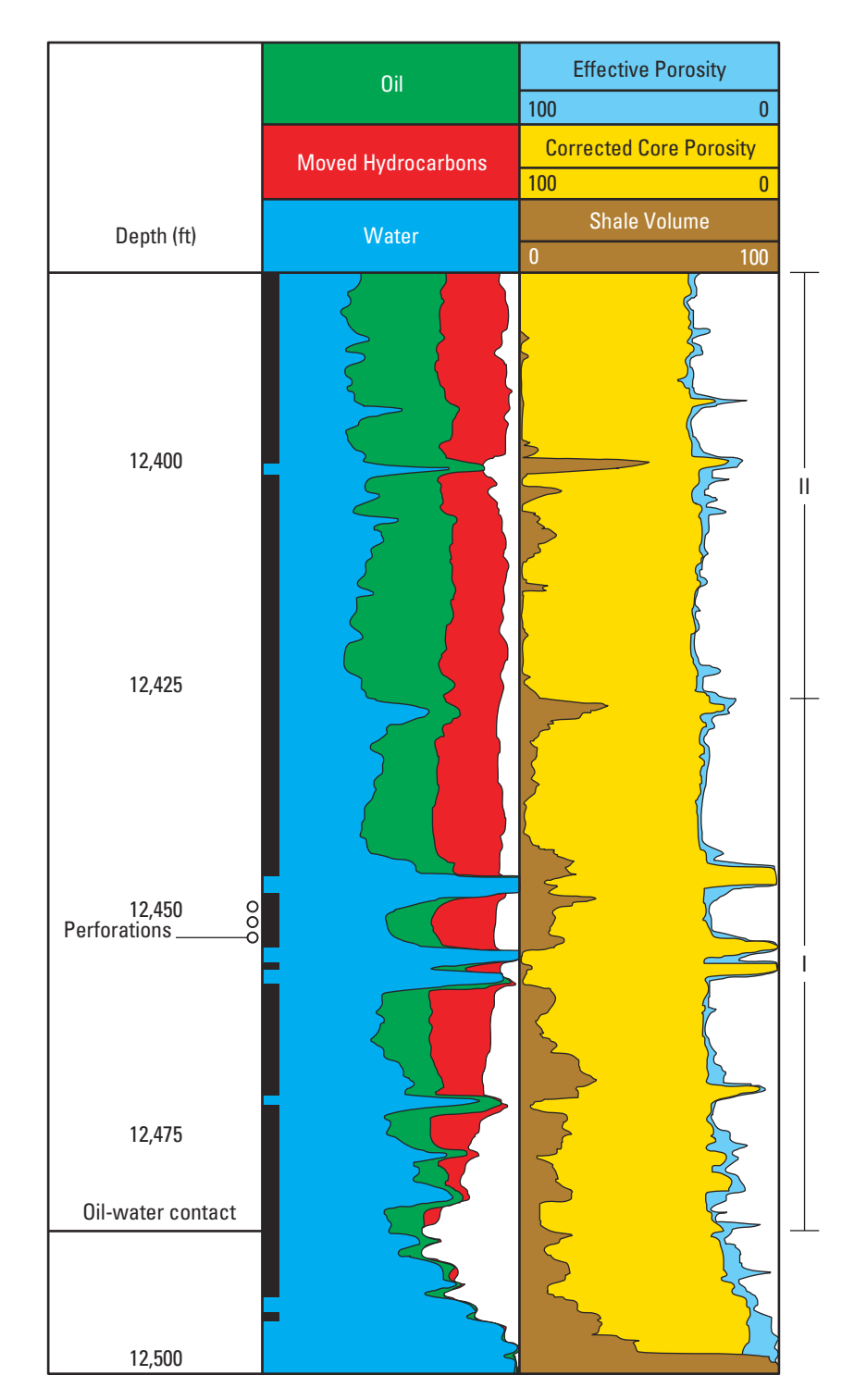


Figure 22. The openhole log shows a partially completed interval (Ehlig-Economides et al., 1994).

Linear flow

The geometry of linear flow streamlines consists of strictly parallel flow vectors. Linear flow is exhibited in the derivative as a positive half-slope trend. Figure 23 shows why this flow regime develops in vertically fractured and horizontal wells. It also is found in wells producing from an elongated reservoir. Because the streamlines converge to a plane, the parameters associated with the linear flow regime are the permeability of the formation in the direction of the streamlines and the flow area normal to the streamlines. The kh value of the formation determined from another flow regime can be used to calculate the width of the flow area. This provides the fracture half-length of a vertically fractured well, the effective production length of a horizontal well or the width of an elongated reservoir.

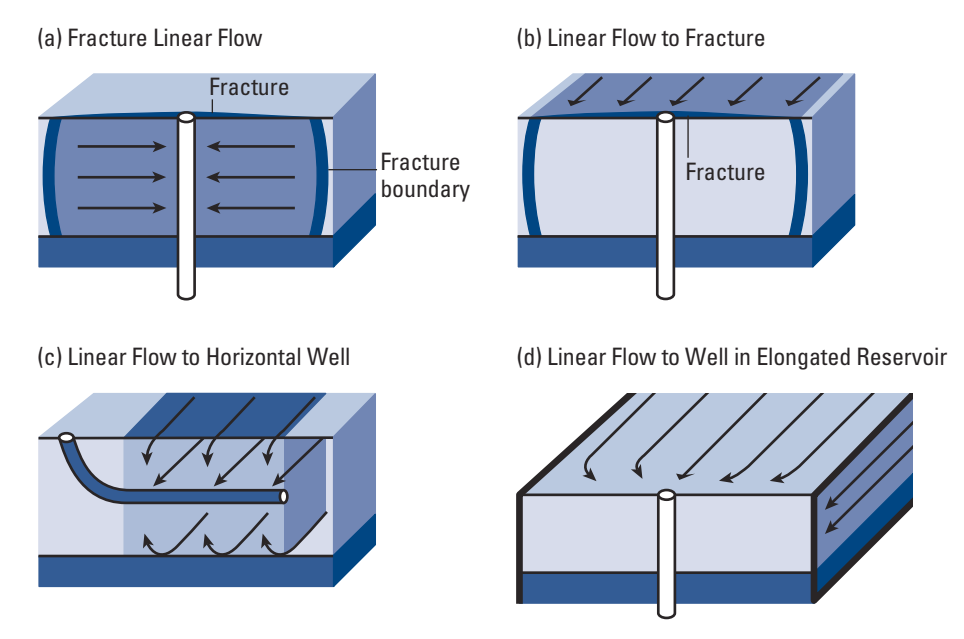


Figure 23. Linear flow regimes have parallel flowlines (Ehlig-Economides et al., 1994).

The combination of linear flow data with radial flow data (in any order) can provide the principle values of k_x and k_v for the directional permeabilities in the bedding plane. In an anisotropic formation, the productivity of a horizontal well is enhanced by drilling the well in the direction normal to the maximum horizontal permeability.

Well C is a water injection well that exhibits linear flow (Fig. 24). Although no radial flow is evident, the time of departure from linear flow coupled with an analysis of the data that follows the half-slope derivative trend provides two independent indicators of the formation permeability and fracture half-length, enabling the quantification of both. The subtle rise in the derivative after the end of linear flow suggests a boundary, which was interpreted as a fault.

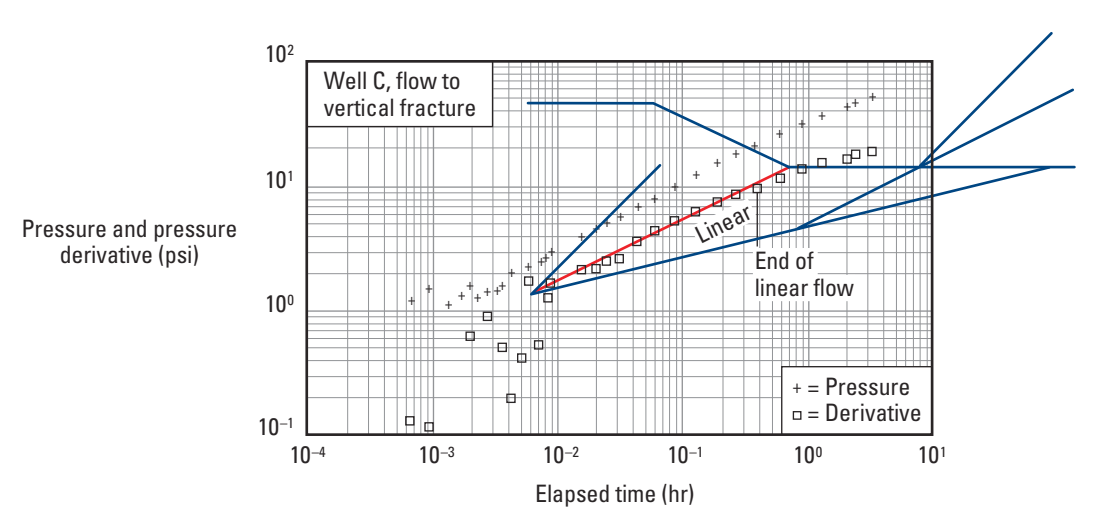


Figure 24. The linear flow regime has a positive half-slope trend in the derivative curve.

■ Bilinear flow

Hydraulically fractured wells may exhibit bilinear flow instead of, or in addition to, linear flow. The bilinear flow regime occurs because a pressure drop in the fracture itself results in parallel streamlines in the fracture at the same time as the streamlines in the formation become parallel as they converge to the fracture (Fig. 25). The term bilinear refers to the simultaneous occurrence of two linear flow patterns in normal directions. The derivative trend for this flow regime has a positive quarter-slope. When the fracture half-length and formation permeability are known independently, the fracture conductivity $k_f w$ can be determined from the bilinear flow regime.

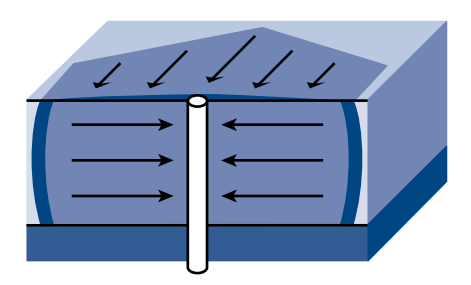


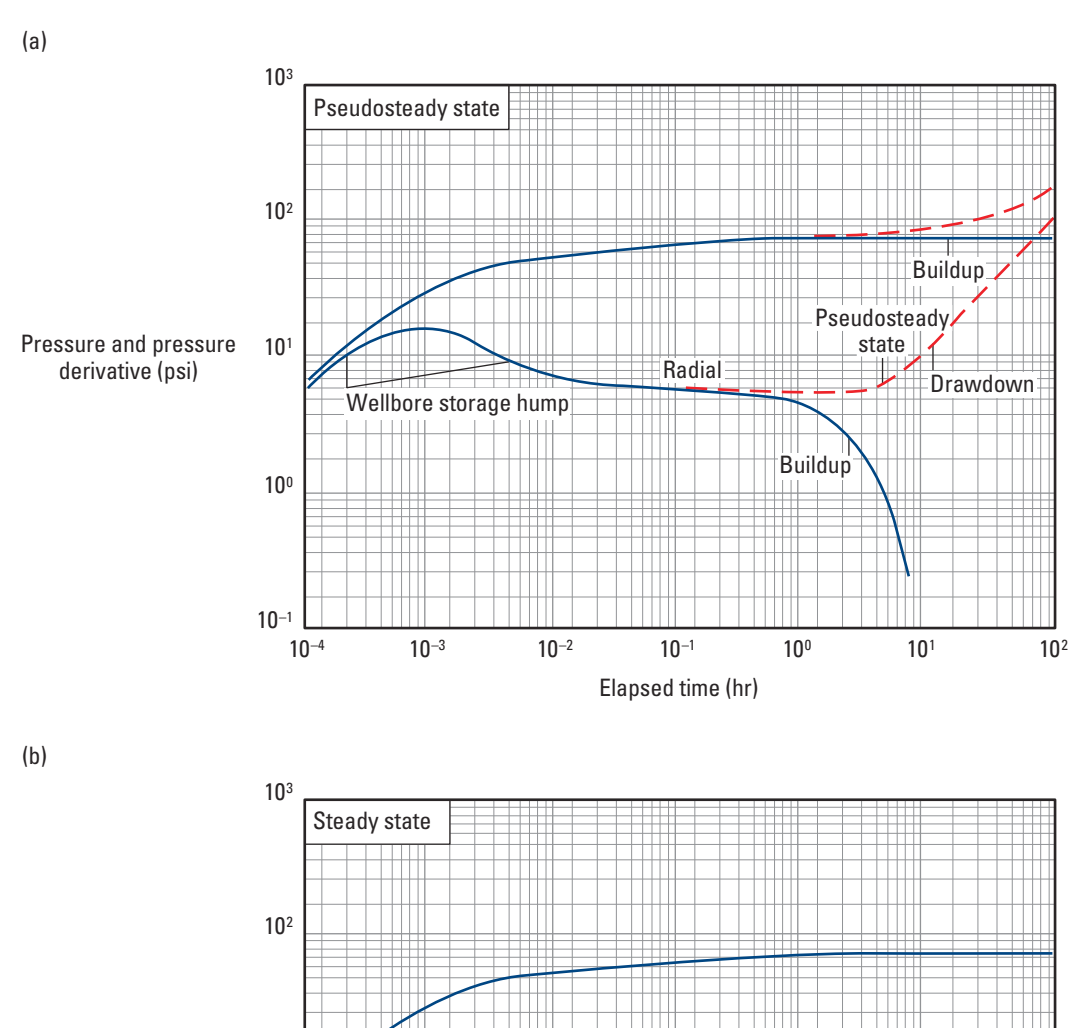
Figure 25. Bilinear flow regime commonly exhibited by hydraulically fractured wells (Ehlig-Economides et al., 1994).

Compression/expansion

The compression/expansion flow regime occurs whenever the volume containing the pressure disturbance does not change with time and the pressure at all points within the unchanging volume varies in the same way. This volume can be limited by a portion or all of the wellbore, a bounded commingled zone or a bounded drainage volume. If the wellbore is the limiting factor, the flow regime is called wellbore storage; if the limiting factor is the entire drainage volume for the well, this behavior is called pseudosteady state. The derivative of the compression/expansion flow regime appears as a unit-slope trend.

One or more unit-slope trends preceding a stabilized radial flow derivative may represent wellbore storage effects. The transition from the wellbore storage unit-slope trend to another flow regime usually appears as a hump (Fig. 26). The wellbore storage flow regime represents a response that is effectively limited to the wellbore volume. Hence, it provides little information about the reservoir. Furthermore, wellbore storage effects may mask important early-time responses that characterize near-wellbore features, including partial penetration or a finite damage radius. This flow regime is minimized by shutting in the well near the production interval. This practice can reduce the portion of the data dominated by wellbore storage behavior by two or more logarithmic cycles in time. In some wells tested without downhole shut-in, wellbore storage effects have lasted up to several days.

After radial flow has occurred, a unit-slope trend that is not the final observed behavior may result from production from one zone into one or more other zones (or from multiple zones into a single zone) commingled in the wellbore. This behavior is accompanied by crossflow in the wellbore, and it occurs when the commingled zones are differentially depleted. If unit slope occurs as the last observed trend (Fig. 26a), it is assumed to indicate pseudosteady-state conditions for the entire reservoir volume contained in the well drainage area. Late-time unit-slope behavior caused by pseudosteady state occurs only during drawdown. If the unit slope develops after radial flow, either the zone (or reservoir) volume or its shape can be determined.



Pressure and pressure 10¹ Steady state derivative (psi) Radial Buildup Wellbore storage hump Drawdown 10⁰ 10-1 10-3 10-2 10-1 10° 10¹ 10-4 10² Elapsed time (hr)

Figure 26. Flow regime trends exhibited by wellbore storage, boundaries and pressure maintenance.

Steady state

Steady state implies that pressure in the well drainage volume does not vary in time at any point and that the pressure gradient between any two points in the reservoir is constant. This condition may occur for wells in an injection-production scheme. In buildup and falloff tests, a steeply falling derivative may represent either pseudosteady or steady state.

Dual porosity or permeability

Dual-porosity or -permeability behavior occurs in reservoir rocks that contain distributed internal heterogeneities with highly contrasting flow characteristics. Examples are naturally fractured or highly laminated formations. The derivative behavior for this case may look like the valley-shaped trend shown in Fig. 27a, or it may resemble the behavior shown in Fig. 27b. This feature may come and go during any of the previously described flow regimes or during the transition from one flow regime to another. The dual-porosity or -permeability flow regime is used to determine the parameters associated with internal heterogeneity, such as interporosity flow transmissibility, relative storativity of the contrasted heterogeneities and geometric factors.

■ Slope doubling

Slope doubling describes a succession of two radial flow regimes, with the slope of the second exactly twice that of the first. This behavior typically results from a sealing fault (Fig. 28), but its similarity to the dual-porosity or -permeability behavior in Fig. 27b shows that it can also be caused by a permeability heterogeneity, particularly in laminated reservoirs. If slope doubling is caused by a sealing fault, the distance from the well to the fault can be determined.

38 Schlumberger

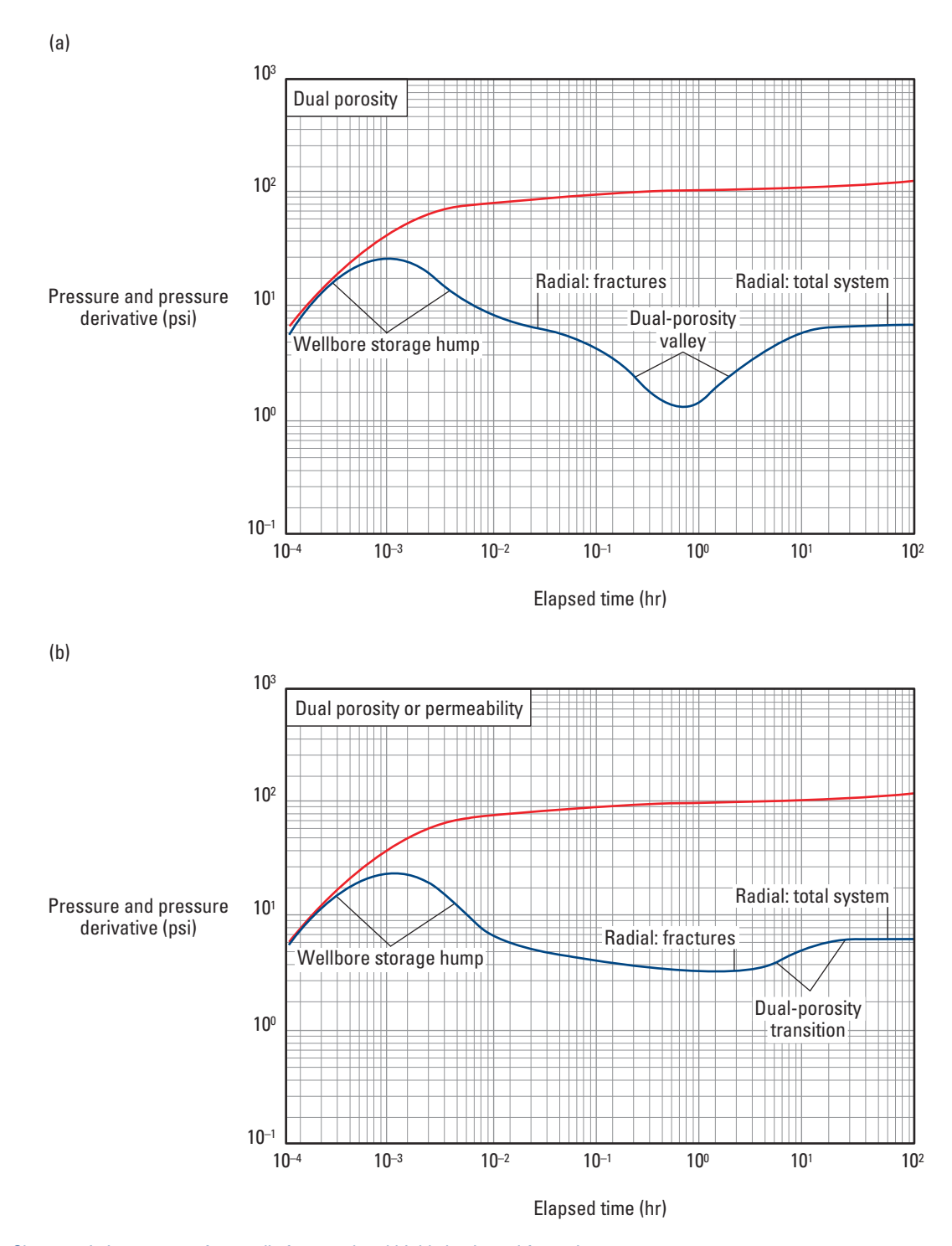


Figure 27. Characteristic patterns of naturally fractured and highly laminated formations.

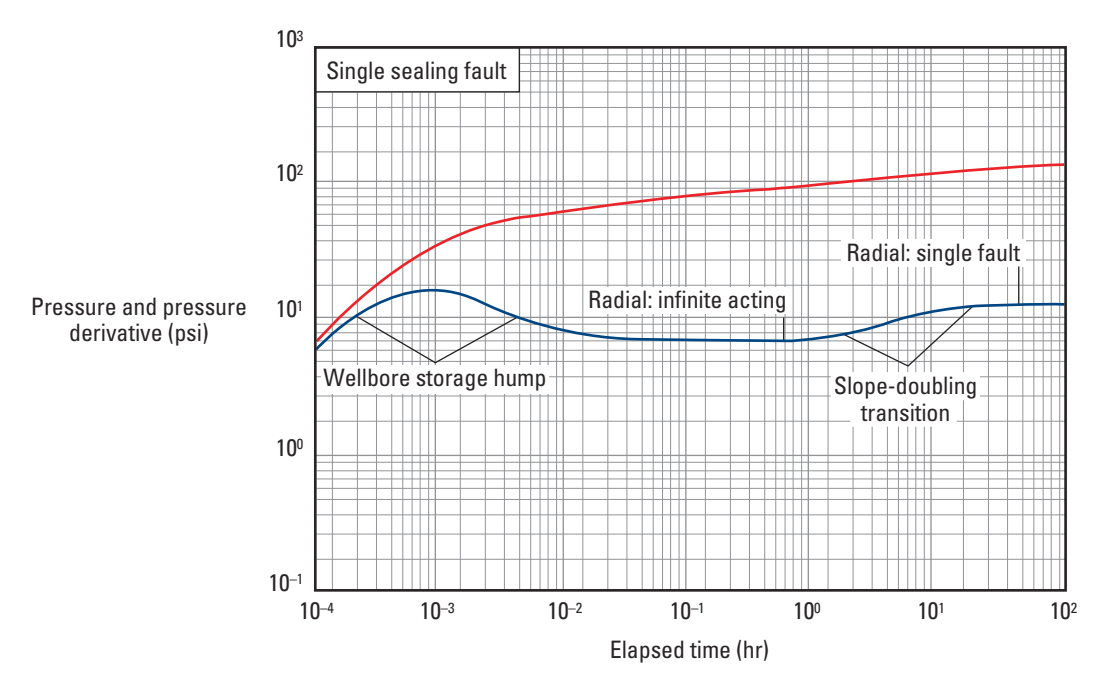


Figure 28. Slope doubling caused by a succession of two radial flow regimes (sealing fault).

The analysis of log-log plots of testing data is an improvement in well testing practice, but, as previously mentioned, it does not preclude following a systematic approach. The preceding steps of test design, hardware selection, and data acquisition and validation are the foundation of effective interpretation.

Use of type curves

The original rationale for type curves was to interpret interference tests using the line source solution. Later type curves for wellbore storage and skin effects were developed to improve on Horner buildup analysis, which was in error whenever an apparent straight-line trend in the transient data that was not due to radial flow in the reservoir was used to compute estimates for k, s and p^* . Over time, models capturing near-well geometry (partial penetration, vertical fracture), reservoir heterogeneity (homogeneous, dual porosity, dual permeability) and outer boundaries (faults, drainage boundaries, constant-pressure boundaries) were presented as families of type curves. Since the advent of the pressure derivative, new models have been introduced in the literature as type-curve pairs for pressure change and its derivative. Expert well test analysts have learned to recognize models for observed transient data as identifiable trends in the pressure derivative.

The Appendix to this book is a library of published type curves along with the reservoir models. The curves were derived for a step rate increase from zero and assume constant wellbore storage. Each log-log plot has a family of paired pressure and pressure derivative curves differentiated by color. Identified flow regimes described previously in this chapter are differentiated by symbols: dashes (radial), dots (linear), triangles (spherical) and squares (closed system).

The generalized models can be matched directly to data from a drawdown period at a constant flow rate or a buildup test preceded by a long drawdown period. With appropriate plotting techniques, as explained later, this library may be extremely useful for the model identification stage of the interpretation process for any type of transient test. Care must be taken when dealing with closed systems because the late-time portion exhibits different features for drawdown than for shut-in periods.

In practice, drawdowns are short or exhibit widely varying flow rates before shut-in. Also, buildup tests are often conducted with surface shut-in and exhibit variable wellbore storage. These situations violate the assumptions on which published type curves are based, impairing their direct usage. The weaknesses inherent in analysis using published models can be avoided by constructing curves that account for the effects of flow changes that occur before and during the test. Improved computing techniques have facilitated the development of custom curves, resulting in a major advance in well test interpretation. The computer-generated models are displayed simultaneously with the data and rigorously matched to produce precise estimates for the reservoir parameters.

Use of numerical simulation

Acquired transient data commonly contains behavior dominated by effects that are not captured in analytical models. Typical departures from the analytical model assumptions are multiphase flow, non-Darcy flow and complex boundary configurations that are not easily generalized in an analytical model catalog. Such features can be addressed with a numerical model, but commercial numerical simulators are designed for full-field simulation with multiple wells and do not readily adapt to the single-well focus and short time frame inherent to well testing.

If they are adapted to focus on the short-term transient behavior of a single well or a few wells, and also designed to present the data in the form used for well test interpretation, numerical models can provide considerable insight beyond that possible from analytical models.

The extremely broad range of what can be modeled with numerical simulation makes this a tool used to refine the interpretation process, not a starting point. When sufficient information supports this level of complexity, the approach is to capture all known parameters in the simulation and use the resulting model to quantify what is not known. For example, if transient data are acquired that encompass a radius of investigation that includes structural or stratigraphic barriers mapped from seismic data, capturing these in the numerical model may enable quantification of areal permeability anisotropy that would otherwise require interference testing to determine. Alternatively, the same scenario in successive tests of the same well may enable insitu characterization of multiphase fluid flow properties.

Data from multiple wells acquired by permanent monitors are more easily interpreted with numerical simulation. Likewise, data acquired in complex wells employing multibranch and smart well technologies require numerical simulation for rigorous analysis.

Three stages of modeling

Modern well test interpretation has three distinct stages. In the model identification stage, the analyst identifies a theoretical reservoir model with pressure trends that resemble those observed in the acquired data. Once the model has been chosen, the model parameters that produce the best match for the measured pressure data are determined in the parameter estimation stage. Finally, in the results verification stage the selected model and its parameters are used to demonstrate a satisfactory match for one or more transient tests in the well. A brief discussion of these three stages follows.

Model identification

For the model identification stage, the analyst should recognize certain characteristic patterns displayed by the pressure transient data. This is greatly facilitated by a knowledge of straight-line pressure derivative response trends associated with the formation flow geometry. As previously discussed, spherical or hemispherical flow to a partial completion exhibits a derivative line with a negative half-slope. Linear flow to a hydraulic fracture or in an elongated reservoir is recognized as a straight trend in the derivative with a positive half-slope. Bilinear flow to a finite-conductivity hydraulic fracture has a derivative line with a positive quarter-slope. The dominant geometry of the flow streamlines in the formation determines which flow regime pattern appears in the pressure transient response at a given time.

The presence of one or more of the recognized derivative patterns marks the need to select a model that accounts for the implied flow regimes. Moreover, each of the several easily recognized derivative trends has a specialized plot that is used to estimate the parameters associated with the trend. The specialized plot for each straight derivative trend is merely a plot of the pressure change versus the elapsed time, raised to the same power as the slope of the derivative line on the log-log plot. The slopes and intercepts of these specialized plots provide the equations for parameter computations. Parameters estimated from a specialized plot may be used as starting values for computerized refinement of the model for the transient response in the second interpretation stage.

Reservoir information collected from geoscientists assists the selection of a reservoir model. The distinctions among the various model options consistent with the transient test data are not always clear-cut, and more than one model may provide similar responses. In this case the analyst may rule out most model options by consulting with colleagues working with other, independent data. If the flow regime responses are poorly developed or nonexistent, interdisciplinary discussion may suggest the selection of an appropriate model and reasonable starting values for the parameter estimation stage of the interpretation.

Flow regime responses may be difficult to recognize because of a problem or procedure that could have been addressed before starting the test. This underscores the need for careful test design. For example, excessive wellbore storage resulting from shutting in the well at the surface can mask important flow regime trends. Furthermore, late-time trends may be distorted by superposition effects that could have been minimized with adjustments in the test sequence or by inadequate pressure gauge resolution that could have been avoided by using a more sensitive gauge. Missing or incomplete late-time trends may result from premature test termination that would have been avoided with real-time surface acquisition and on-site data validation. Even well-designed tests may have flow regimes that are difficult to discern, but this is relatively rare.

Parameter estimation

Once the reservoir model has been identified, it is necessary to compute the model parameters. Using initial parameter estimates from specialized flow regime analysis, interdisciplinary input or both resources, an initial simulation for the transient response is computed. The initial simulated and observed responses usually differ. Modern analysis, however, is assisted by nonlinear regression routines that automatically refine the parameter estimates until the simulation coincides with the observed data for the essential portions of the transient response. Thus, the first interpretation stage of model identification represents the main challenge for the analyst.

The following example illustrates the first two modeling stages. Figure 29a shows a combined pressure and pressure derivative plot, and Fig. 29b shows the generalized Horner plot. At first glance, the plots could be caused by four possible reservoir configurations or characteristics:

- single sealing fault, as indicated by doubling of the slope in the generalized Horner plot
- trough in the derivative plot resulting from a dual-porosity system
- dual-permeability (two-layer) reservoir
- composite system.

44

The composite model was discarded because knowledge of the reservoir made this configuration infeasible. A composite system occurs if there is a change in mobility from the value near the well to another value at some radius from the well. The pressure and pressure derivative plots were then computed by assuming the remaining three models (Fig. 30). The single sealing fault model (Fig. 30a) does not match the observed pressure transient.

Figures 30b and 30c, derived assuming a dual-porosity system, provide a much better match than the two previous models, although they are still imperfect. Figure 30d confirms the extremely good fit of the dual-permeability or two-layer reservoir model with the pressure transient and derivative curves.

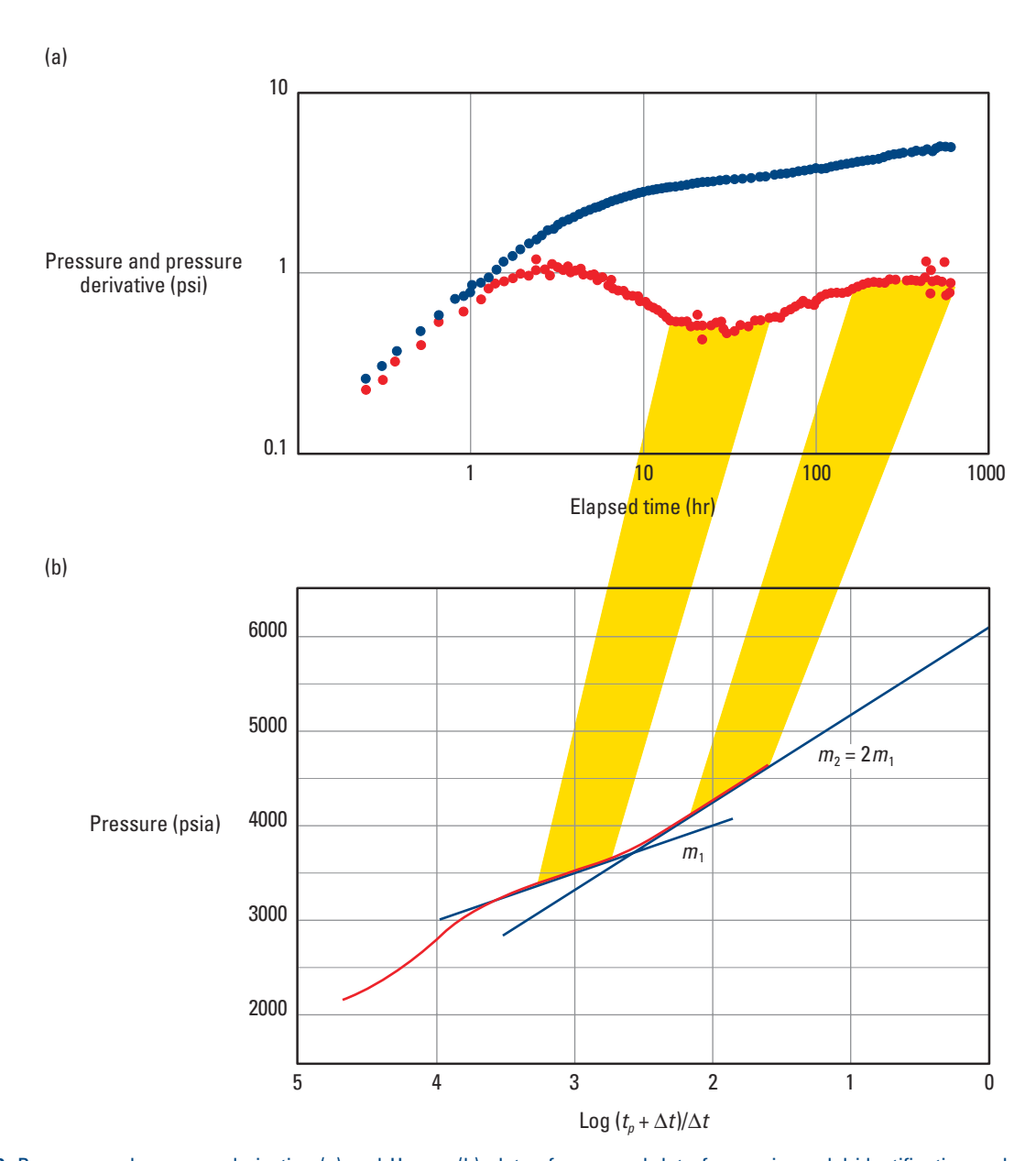


Figure 29. Pressure and pressure derivative (a) and Horner (b) plots of measured data for use in model identification and parameter computation. The doubling of the slope m on the Horner plot simplistically indicates that the sole cause is an impermeable barrier near the well, such as a sealing fault. Closer examination of the data using current computational techniques and interdisciplinary consultation identifies other factors that may cause the change in slope, such as a two-layer reservoir (dual permeability).

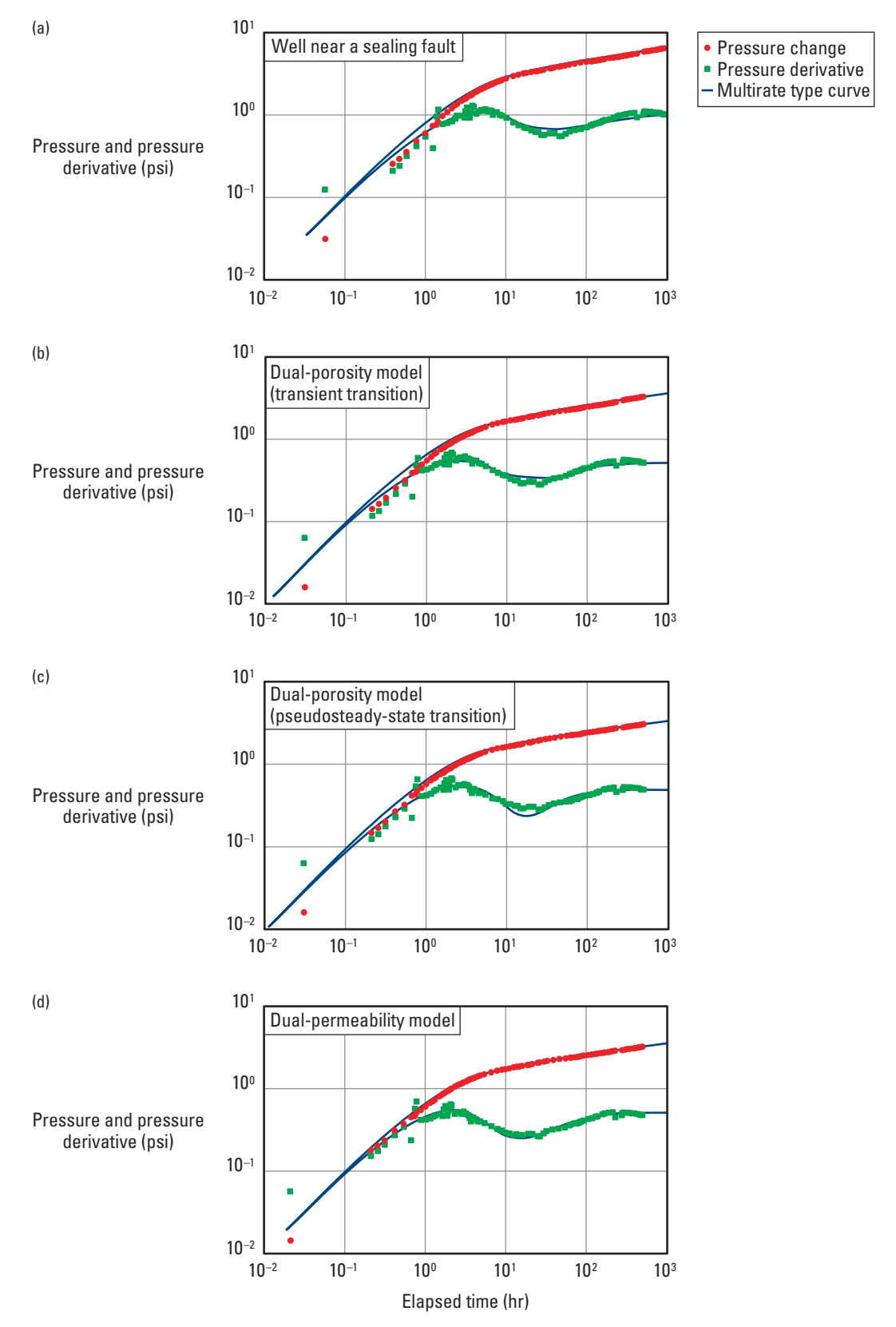


Figure 30. Finding the model. These four plots show the response of various idealized formation models compared with the pressure and pressure transient data plotted in Fig. 29.

46 Schlumberger

Results verification

Several drawdown and buildup periods are typically included in a well test, and it is common to interpret every transient and cross-check the computed reservoir parameters. However, analysis of all the transients in a test is not always possible. In this situation, forward modeling may help confirm the validity of a reservoir model.

Basically, forward modeling involves simulating the entire series of drawdowns and buildups and using the reservoir model and its parameters (Fig. 31). Because the simulation continues for much longer than an individual transient, the effects of reservoir boundaries are more likely to be noticed. If the simulation does not match the entire pressure history, then the assumed reservoir model should be reassessed.

For example, if an infinite-acting reservoir model is assumed from the analysis of a single transient, the forward-modeling technique will show whether the model is correct. If the reservoir is actually a closed system, the simulation will not reveal realistic reservoir depletion.

Changes in model parameters may be required to match each transient, especially the skin factor. The skin factor usually decreases during cleanup. For high flow rates, especially in gas wells, the skin factor may be rate dependent. In these cases no single model matches the entire pressure history.

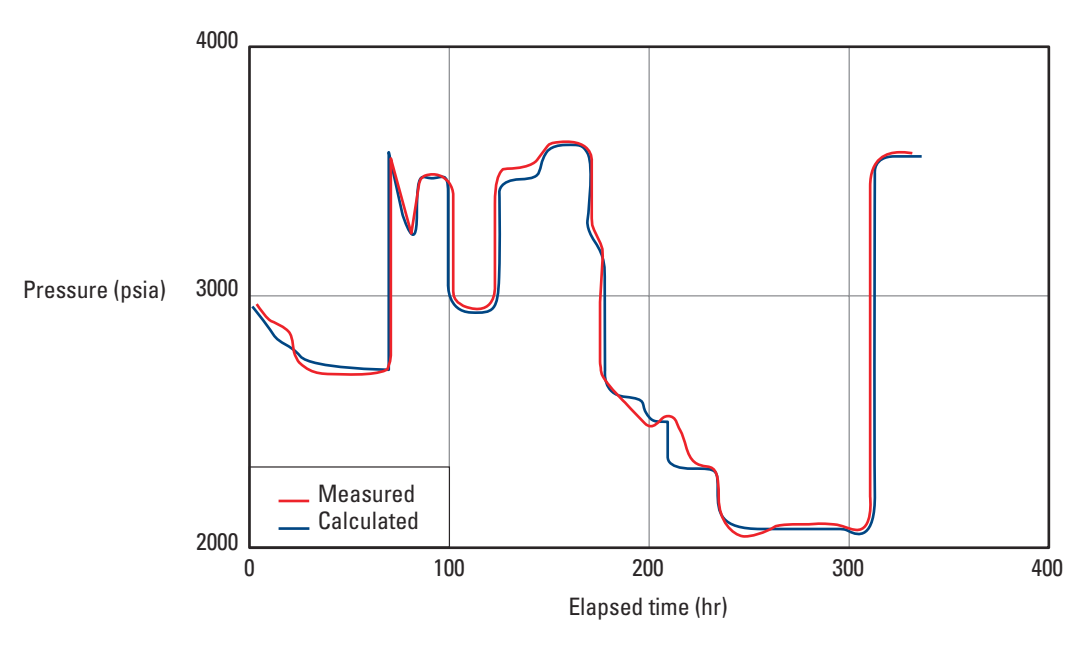


Figure 31. Forward modeling used to reproduce the entire data set. The model and parameters were selected by analyzing one of the pressure transients.

Use of downhole flow rate measurements

The techniques described for analyzing transient tests rely on only pressure measurements and were derived assuming a constant flow rate during the analyzed test period. The constant flow rate situation, in practice, prevails only during shut-in conditions. Because of this, buildup tests are the most commonly practiced well testing method.

A buildup test is undesirable if the operator cannot afford the lost production associated with the test or because the well would not flow again if shut in. For these circumstances drawdown tests are preferable. In practice, however, it is difficult to achieve a constant flow rate out of the well, so these tests were traditionally ruled out.

Advances in measurement and interpretation techniques now enable the analysis of tests that exhibit variable flow rate conditions to obtain the same information furnished by buildup tests, provided that the flow rate variations are measured in tandem with changes in pressure. Today, pressure transient tests can be run in almost any production or injection well without shutting in the well and halting production.

Furthermore, drawdown data are not ambiguous like buildup data (varying between steady-state and pseudosteady-state responses). Boundary geometries are easier to diagnose because there is less distortion caused by superposition, provided that the downhole flow rate is measured. Consequently, the results are more definitive.

This section briefly describes a procedure for well test analysis in a single-layer reservoir with combined downhole flow rate and pressure measurements. The method enables the analysis of drawdown periods and the afterflow-dominated portion of a buildup test. It also constitutes the fundamental basis for testing multilayered reservoirs with rigless operations—a subject discussed in the next chapter.

Description of the problem

Flow rates and pressure changes are closely associated: any change in the flow rate produces a corresponding change in pressure, and vice versa. The challenge for the analyst is to distinguish the changes in the pressure response curve that have been caused by a genuine reservoir characteristic from those created by varying wellbore flow rates (i.e., the pure reservoir signal versus noise).

The pure reservoir signal can be separated from the noise by acquiring simultaneous measurements of flow and pressure. Production logging tools can acquire both variables simultaneously and accurately, extending the range of wells in which well testing can be successfully performed.

In a typical test, a production logging tool is positioned at the top of the producing interval (Fig. 32). The tool records flow and pressure data for the duration of the test. Figure 33 shows a typical data set acquired during a drawdown test, with changes in the shape of the pressure curve matching those on the flow rate curve.

The analysis of transient tests with simultaneously recorded flow rate and pressure measurements involves the same three basic stages as pressure data analysis—model identification, parameter estimation and verification. The same plotting techniques are used, except that the scales contain functions that account for all observed flow rate changes. The three stages are explained and illustrated using the example drawdown data in Fig. 33.

48 Schlumberger

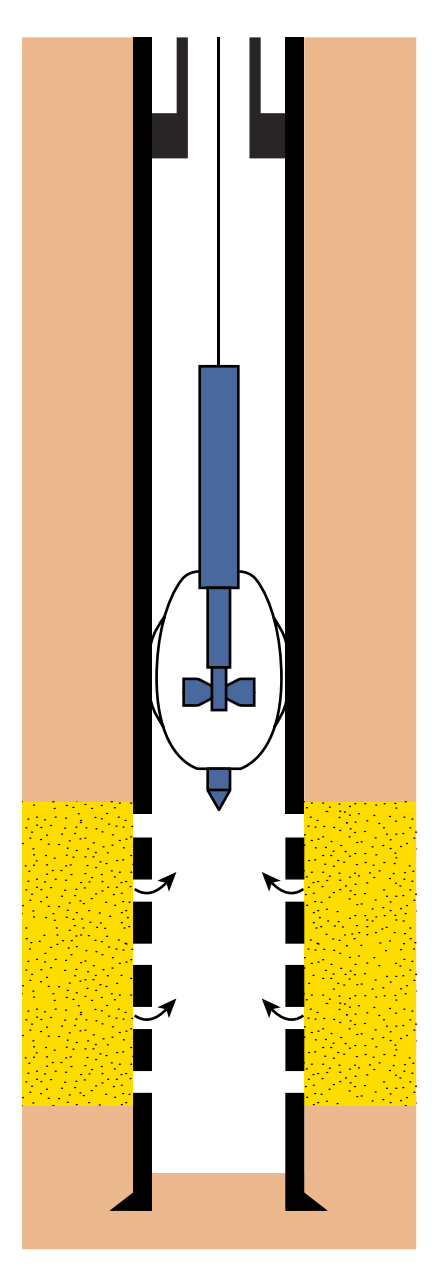


Figure 32. Production logging tool in position for a well test in a single-layer reservoir.

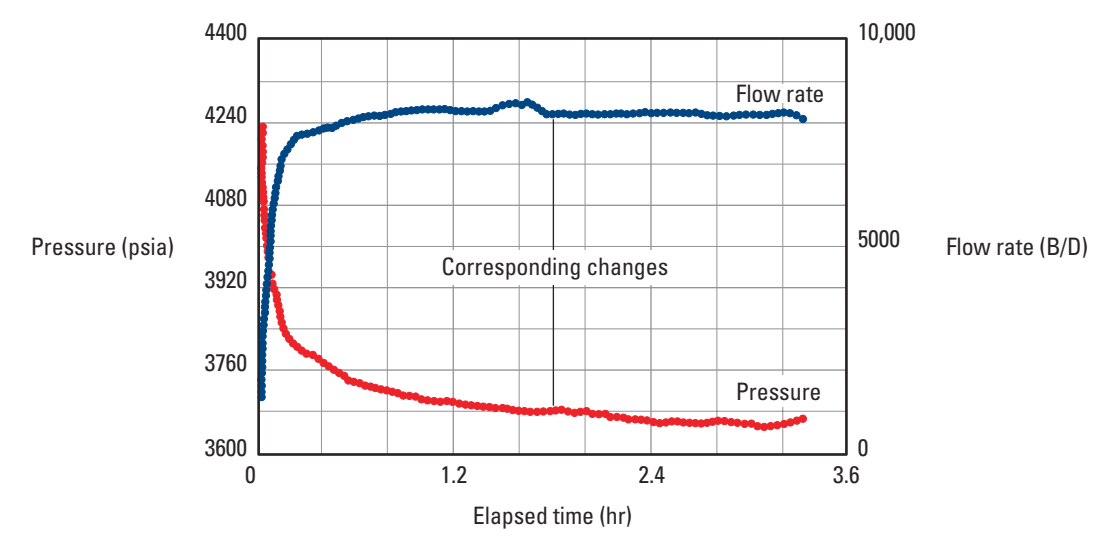


Figure 33. Flow rate and pressure data recorded during a drawdown test. Changes in the pressure curve correspond to changes in the flow rate curve.

Model identification

The library of type curves in the Appendix constitutes an excellent tool for the model identification process. Although measured pressure values can be compared directly with the theoretical curves only when the flow rate from the reservoir is constant, the curves can also be used for variable rate cases if mathematical transforms are applied to the test data. The transforms account for the flow rate variations observed during the transient.

Figure 34 shows the log-log plot of the pressure and pressure derivative curves of the data shown in Fig. 33. The data are from a well in which the flow rates were changing before and during the test. The flow rate changes had a dominating effect on the well pressure, to the point where the pressure and pressure derivative curves lack any distinct shape that could be used for model identification. It would be incorrect to attempt identification of the reservoir model by comparing these raw data with the library of type curves, which were constructed using a single-step change, constant flow rate.

Rather, the data are transformed to a form that can be more readily analyzed. One such transform is deconvolution— a process that enables construction of the raw pressure curve that would have occurred in response to a single-step change, constant flow rate.

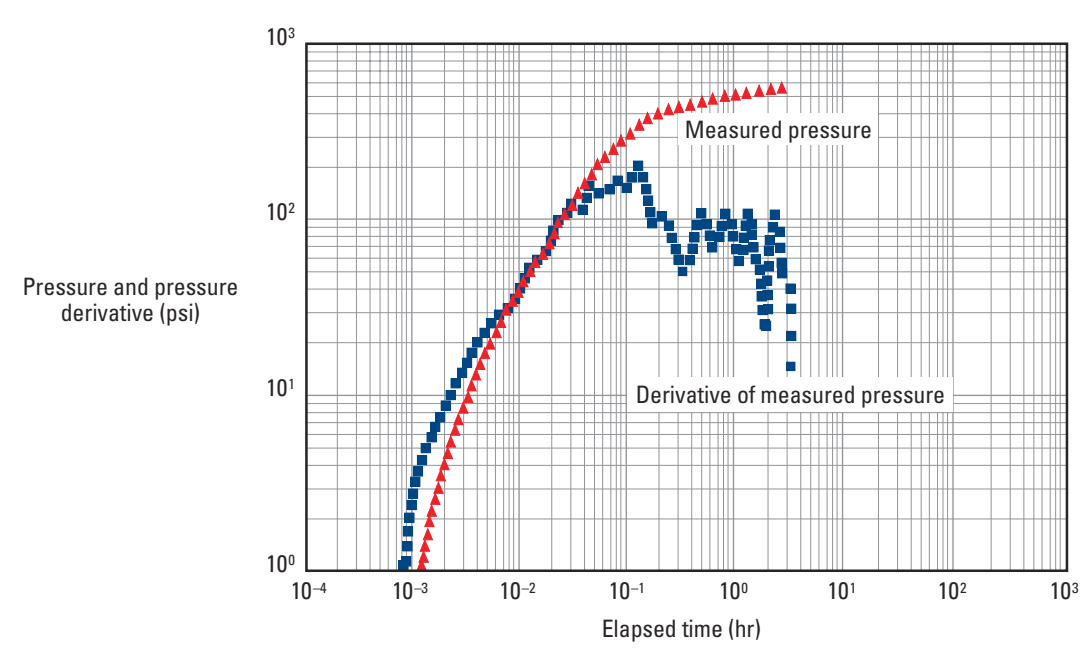


Figure 34. Flow rate changes before and during a well test can dominate the measured well pressure. Because the pressure and pressure derivative curves lack any distinct shapes, they cannot be compared with published type curves to identify the reservoir model.

The pressure response for a transient test under variable flow rate conditions is given by the convolution integral, which can be expressed in dimensionless variables as

$$p_{wbD}(t_D) = \int_0^{t_D} q_D(\tau) p_{wD}'(t_D - \tau) d\tau, \tag{6}$$

where

 p_{wbD} = dimensionless wellbore pressure

 p_{wD} = derivative of the dimensionless wellbore pressure at constant flow rate,

including wellbore storage and skin effects

 q_D = dimensionless flow rate.

Mathematically, deconvolution is the inversion of the convolution integral. The constant flow rate response (including wellbore storage and skin effects) is computed from measurements of the wellbore flowing pressure p_{wbf} and flow rate q_{wbf} . Ideally, deconvolved pressure data can be compared directly with published type curves. Then, straightforward conventional interpretation techniques and matching procedures can obtain the model and its parameters simultaneously.

Although simple in concept, deconvolution suffers from certain drawbacks related to errors in the flow measurements and the intrinsic difficulties of the numerical inversion. An approximation is usually used as a simple alternative technique to produce results close to those that would have been obtained from deconvolution of the raw data. The approximation technique is applied to the rate-normalized pressure derived from the simultaneously measured flow and pressure data. The rate-normalized pressure p/q at any point in a test is determined by dividing the pressure change since the start of the test by the corresponding flow rate change.

Using rate-normalized pressure and its derivative curve makes it possible to conduct conventional flow regime identification—similar to that used during the analysis of data acquired with downhole shut-in tools. The difference is that the data are plotted in terms of p/q and $\partial(p/q)/\partial(\mathrm{SFRCT})$ versus t, where SFRCT is the sandface rate-convolution time function, which accounts for all flow rate variations during the transient. In the case of a buildup preceded by a single drawdown, this function is similar to the Horner time function except that it also accounts for flow rate change during the transient.

The rate-normalized pressure and pressure derivative obtained from the flow rate and pressure data in Fig. 33 are plotted in Fig. 35. Although this is the same data set as in Fig. 34, it has a sufficiently distinct shape that can be compared with type curves to guide the search for the reservoir model. In this case, the model is for a well in an elongated reservoir. This hypothesis was confirmed by geologic evidence that the reservoir is between two impermeable faults.

Once the model that suites the wellbore reservoir system has been identified using the deconvolution approximation, the interpretation proceeds to the quantification of model parameters such as k, s and the distance from the well to the nearest faults.

Parameter estimation

Initial estimates of the model parameters are determined in this stage of the analysis. The rate-normalized pressure data are again used in the same way as pressure data are for flow regime identification and computation of the well and reservoir parameters. Figure 35a shows the conventional type-curve match made between the rate-normalized pressure data and drawdown type curves.

In Fig. 35b the radial flow portion of the flow regime is similarly analyzed. A plot of the variations in the rate-normalized pressure against the SFRCT produces a straight line between 0.014 and 0.063 hr. From the slope and intersect of this line, the values of kh and s can be computed, similar to the analysis performed with generalized superposition plots. The next stage is to verify these preliminary results.

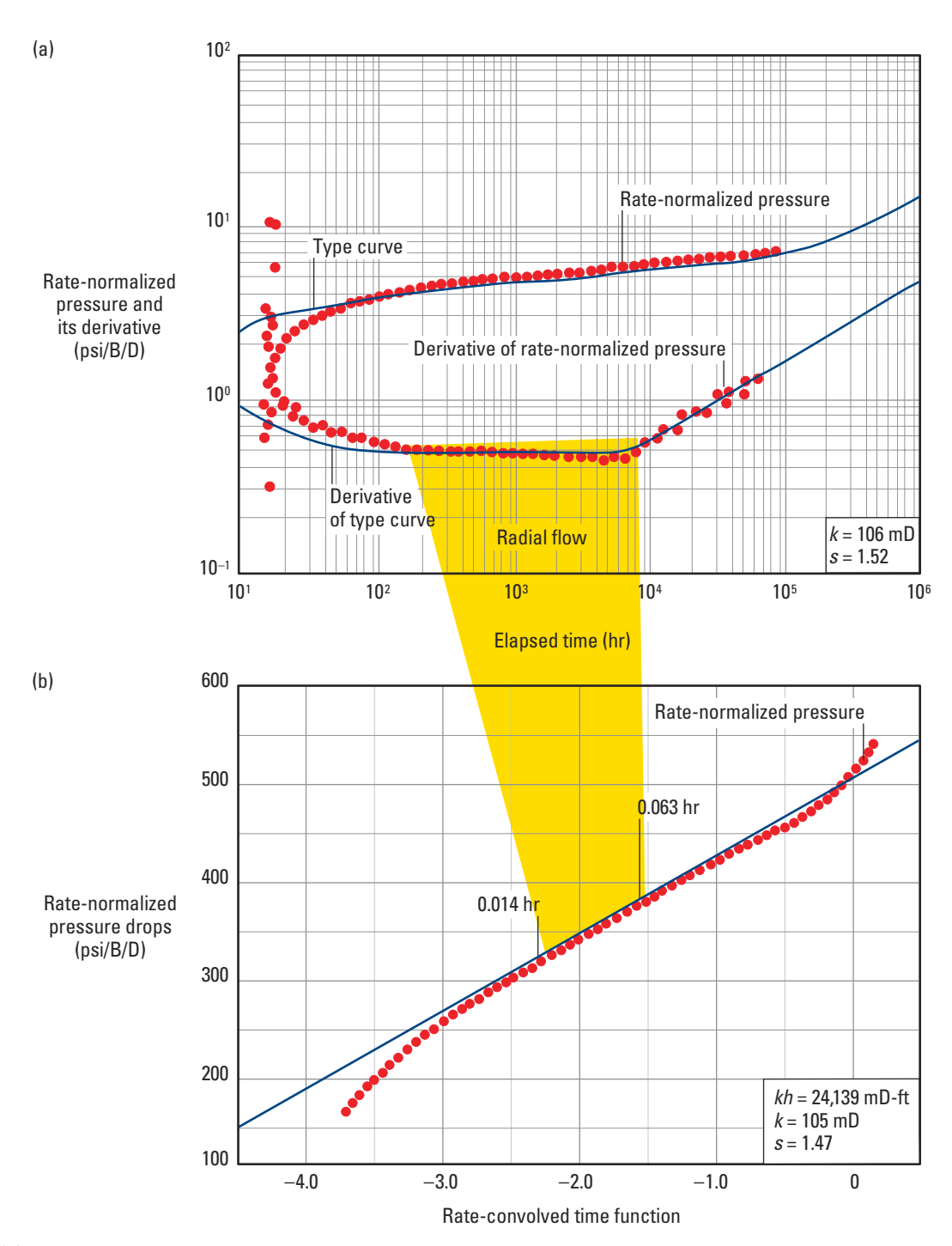


Figure 35. (a) Log-log plot of rate-normalized pressure and its derivative curve used for flow regime identification and type-curve matching analysis. This method is similar to that used for the analysis of data acquired at a constant flow rate. **(b)** Sandface rate-convolution plot of pressure data normalized with flow rate data versus a time function that accounts for all observed flow rate changes (Ayestaran *et al.*, 1988).

Model and parameter verification

With model and parameter information, it is a simple step to construct variable-rate type curves, which should closely match the raw pressure and pressure derivative data if the model and parameter estimates are correct.

To produce a variable-rate type curve, the model uses the actual flow history of the well. The measured flow rate during the transient is convolved with the selected model pressure response, and the effects of the flow rate changes before the test are added. The resulting curve has been called a convolution type curve (CTC). In reality, it is computed in the same manner as the forward model shown in the preceding "Results verification" section and should be called a history match. Figure 36 shows the information used in the construction of a CTC. The mathematical expression for the model response includes not only the flow rate variations before the transient test but also changes that occurred during the transient:

$$p_{wDC}(t_D) = \sum_{j=1}^{M} \left[\left(q_D \right)_j - \left(q_D \right)_{j-1} \right]$$

$$\times \left\{ p_{wD} \left[\left(T_M \right)_D - \left(T_{j-1} \right)_D \right] - p_{wD} \left[\left(T_M \right)_D + t_D - \left(T_{j-1} \right)_D \right] \right\}$$

$$= \int_0^{t_D} \Delta q_D'(\tau) \ p_{wD}(t_D - \tau) d\tau,$$

$$(7)$$

where

$$p_{wDC}(t_D) = \frac{\Delta p_{wbf} t}{-\mu q_r}$$

$$= \frac{\mu q_r}{2\pi b h}$$
(8)

and

 p_{wDC} = convolved dimensionless wellbore pressure

T = time starting with first flow rate

 q_r = constant surface flow rate.

The subscript M denotes the number of flow steps preceding the transient.

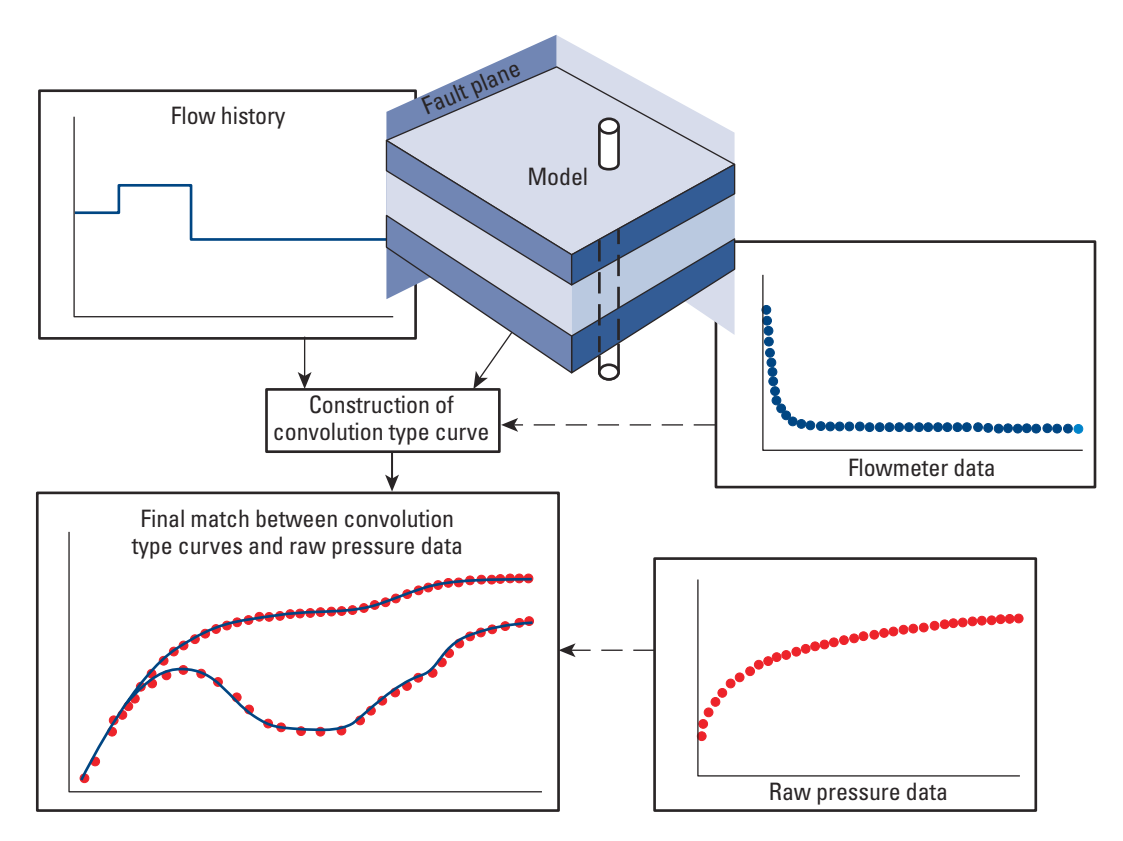


Figure 36. The construction of convolution type curves. Pressure is computed from flow rate data and from the theoretical pressure response (model) to a single-step rate change. The CTC accounts for all rate variations before and during the test (Ayestaran *et al.*, 1988).

Figure 37 is the CTC constructed for the example drawdown data set. The CTC and its derivative match the raw pressure and pressure derivative data almost perfectly. The flow rate and pressure data obtained using a production logging tool are extremely useful for analysis because they enable interpretation of the drawdown periods together with the pressure buildups.

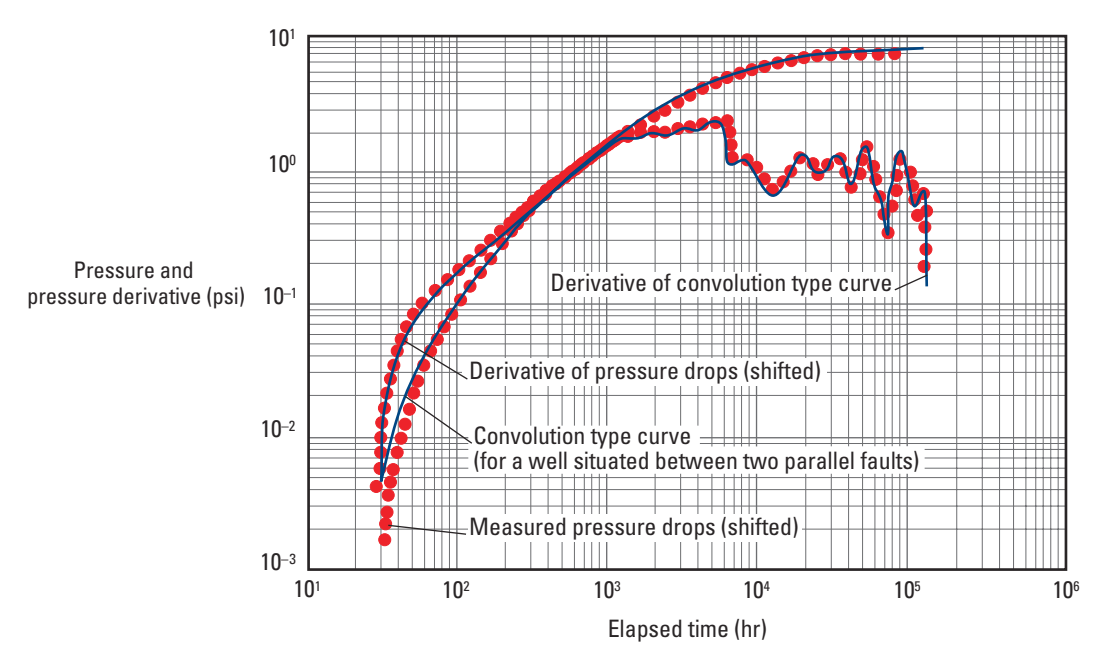


Figure 37. CTC and its derivative matched to the measured pressure response (Ayestaran et al., 1988).

Gas well testing

There are two main differences between gas well testing and liquid well testing. First, because gas properties are highly pressure dependent, some of the assumptions implicit in liquid well testing theory are not applicable to gas flow. Second, high gas velocity usually occurs near the wellbore and an additional pressure drop is caused by visco-inertial effects. The additional pressure drop is called the rate-dependent skin effect.

The variations of gas properties with pressure are accounted for by introducing the real gas pseudopressure function (Al Hussainy $et\ al.$, 1966)

$$m(p) = \int_{p_0}^{p} \frac{2p \times dp}{\mu(p) \times z(p)}$$
(9)

and the real gas pseudotime function (Agarwal, 1979)

$$t_{a}\left(p\right) = \int_{t_{0}}^{t} \frac{dt}{\mu \times c_{t}} = \int_{p_{0}}^{p} \frac{\left(\frac{dt}{dp}\right) \times dp}{\mu(p) \times c_{t}(p)},$$
(10)

where

 p_0 = arbitrary reference pressure

 t_0 = time corresponding to p_0

z = gas deviation factor.

All the equations used for gas well test analysis may be obtained from the liquid equations by replacing p with m(p) and t with t_a . Consequently, all the liquid solutions can be applied, and the techniques used for the analysis of oil well testing are applicable to gas well testing.

Analysis based on pseudopressure may be used for all ranges of pressure. However, simplifications can be made for certain limits. Although these limits are approximate, apply to certain temperature ranges and depend on gas properties, the following rules are usually valid:

- For pressures less than 2500 psi, the z product is constant and the pseudopressure m(p) is proportional to p^2 (Fig. 38a). The analysis can be performed using p^2 instead of m(p).
- For pressures greater than 3500 psi, the term z/p is constant and m(p) is proportional to the pressure. The analysis can be performed using p instead of m(p).

However, for pressures between 2500 and 3500 psi, no simplification can be made and the use of m(p) is mandatory.

If the pressure drawdowns are large, changes in the product c_t are important (Fig. 38b) and pseudotime must be used. For small pressure variations, however, the effect of changing gas properties is minimal and real time may be used.

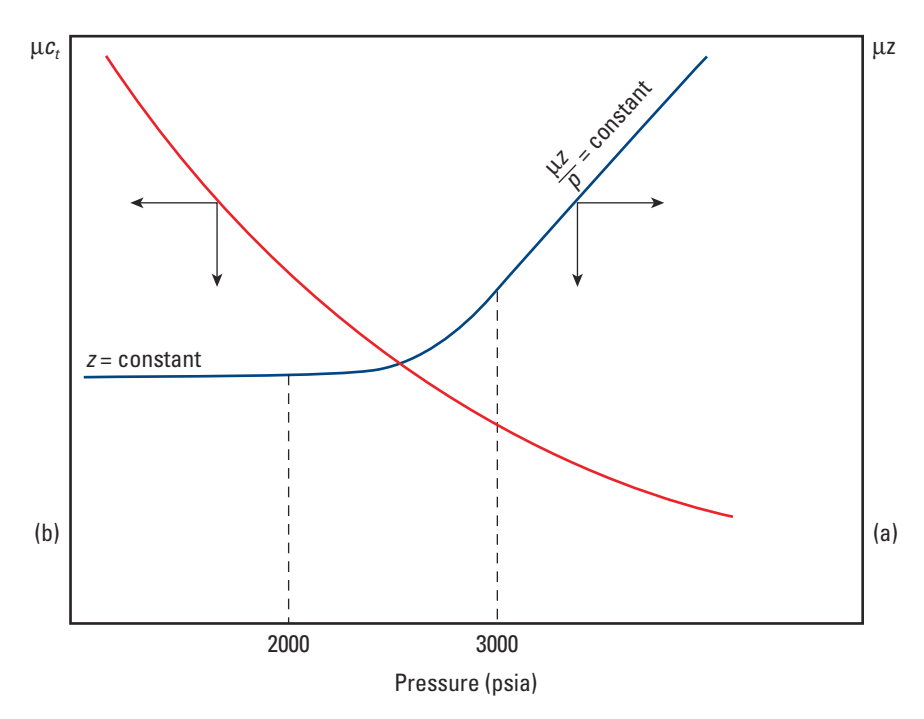


Figure 38. Typical pressure dependency of the viscosity—real gas deviation factor product (a) and the viscosity—total compressibility product (b).

For convenience, the pseudofunctions are normalized with reference to conditions at static reservoir pressure. The pseudopressure is expressed in dimensions of pressure, and the pseudotime is expressed in units of time. Figure 39 shows type-curve matching for a gas well test performed in an Oklahoma well. The log-log plot of the normalized pseudopressure variations versus normalized pseudotime changes has been superimposed on a computed model that includes variable wellbore storage. The reservoir parameters are obtained the same way as for oil wells, but with the appropriate units and corresponding conversion factors.

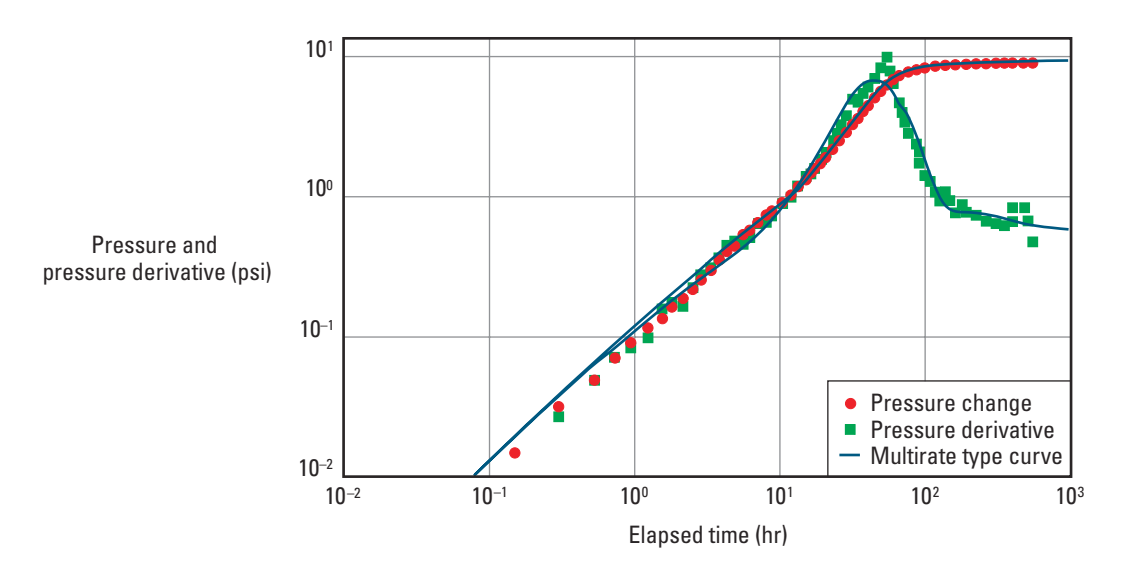


Figure 39. Type-curve match for a pressure data set from a gas well test (Hegeman et al., 1993).

The second problem posed by gas wells is addressed by multipoint well testing. In a conventional well, the additional pressure drop induced by high gas velocities, together with the one caused by formation damage, is manifested as a high skin factor. To distinguish between these two effects, gas wells are usually tested with a sequence of increasing flow rates. Theoretically, two transients are sufficient to separate the two skin effects, but in practice a multipoint test is usually conducted. The value of s is determined for each transient, and a plot similar to the one shown in Fig. 40 yields the formation damage skin or true skin effect.

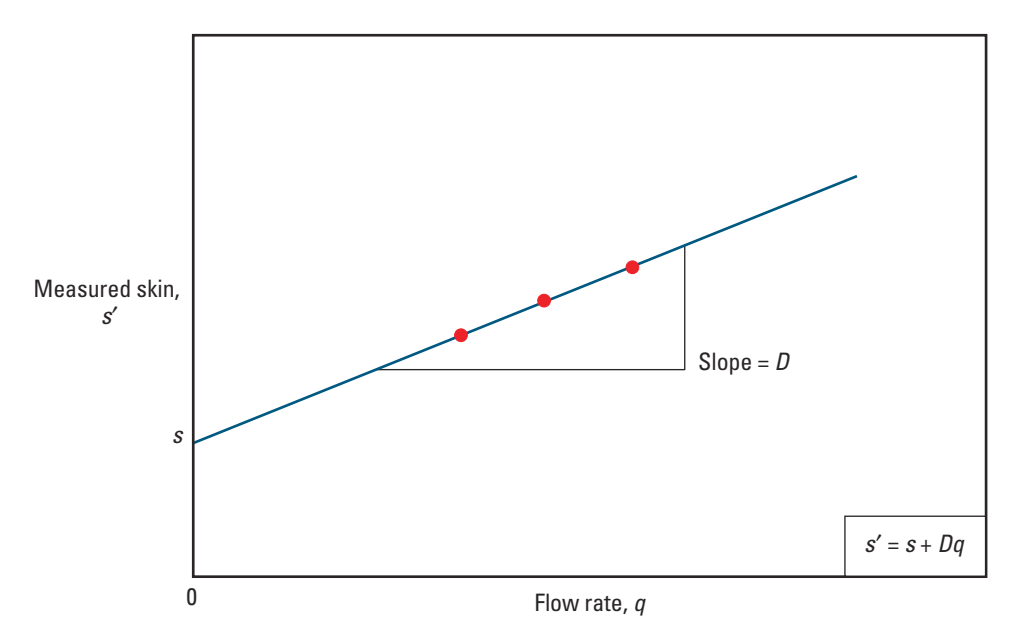


Figure 40. Measured skin effect versus flow rate in a multirate transient test. The slope of the curve is called the non-Darcy coefficient and indicates the inertial effects occurring near the wellbore. The intercept represents the skin effect resulting from formation damage.

Multipoint or backpressure tests are conducted not only to estimate the true skin effect but also to determine deliverability curves and the potential absolute open flow (AOF). Deliverability curves are used to predict flow rates against values of backpressure. For gas wells the relationship between rate and bottomhole pressure is given by the so-called backpressure equation:

$$q = C \left(p_{ws}^{2} - p_{wf}^{2} \right)^{n}, \tag{11}$$

where

C = performance coefficient p_{ws} = bottomhole shut-in pressure p_{wf} = wellbore flowing pressure n = inertial effect exponent.

Deliverability curves can also be used for determining the number and location of wells in a field, designing compressor requirements and establishing base performance curves for future comparisons.

The AOF of a well is defined as the rate at which a well would produce at zero sandface pressure. Although this rate cannot be achieved, regulatory authorities use it to set maximum allowable rates.

Backpressure tests are usually conducted with an increasing rate sequence. However, gas well test sequences vary according to stabilization times. High-productivity formations are usually tested with a four-point backpressure test, commonly called a flow-after-flow test. In this test, the well is flowed at four different stabilized flow rates for periods of equal duration. At the end of each flow period, the rate is changed without closing the well (Fig. 41A).

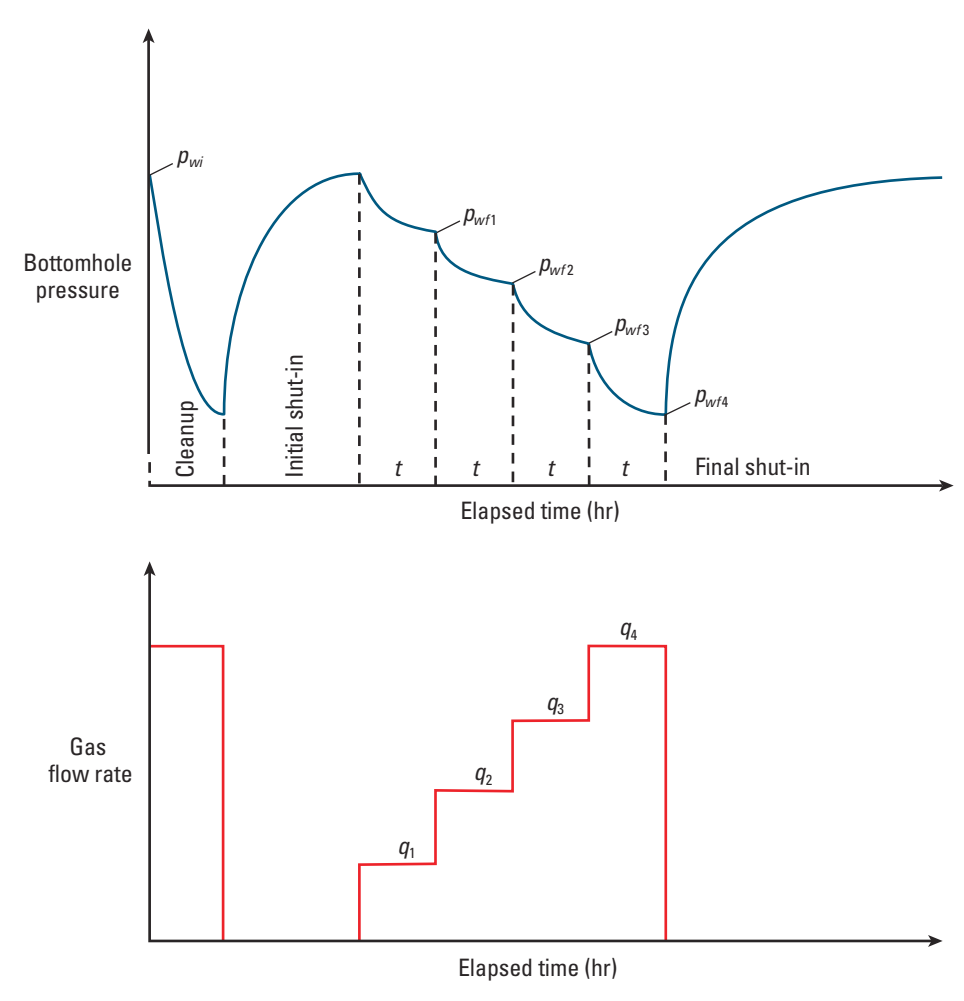


Figure 41A. Schematic of rate sequence and pressure variations in a flow-after-flow multipoint test. p_{wi} = initial wellbore pressure.

Schlumberger Schlumberger

In low-productivity formations stabilization times can be too long, so an isochronal test is preferred to a flow-after-flow test. In an isochronal test, the well is flowed at four or more different rates for periods of equal duration. Between flow periods, the well is shut-in until static conditions are reached. The last flowing period is extended until stabilized flowing conditions are reached (Fig. 41B).

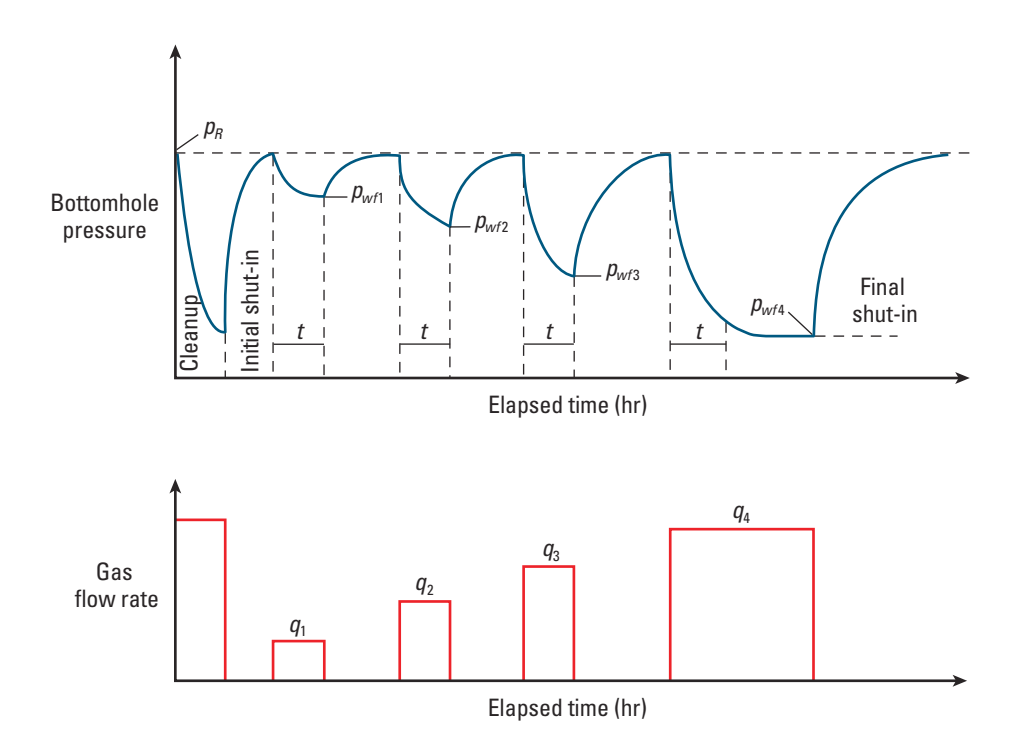


Figure 41B. Schematic of rate sequence and pressure variations in an isochronal multipoint test. p_R = reservoir pressure.

In practice, the true isochronal test is usually replaced by a modified test sequence with flow and shut-in periods of equal duration. The modified isochronal test is faster because it is not necessary to wait for stabilization. Like the isochronal test, however, the last flowing period is extended until stabilization is reached (Fig. 41C). This test is called a modified isochronal test.

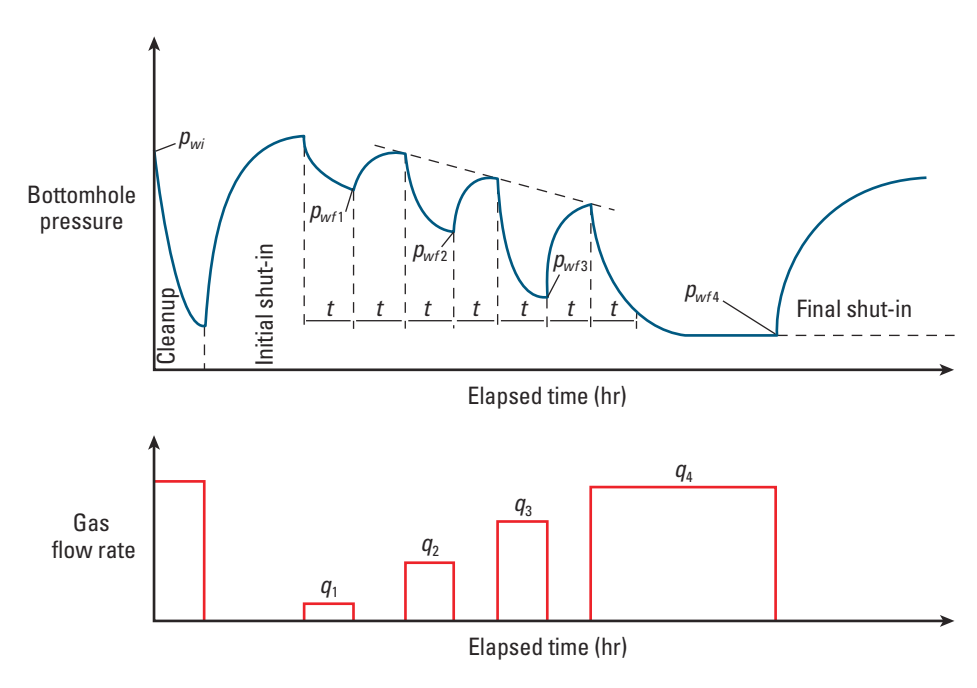


Figure 41C. Schematic of rate sequence and pressure variations in a modified isochronal multipoint test.

The results of backpressure tests are conventionally presented as log-log plots of $(p_{ws}^2 - p_{wf}^2)$ versus flow rate. The resulting straight line is used to obtain the exponent n, which varies between 0.5 (high inertial effects) and 1 (negligible inertial effects). For isochronal or modified isochronal tests the resulting curve is termed the transient deliverability curve. The stabilized curve is drawn through the extended data point using a line parallel to the transient deliverability curve. The modified isochronal test does not yield a true stabilized deliverability curve but rather a close approximation. Figure 42 shows a log-log plot for a modified isochronal test.

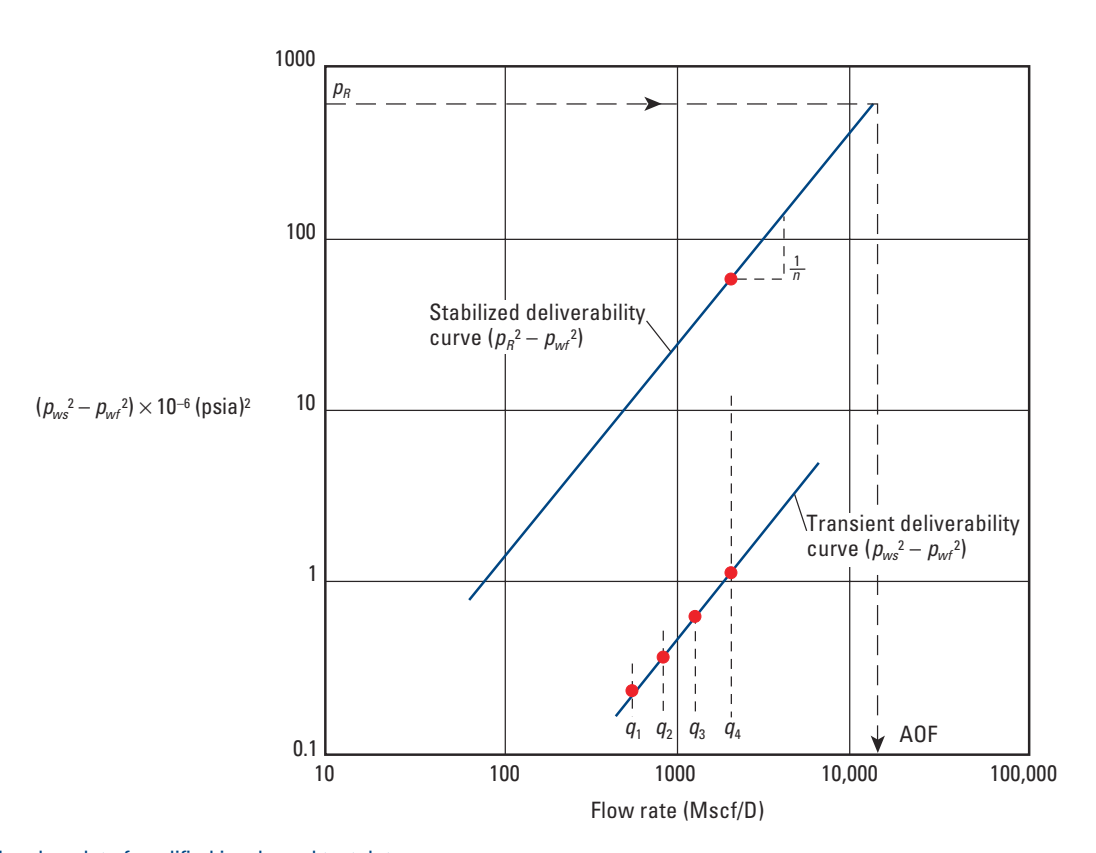


Figure 42. Log-log plot of modified isochronal test data.

Specialized Test Types

This chapter reviews specialized pressure transient tests for testing layered reservoirs and horizontal wells, multiple-well testing, vertical interference, and combined perforation and testing techniques. Testing low-energy wells, water injection wells and sucker-rod pumping wells is also included.

Layered reservoir testing

Most of the world's oil fields comprise layers of permeable rock separated by impermeable or low-permeability shales or siltstones. Each layer may have different pressure and reservoir properties (Fig. 43A). Testing all the layers simultaneously cannot determine individual layer parameters, as explained in Fig. 43B. Therefore, special testing techniques must be applied to obtain the parameters of individual layers. One way to test wells in layered reservoirs is to physically isolate each layer before performing conventional tests in it (e.g., straddle DST jobs). A rig is required, and the testing may be prohibitively expensive. A cost-effective alternative, which eliminates the need for a rig, consists of separating the layers "implicitly" using a production logging tool.

There are two rigless testing techniques for layered reservoirs. Selective inflow performance (SIP) tests are performed under stabilized conditions and are suitable for medium- to high-permeability layers that do not exhibit crossflow within the reservoir. The other test is conducted under transient conditions and is known as layered reservoir testing.

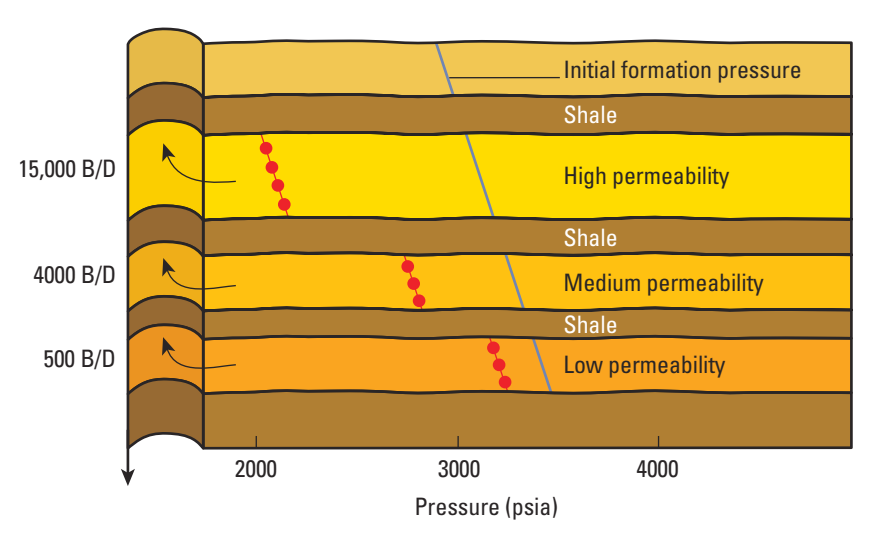


Figure 43A. Pressure profile showing differential depletion of up to 800 psi between layers. The most permeable layer has the greatest depletion because it has the largest cumulative production. In this reservoir, crossflow will develop when the well is shut in.

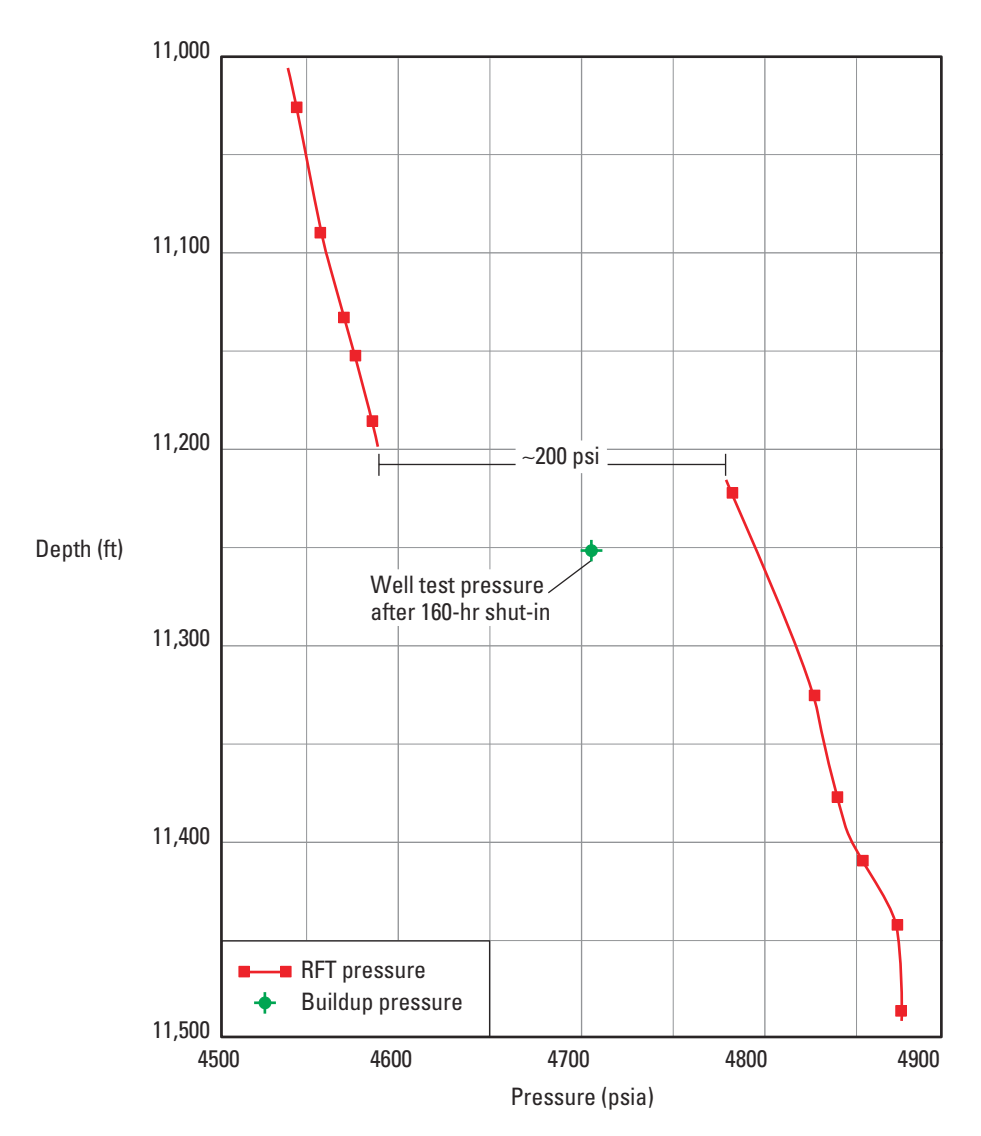


Figure 43B. Comparison of a spot pressure profile with formation pressure obtained using a well test. The pressure values from the transient well tests do not represent those of the top or bottom layers because of crossflow. The well test pressure tends to be close to the pressure of the most permeable layer.

Selective inflow performance

The SIP test provides an estimate of the inflow performance relationship curve for each layer. Measurements are made with a production logging tool, which records the bottomhole pressure and flow rate simultaneously. The SIP test is run by putting the well through a stepped production schedule with various surface flow rates (Fig. 44a). The bottomhole pressure changes follow the pattern shown in Fig. 44b. The production logging tool is used to measure the bottomhole pressure and obtain a flow profile at the end of each flow step. From the production profile, the flow rates of the individual layers can be determined. Figure 45 shows an example of a flow profile in a layered reservoir. An inflow performance relationship (IPR) curve can be constructed for each layer using the data from all the flow profiles: $p_{wf}(i,j)$ and q(i,j) for i=1 to L and for j=1 to F, where L is the number of layers and F is the number of flow steps.

Schlumberger

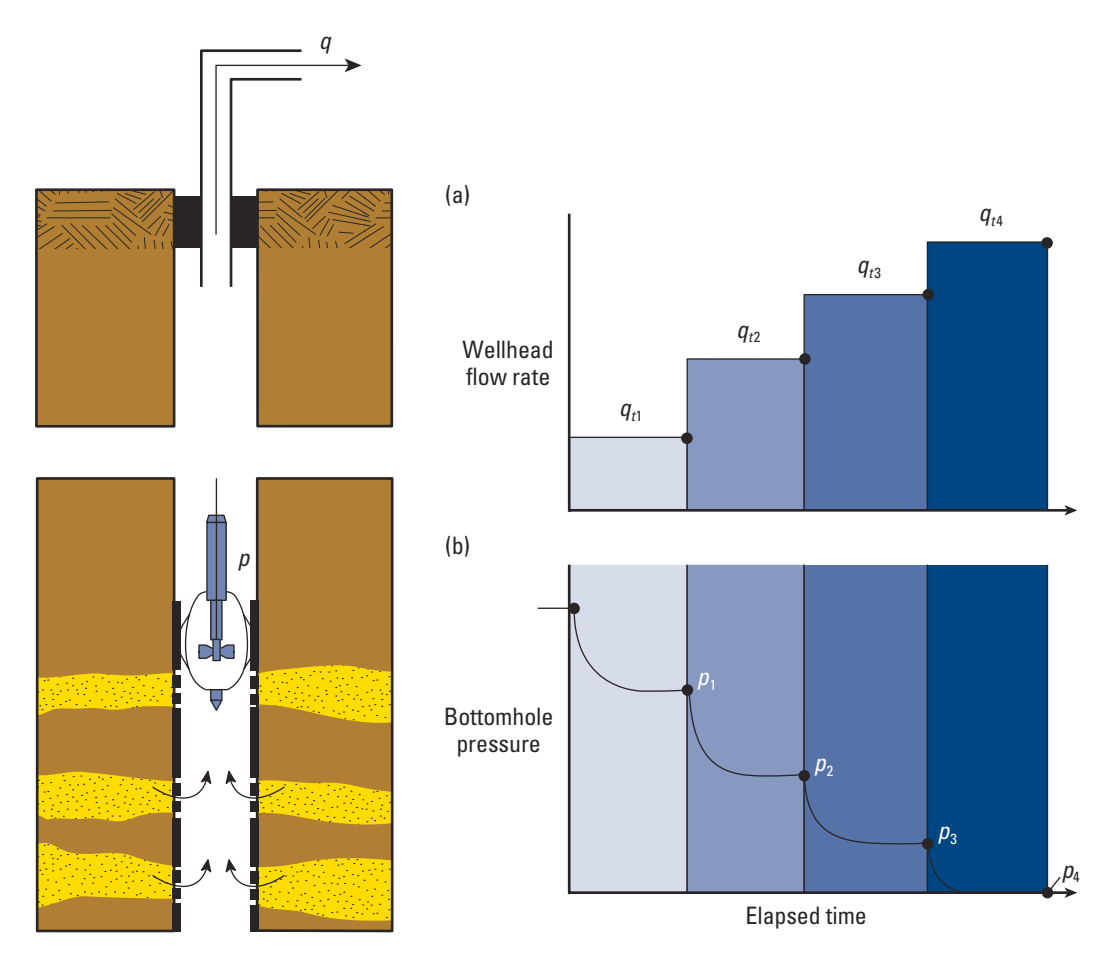


Figure 44. Surface flow rate history (a) and associated changes in bottomhole pressure (b) during an SIP test. q_t = total flow rate.

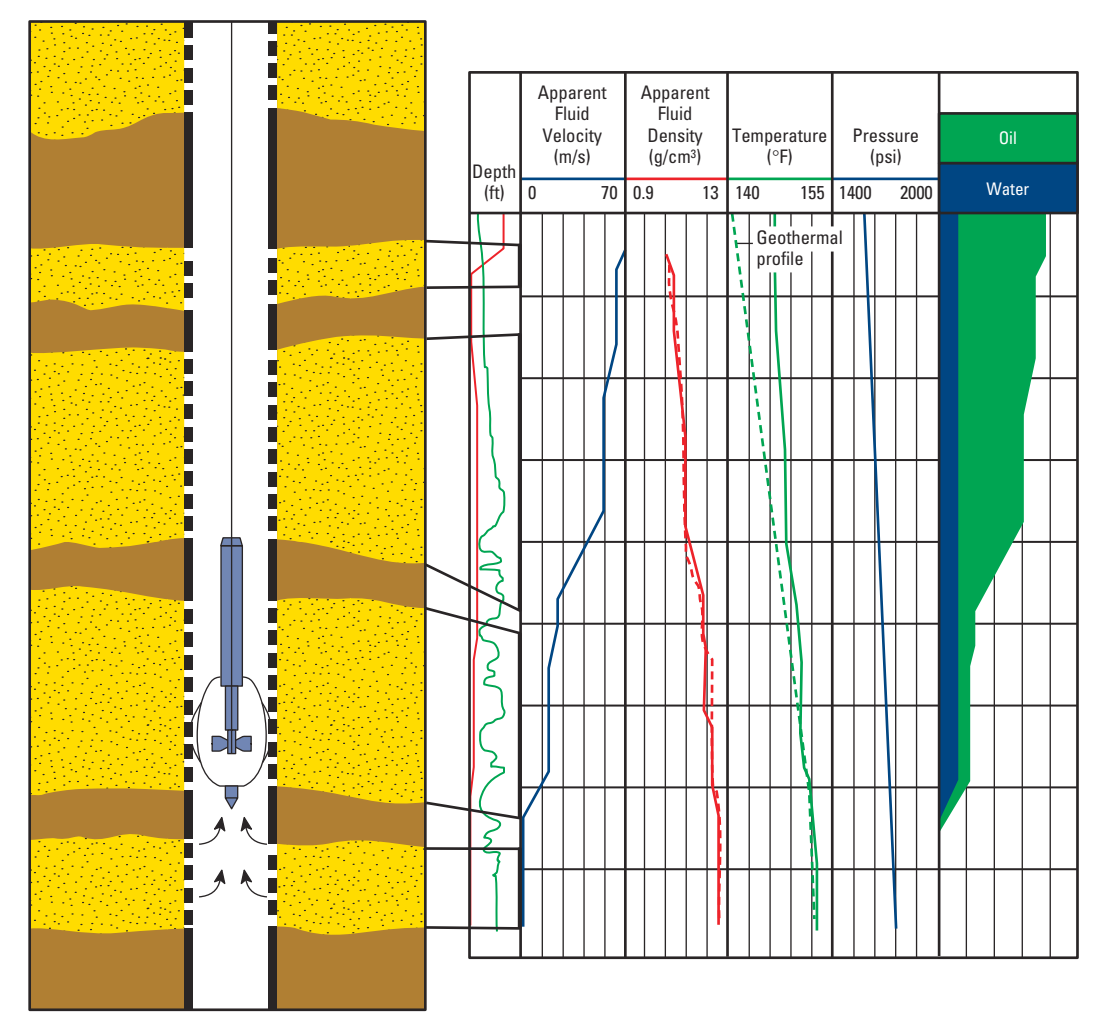


Figure 45. Typical flow profile acquired in a multilayered reservoir.

Figure 46 is an SIP plot from a well that produces from a four-layer reservoir. The SIP survey was conducted using six flow steps. The shape of the IPR curves is characteristic of oil wells that flow below bubblepoint pressure or, alternatively, that have rate-dependent pressure drops. The static pressure of each layer can be estimated from the point at which the IPR curve of the layer intersects the vertical axis. This estimate is valid provided that the flow steps during the SIP survey are sufficiently long to ensure that at the end of each step the pressure drop stabilizes both in the layer and within the well drainage area.

SIP tests provide the formation pressure and IPR for each layer but do not give unique values of k and s for an individual layer. A transient test is required to determine those parameters.

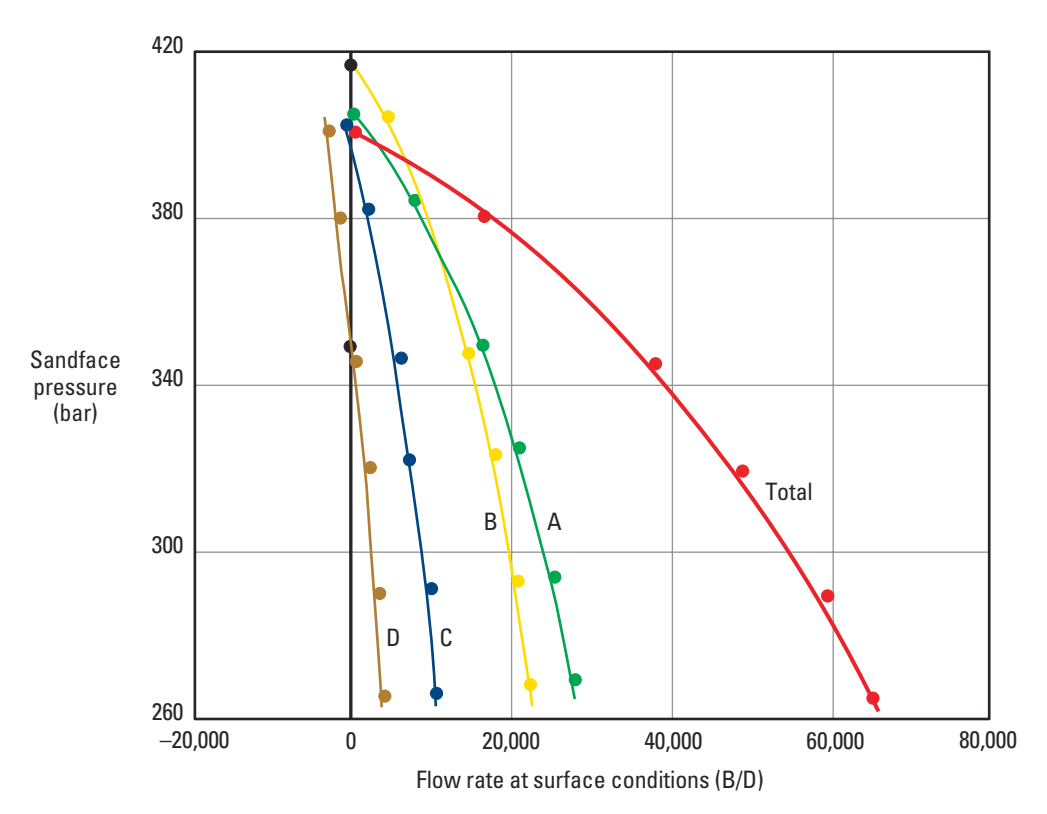


Figure 46. IPR curves of a multilayered reservoir showing uneven depletion between layers. The pressure is highest in layer B and lowest in layer D.

Transient layered testing

Layered reservoir tests differ from SIP tests in that, in addition to the acquisition of a flow profile, the downhole pressure and flow rate are simultaneously recorded versus time during each flow period. These measurements are obtained with the tool stationed at selected locations—between layers and above the topmost layer—which implicitly separates the layers.

The LRT procedure uses a continuous recording of the bottomhole pressure, whereas the rate per layer is measured only at discrete time intervals. During the first transient, only the bottom-layer flow rate is measured. Flow rate changes in all layers above the bottom one cannot be measured directly because the flowmeter sensor measures the combined flow from all the layers below the tool.

The LRT test requires careful planning and rigorous wellsite logging procedures because of the numerous events that occur during the test. The tool must be equipped with sensors that can monitor flow rate, pressure, density and temperature. In addition, changes in flow rates are critical and must be controlled precisely using fixed choke sizes.

Low flow rates generally occur during the survey of the bottom layers, while recording the afterflow during a buildup and when investigating crossflow during the final buildup. The survey must be conducted using surface recording equipment that enables real-time test follow-up and data quality control. This procedure is particularly critical in LRT operations because it is often necessary to adjust the original test program according to the well's behavior.

Figure 47 shows a simplified job sequence. For a two-layer test, the flowmeter is stationed at only two locations: station 1, above the topmost layer, and station 2, between the two layers. The green line is the trajectory of the production logging tool. The top and bottom graphs show the behavior of the wellhead flow rate and bottomhole pressure and flow rate, respectively.

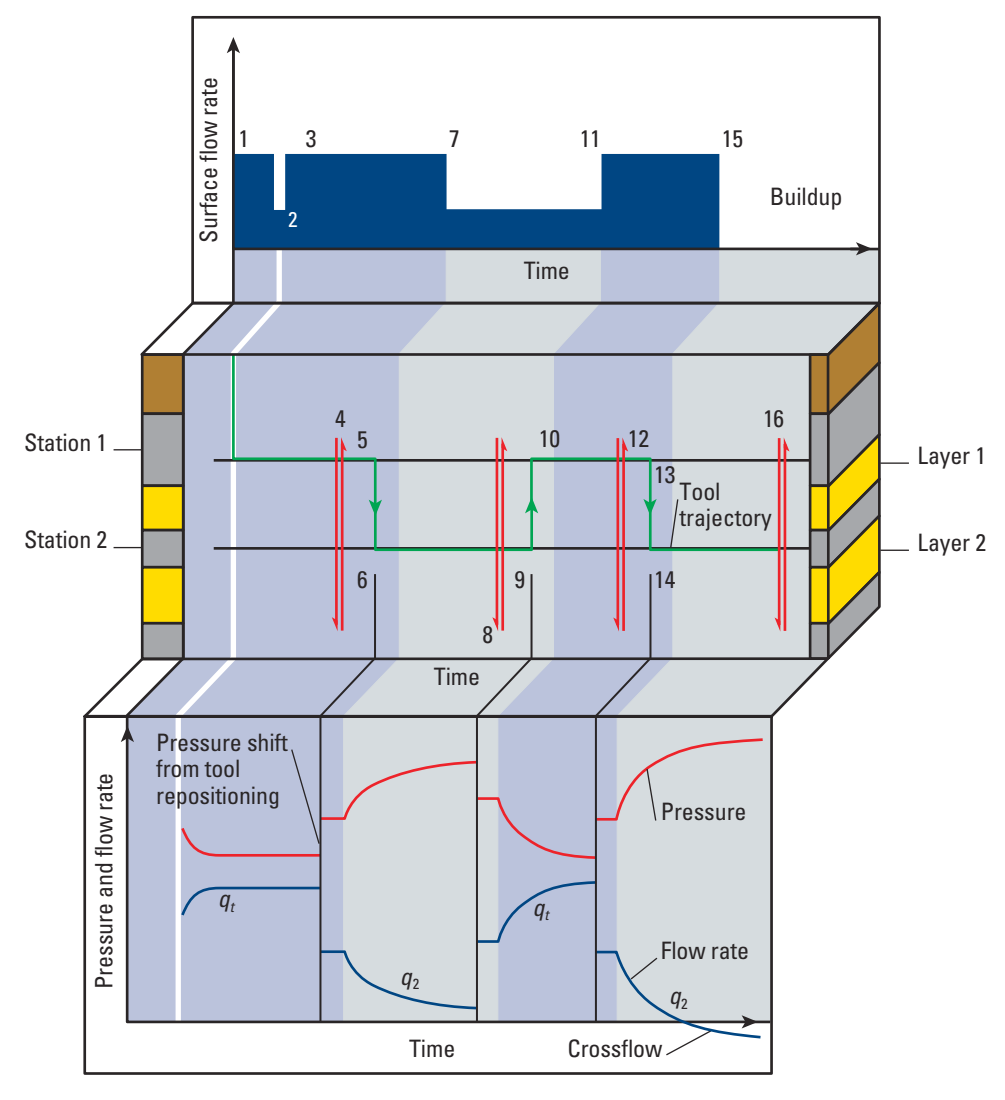


Figure 47. Simplified layered reservoir test sequence.

Interpretation of layered reservoir testing

Interpreting layered reservoirs is complex because it not only involves identification of the reservoir model but also requires the estimation of a large number of unknown parameters such as the values of k and s and the reservoir geometry and pressure for each layer. For example, a simple three-layer reservoir has at least nine unknowns (permeability, skin effect and pressure for each layer) in addition to the task of model identification. For these reasons, LRT interpretation relies heavily on techniques that indicate the reservoir model and initial parameter values, which are necessary input for the history-matching process used for interpretation.

The first step is preparation of the data to a suitable form for interpretation. Pressure values are referred to the same datum to remove gravity effects. Once this is done, the pressure potential plot becomes a continuous curve— a useful feature for subsequent history matching.

LRT interpretation is conducted by seeking a match between the behavior of the reservoir and the modeled response. The model has as many individual layers as tool stations used during the test, and each layer model can be different. The total reservoir response is calculated by stacking the single-layer models. The three stages for analyzing a single-layer test—model identification, parameter estimation, and model and parameter verification—are also followed during LRT interpretation.

Sequential analysis

The simplest approach to identifying reservoir geometry is to start by examining the response of the bottom layer. When the production logging tool is stationed at the top of the bottom layer, it measures only the flow rate changes induced in the bottom layer. Thus, interpreting the response of the bottom layer is a single-layer interpretation problem. As with single-layer drawdown tests, the reservoir model and the dominant flow regimes must first be identified.

The first step is to calculate the pressure and flow rate changes that occur after the stabilized trend is established and to generate an approximate flow history of the layer. The pressure values are then normalized using the corresponding flow rate changes. A log-log plot of the rate-normalized pressure change and its derivative with respect to the SFRCT function is used to identify the model and flow regime. The relevant reservoir parameters are then calculated using specialized interpretation plots.

■ Initial parameter estimation for the remaining layers

Once a satisfactory model of the lowest layer is established, the interpretation proceeds with the next layer above it. During this transient, the measured flow rate is the cumulative total of the two layers.

Under these circumstances, analysis of the cumulative flow rate and wellbore pressure provides a close estimate of the "average" values of k and s for the two-layer system. Initial estimates of the reservoir parameters k_i and s_i for next-to-lowest layer can easily be computed from the following relationships:

$$kh_{ave} = k_i h_i \tag{12}$$

$$s = \frac{s_i q_i}{q_t}, \tag{13}$$

where

 kh_{ave} = average permeability-thickness product

s = measured pseudoskin

 q_t = total flow rate

and i varies from 1 to the number of layers.

The sequential analysis continues until all the layers are included in the interpretation process. In a three-layer reservoir, this method uses a three-layer model to estimate the parameters of the newly added top layer. The analyst assumes that the parameters for the two lower layers are known and searches for the parameters of only the new layer, and so on.

The disadvantage of this method is that errors are propagated as the bottom-up analysis progresses, but these errors may be corrected during the simultaneous history matching performed in the final stage of LRT interpretation.

Verification of the model and its parameters— simultaneous history matching

Once the model is identified and an initial estimate of the parameters is available, the next stage is the simultaneous history-matching process. In this procedure, the pressure history is used as the boundary condition and history matching is conducted by reproducing the observed flow rates.

It is also valid to use downhole or surface flow rates as the boundary condition and then match the pressure history. The use of pressure or surface flow rate measurements as the boundary condition has the added advantage of providing a continuously measured boundary condition during the intermittent recording of downhole flow rates.

The following example corresponds to a severely faulted field, crossed by volcanic dikes that create reservoir compartments, the extent of which is difficult to evaluate because of the poor quality of the seismic data. Before embarking on a waterflooding project, the operator needed insight into the extent of the compartments and the parameters that control the reservoir dynamic response.

LRT was conducted in a representative well to determine the layer pressures and properties and define the geometry of the fault block in which the well is situated. The reservoir has four layers, and the test was composed of five transients. As a result of the test, values of kh, s and formation pressure were obtained for all four layers. Furthermore, the test indicated that the well is located in a channel and established the width of the channel and the location of the nearest boundary to the well.

Flow rate history matching was performed using the measured pressure as the boundary condition. Figure 48A is a comparison of the simulated flow profiles and the vertical fluid flow distribution observed with the production logging flowmeter at the end of each transient. Figure 48B shows the flow rate versus time match. The quality of both matches—against depth and time—indicates that the selected model and its parameters properly describe the dynamic behavior of the tested reservoir compartment.

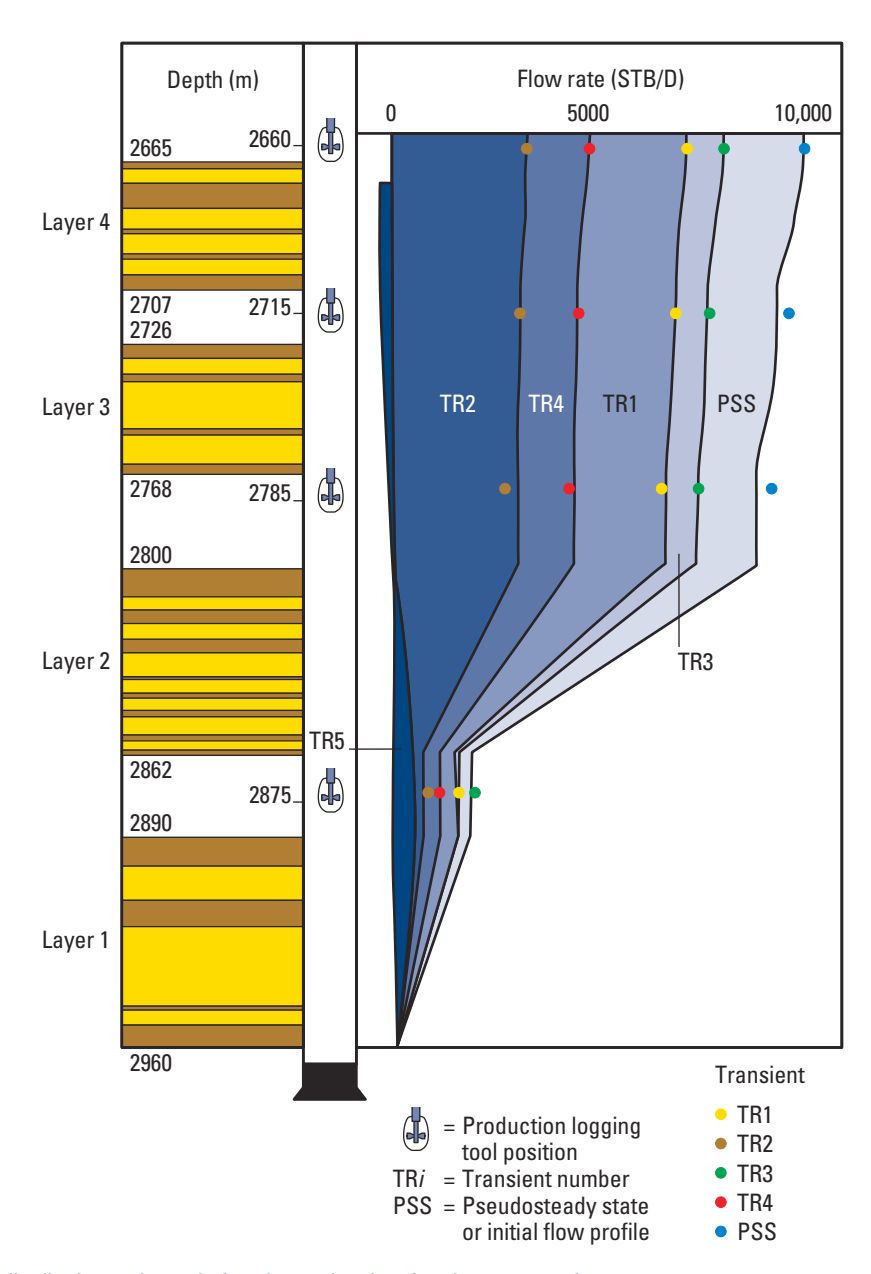


Figure 48A. Fluid flow distribution at the end of each transient in a four-layer reservoir.

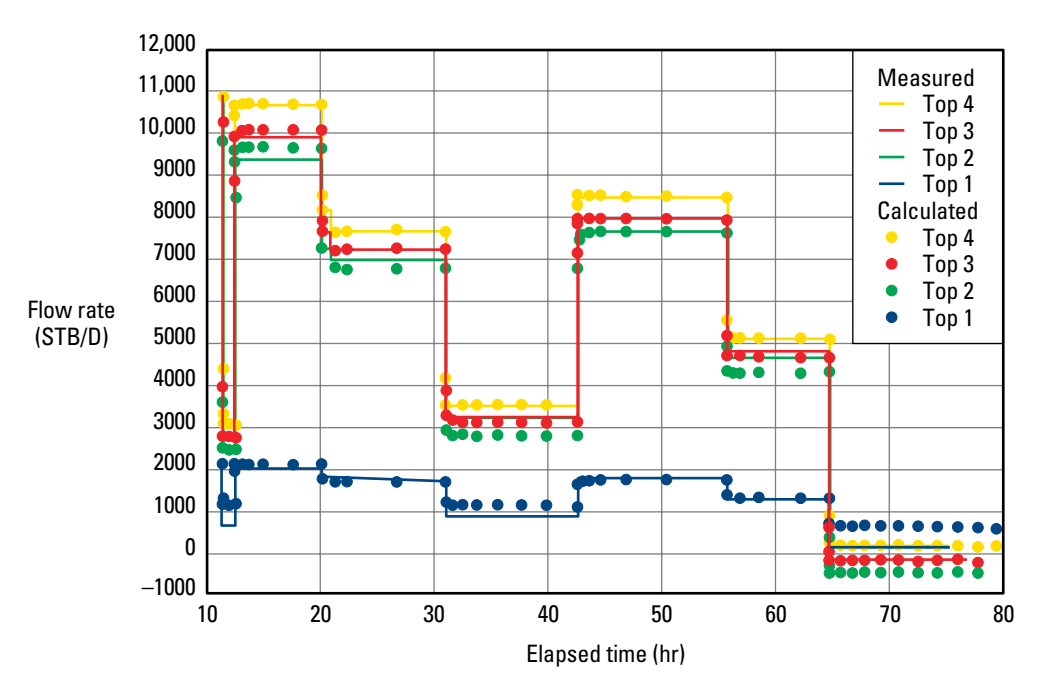


Figure 48B. Flow rate match using the measured pressure as the inner boundary condition.

Horizontal wells

With the significant increase in horizontal drilling activity during recent years, pressure transient behavior in horizontal wells has received considerable attention. In this section, the specific flow regimes developed during a horizontal well test and the interpretation methodology used are briefly described and illustrated with a field example.

Pressure transient behavior in a horizontal well test is considerably more complex than in a conventional vertical well test because of its three-dimensional nature. In a horizontal well, instead of the radial flow regime that develops for a conventional test, three flow regimes may occur after the effects of wellbore storage disappear.

Figure 49 shows the different phases in a horizontal well transient test. Initially flow occurs radially in a vertical plane toward the well, indicated by a plateau on the derivative curve of the log-log plot. This regime is termed early-time pseudoradial flow because of the elliptical flow pattern resulting from the vertical to horizontal permeability anisotropy. The second flow regime begins when the transient reaches the upper and lower boundaries of the producing interval and flow becomes linear toward the well within a horizontal plane. This intermediate-time regime is characterized by a half-slope trend in the derivative curve. The third flow regime occurs as the transient moves deeper into the reservoir and the flow becomes radial again, but in the horizontal plane. This late-time regime is indicated by a second plateau in the derivative curve.

The first radial flow regime yields the mechanical skin factor and the geometric average of the vertical and horizontal permeabilities. The intermediate-time linear flow regime can be analyzed to estimate the length of the producing interval, as long as the horizontal plane can be considered isotropic. The late-time radial flow yields the average permeability in the horizontal plane and the total skin factor (mechanical and geometrical skin factors).

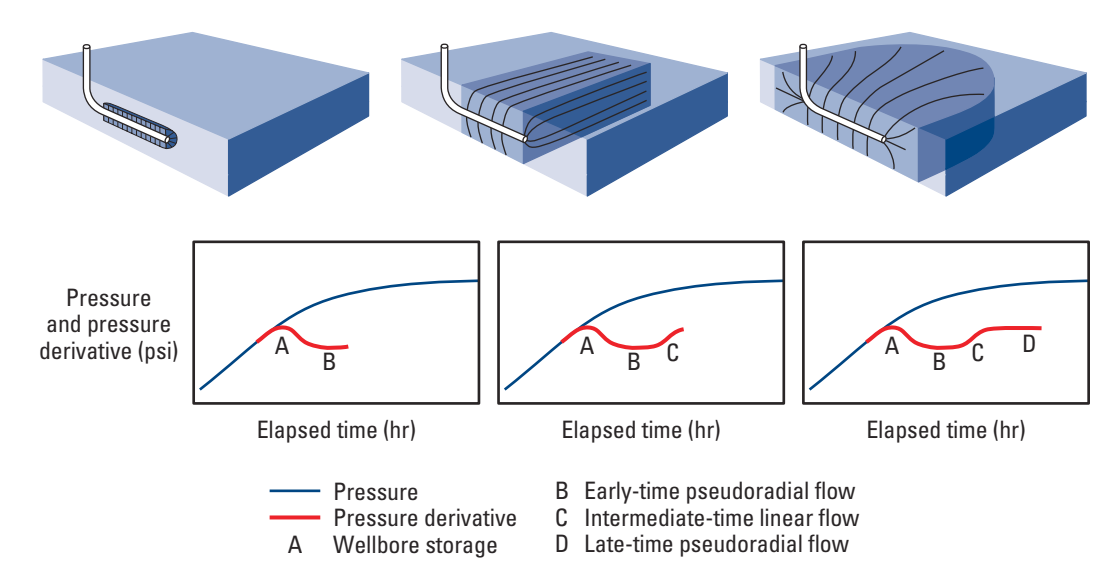


Figure 49. Phases in a horizontal well transient test. After wellbore storage effects have disappeared, the flow is radial toward the well in the vertical y-z plane (first plateau in the derivative curve). The next phase is linear flow in the y-z plane (straight line with half-slope in the derivative curve). Finally flow is radial in the x-y plane (second plateau in the derivative curve).

The geometrical skin factor is important for horizontal wells drilled in thick formations or in formations that exhibit a high contrast between kh and kv. Furthermore, in these circumstances neither the early-time flow regime nor the linear one develops (Fig. 50).

The identification of the first pseudoradial flow is crucial for a complete interpretation because it provides the formation damage. This regime is often masked by the unavoidably large wellbore storage effects in horizontal wells. The key to successful horizontal well testing is full control of the downhole environment. Full control can be achieved by using simultaneous measurements of flow rate and either pressure or downhole shut-in or both. Moreover, the identification of all three flow regimes is not always possible from one transient. Combining drawdown tests in which the flow rate and pressure are measured simultaneously with buildup tests using downhole shut-in maximizes the likelihood of identifying all three flow regimes.

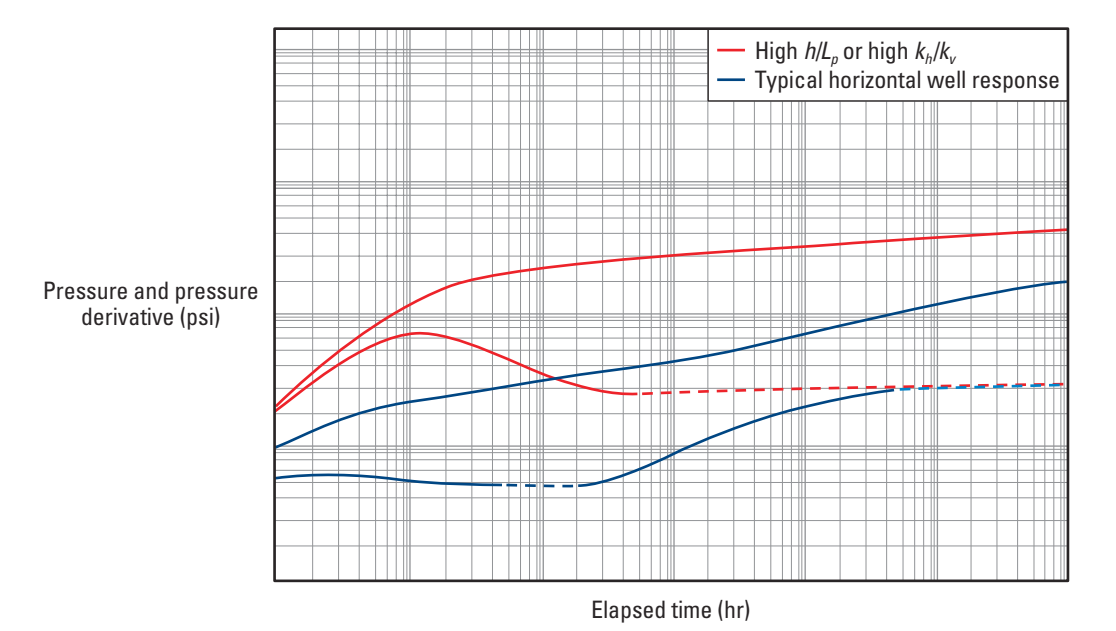


Figure 50. Theoretical pressure response of a horizontal well drilled in a thick reservoir or in a reservoir with high vertical to horizontal permeability anisotropy. $h/L_p = \text{ratio of reservoir height to length of the horizontal well perforated interval.}$

Supplementing the transient test data with flow profiles along the trajectory of the horizontal well facilitates identifying the producing zones and determining the effective flowing interval. Deriving this parameter from the transient data is more complicated because, in addition to the inherent wellbore storage difficulties, other parameters may also be determined from a horizontal well test: wellbore storage coefficient, vertical permeability, maximum and minimum horizontal permeabilities, standoff from the nearest bed boundary, effective flowing length and skin effect. This list can be reduced by running tests in the pilot hole before going horizontal to determine the geometric means of k_h and k_v . These parameters are crucial for estimating horizontal well productivity and have a major influence on the decision whether to drill the well.

Flow profiles are also extremely valuable for pinpointing possible crossflow. Crossflow is more likely to occur during buildup tests and may seriously jeopardize the interpretation. Therefore, drawdown tests are recommended for developed fields where pressure differentials have already developed and may induce crossflow.

The interpretation of horizontal well test pressure measurements involves the same three stages used for vertical well test analysis. First, the pressure response and its derivative are analyzed to diagnose the characteristic behavior of the system and identify specific flow regimes. Second, specialized plots are used to extract the effective parameters for each flow regime, typically the values of k and s. Third, these reservoir parameter estimates are refined by history matching the measured transient response to that predicted by a mathematical model for the well and reservoir system.

As always, history matching is expected to produce more accurate results because the features of the various flow patterns are rigorously taken into account. Moreover, the match involves the entire set of transient data, including transition periods between specific flow regimes, whereas direct analysis uses only the data subset of identifiable flow regimes. This stage also offers the possibility of simultaneously matching more than one transient, which further constrains the model to accurately represent the well and reservoir system.

The following example illustrates the importance of analyzing both the buildup and drawdown periods during which simultaneous downhole rate and pressure measurements are obtained. Figure 51 shows the comparative log-log plot of both transients from a drawdown and buildup test conducted in a well in India. The data are noisy and do not display sufficient character to indicate a unique solution, but knowing that these data were acquired in a horizontal well makes a reasonable flow regime identification feasible. The derivative and convolution derivative curves in Fig. 51 exhibit plateaus that suggest the existence of two pseudoradial flow regimes. The first plateau, indicative of early-time pseudoradial flow, is visible only in the convolution derivative of the drawdown transient. This plateau should also have developed during the buildup, but it is masked by wellbore storage. On the other hand, the second plateau is visible only in the derivative curve of the buildup, which lasted long enough for radial flow to develop. Between these plateaus, the derivative curves of both transients exhibit slopes close to a half-slope trend, indicating the presence of linear flow.

Analysis of these individual flow regimes yielded values for the vertical and horizontal permeabilities and mechanical skin factor. These parameters were refined by history matching both transients with the response of a horizontal well model. For the buildup period, the pressure and pressure derivative were history matched using downhole flow rates as input to the model. For the drawdown period, the measured pressure was used as the boundary condition and the match was performed on the measured downhole flow rate. As shown in Fig. 52, the good quality of the resulting matches gives confidence in the estimated values of the reservoir parameters and supports the conclusion that they are representative of the formation. Furthermore, these results compare well with those obtained from a long-duration pressure buildup test conducted in the well more than a year later.

The information obtained from this horizontal well test analysis enhanced the operator's knowledge of the reservoir, which was used to improve the design of future horizontal wells in the field.

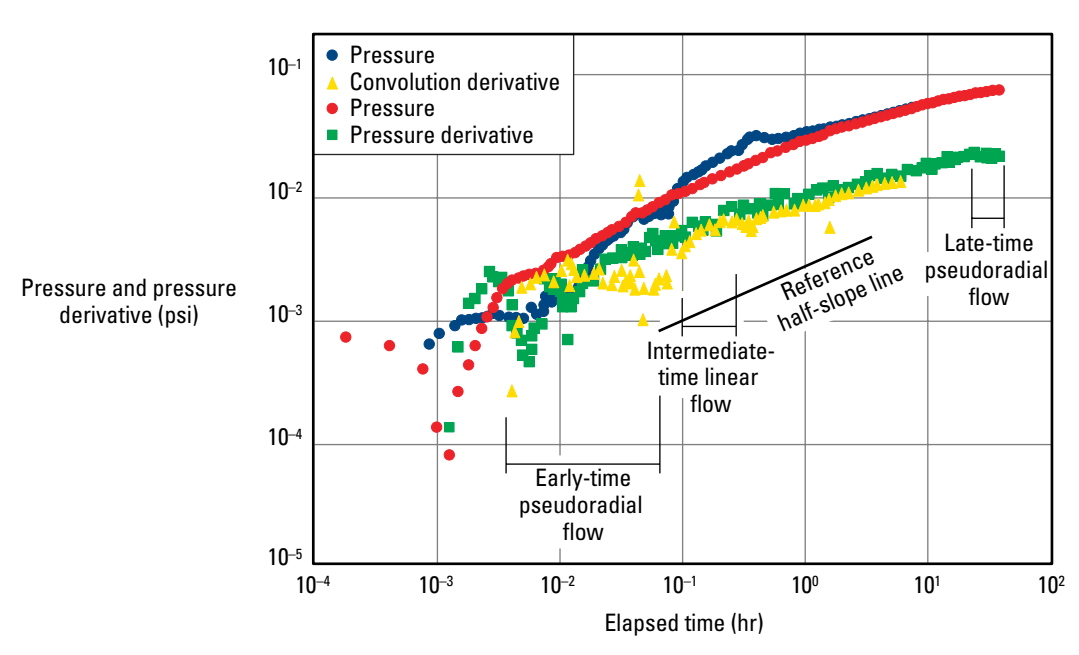
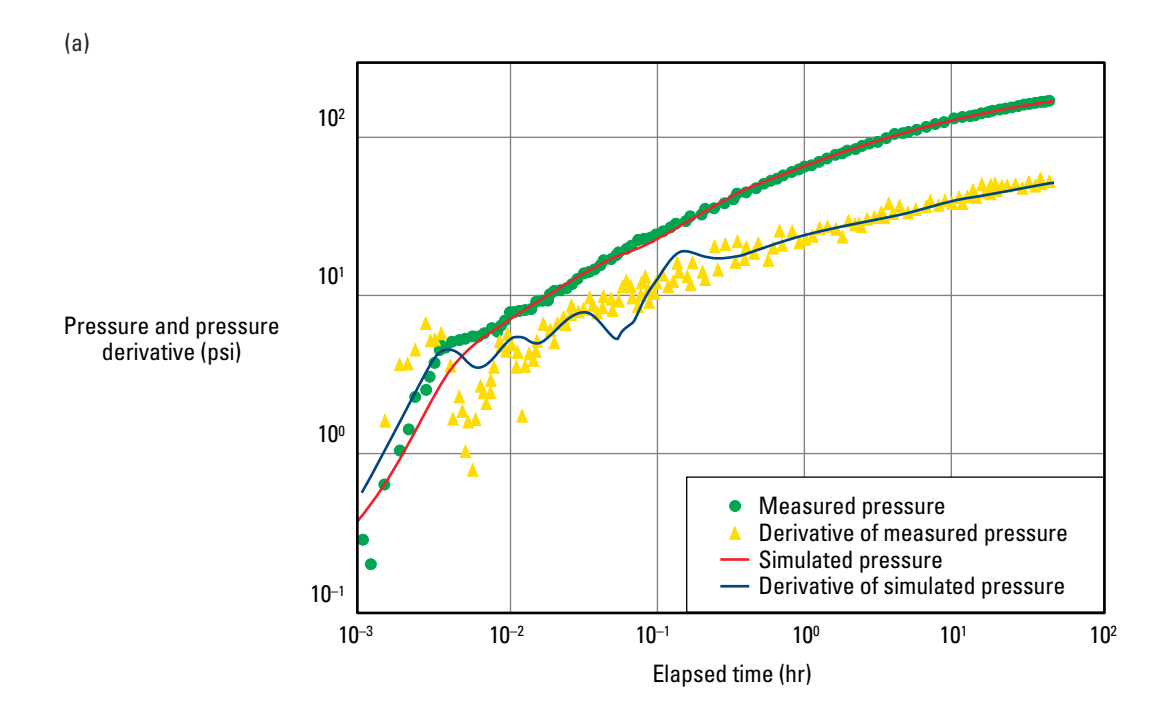


Figure 51. Comparison diagnostic plot used for horizontal well flow regime identification (Shah et al., 1990).



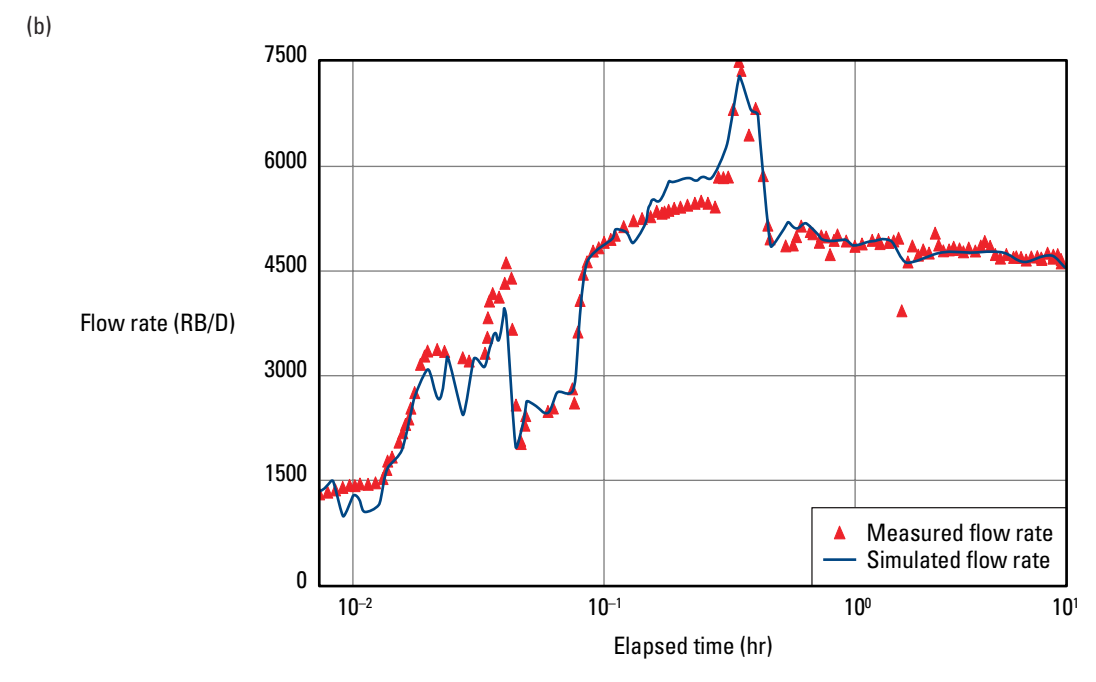


Figure 52. History matching of (a) pressure and pressure derivative for the buildup transient and (b) flow rate for the drawdown period (Shah *et al.*, 1990).

Multiple-well testing

In single-well testing, the primary target is the nearby well region. However, to investigate the interwell region, more than one well must be directly involved in the test. In multiple-well testing, the flow rate is changed in one well and the pressure response is monitored in another. These tests are conducted to investigate the presence or lack of hydraulic communication within a reservoir region. They are also used to estimate interwell reservoir transmissivity and storativity.

The two main types of multiple-well testing are interference tests and pulse tests. Some vertical interference tests are classified as multiple-well tests. As subsequently discussed, they are performed between two sets of perforations or test intervals in a well to investigate vertical communication and estimate vertical permeability. Multiple-well tests are more sensitive to reservoir horizontal anisotropy than single-well tests. Therefore, multiple-well tests are typically conducted to describe the reservoir anisotropy based on directional permeabilities.

Interference testing

Interference tests require long-duration production or injection rate changes in the active well. The associated pressure disturbance recorded in the observation well yields valuable information regarding the degree of hydraulic communication within the interwell region. Figure 53 shows a plan view of two wells used in an interference test, the rate history of the active well and the pressure response in the observation well.

If single-phase conditions prevail within the investigated region of the reservoir, the pressure response can be analyzed to estimate interwell reservoir properties. The analysis technique uses the same type-curve matching approach as for drawdown tests, but with a different type curve because, unlike for single-well tests, the pressure response is observed at some distance from the location where the perturbation was originally created. Figure 54 shows a type-curve match for an interference test using the homogeneous line-source solution (also known as the exponential integral solution) as the referenced theoretical model.

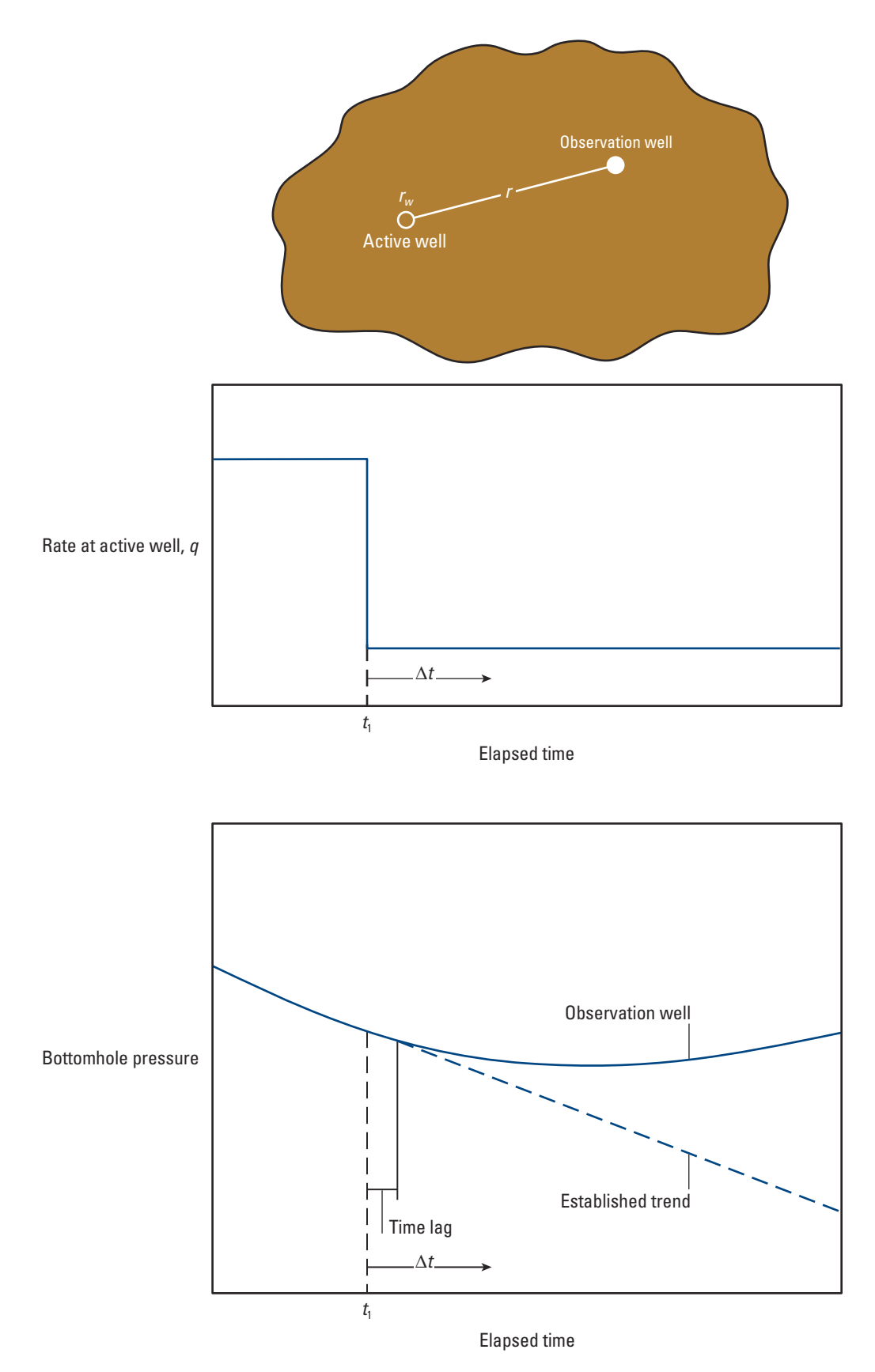


Figure 53. Active and observation wells and their respective rate and pressure changes during an interference test.

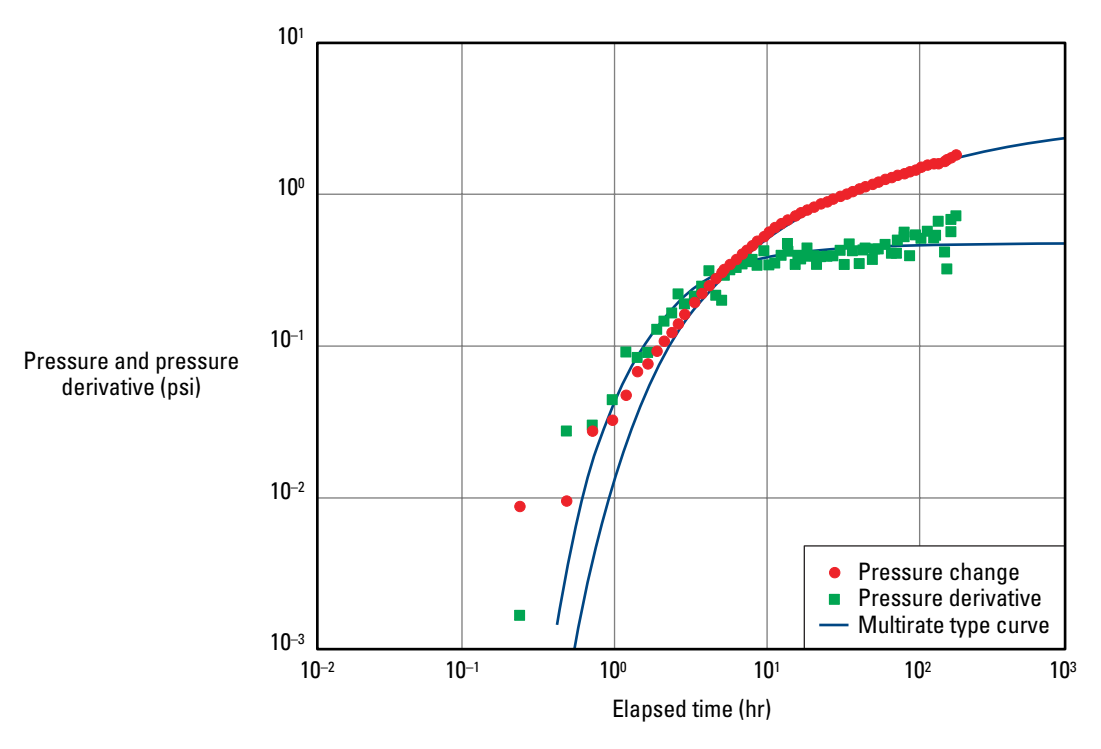


Figure 54. Type-curve match of an interference test.

Pulse testing

Pulse testing is a special form of multiple-well testing that may last from a few hours to a few days. The technique uses a series of short rate perturbations at the active well. Pulses are created by alternating periods of production or injection and shut-in. The pressure response to the pulses is measured at one or more observation wells. Because the pulses are of short duration, the pressure responses are small. Therefore, high-resolution gauges are usually required to measure the small variations in pressure. The advantages of pulse testing compared with interference testing derive from the relatively short pulse length; reservoir pressure trends and noise are removed with appropriate analysis techniques.

The following example illustrates how pulse testing was used to understand the degree of hydraulic communication within a Middle Eastern reservoir and to investigate suspected fluid migration toward a nearby field. The test involved six wells, including the active well. The pulses were created by an alternating sequence of injection and shut-in periods of 36 hr each. The resulting pressure pulses were monitored in the observation wells for 12 days. Downhole memory recorders were used to acquire the pressure data.

The observed pressure responses were analyzed with history-matching techniques. The analytical solution of the diffusivity equation for a homogeneous rectangular reservoir with mixed boundary conditions (i.e., both no flow and constant pressure) yielded an excellent match between the measured and simulated pressure responses (Fig. 55). Figure 56 shows the configuration of producing and injection wells within the area modeled in the study.

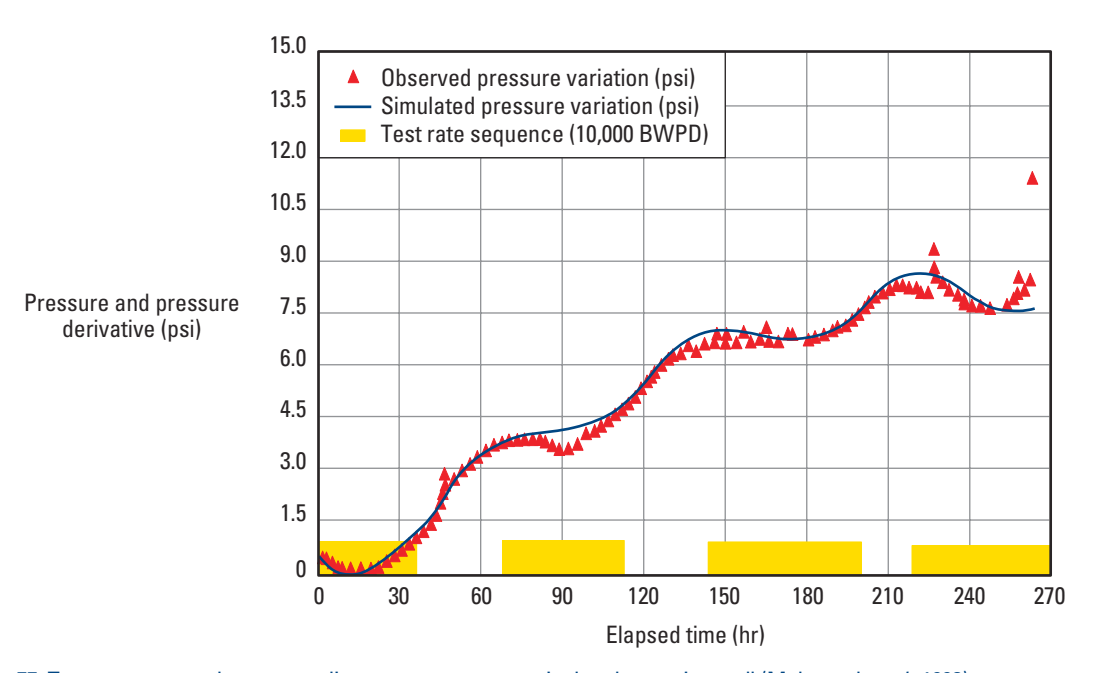


Figure 55. Test sequence and corresponding pressure response in the observation well (Mahmoud et al., 1993).

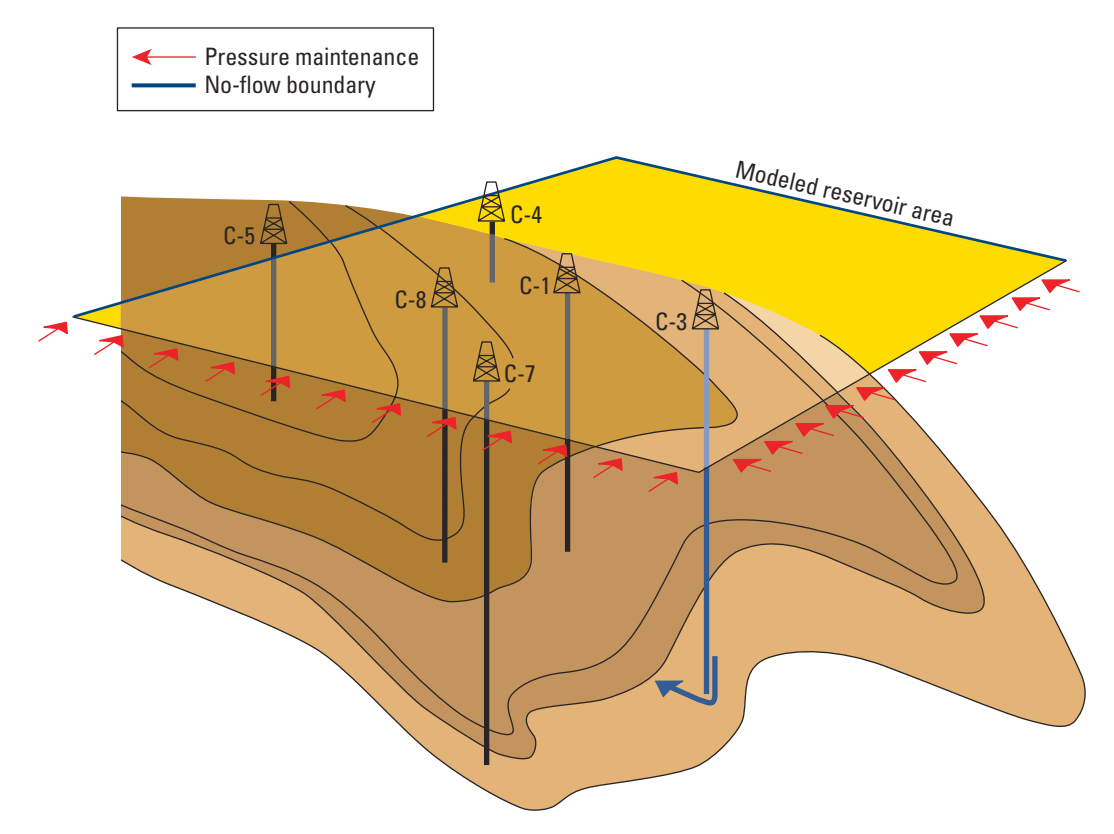


Figure 56. Configuration of producing and injection wells for the example pulse test. The yellow rectangle delineates the area modeled by the reservoir study (Mahmoud *et al.*, 1993).

The test indicated good hydraulic communication within the area investigated. It was also possible to determine the interwell reservoir properties and geometry of the area. The good match of constant-pressure boundaries to the data implied that there was no leakage toward the neighboring field as previously suspected.

The small amplitude of the signal detected in two of the observation wells suggested the presence of free gas in the upper part of the structure. This result was confirmed by other sources of information and proved particularly useful to the operator in locating future water injection wells and optimizing reservoir management.

Vertical interference testing

Understanding vertical flow behavior is essential for effective reservoir management. Vertical permeability is an important parameter, particularly for completion decisions in thick or layered reservoirs. It is even more critical for working with secondary or enhanced recovery processes. The value of k_v can be determined by a type of pressure transient testing called vertical interference tests. These tests are also conducted to determine crossflow between two layers separated by a low-permeability layer and to detect leaks behind the casing.

Figure 57 shows the vertical interference test configuration and reservoir geometry. Two permeable layers are separated by a tight, low-permeability zone. Layer 1 flows to the well, while flow to the well from layer 2 is prevented by a packer assembly. In theory, if both permeable layers have similar or identical flow properties, the wellbore pressure versus time opposite the packed-off zone should yield k_v and an average value of k_h for both layers. However, this assumption rarely holds in practice, and the simultaneous recording of pressure in both the producing and packed-off layers is preferred. The simultaneously recorded measurements enable not only the determination of k_v in the tight zone but also the estimation of individual flow properties for both permeable zones (i.e., the total system).

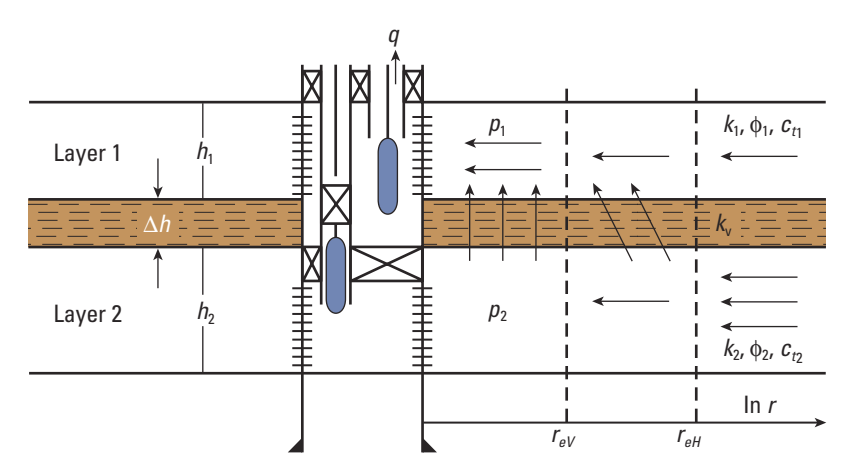


Figure 57. Test and reservoir configuration for a vertical interference test across a tight zone (Ehilg-Economides *et al.*, 1994). r_{eH} = inner radius of the horizontal flow region, r_{eV} = outer radius of the vertical flow region.

The interpretation of a vertical interference test with simultaneous recording is fairly straightforward and requires the use of only one new type curve, shown in red in Fig. 58. The figure shows the theoretical responses of the flowing zone (blue curves) and the packed-off interval (red curves), both hydraulically communicated through the reservoir as shown in Fig. 57. The initial response is that of the producing zone. Once the value of t reaches 70 hr in Fig. 58, the curves diverge as a result of the production of fluids from the packed-off zone to the flowing layer. The observation layer response (green curves) is characterized by a 2-to-1 slope in the early-time storage-dominated response, a unit-slope during the transition from single-layer radial flow to total-system radial flow, and a final derivative response that overlies the pressure derivative for the flowing layer.

The early-time data in the flowing zone are analyzed using conventional methods for a homogeneous system, yielding k and s for the producing zone. The late-time data of the producing zone—when the derivative type curves coincide—are used to obtain the permeability of the observation interval. The difference between the formation pressure of the packed-off interval and the flowing pressure of the producing zone may be used to estimate k_v .

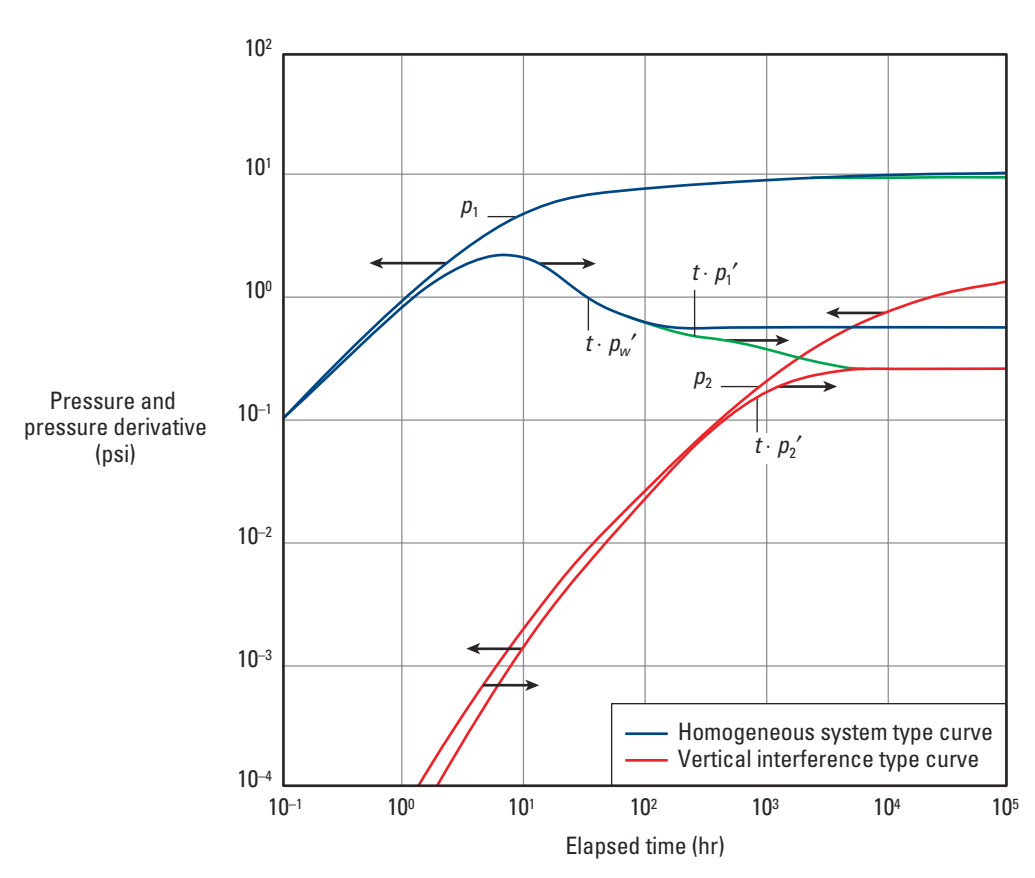


Figure 58. Pressure and pressure derivative curves for the producing and packed-off intervals in a vertical interference test (Ehlig-Economides and Ayoub, 1986).

When the test is not long enough to detect the response of the total system, the analysis is performed by matching the pressure response of the observation interval to the red type curves on Fig. 58. The pressure match provides the total flow capacity, and the time match provides k_v . A similar procedure is followed when the pressure response from the flowing zone is not recorded. However, this approach is not recommended because of the highly nonunique nature of the model for the observation zone. Recording and matching the responses in both layers simultaneously yield the best results.

Figure 59 shows a vertical interference type-curve match for a test conducted in a carbonate reservoir with two layers separated by a streak of low permeability. The early-time response is distorted by changing wellbore storage, which rendered most of the wellbore-dominated transient uninterpretable. However, the simultaneous match of the transition period for both layers is of good quality, giving confidence in the estimated values of the horizontal and vertical permeabilities listed in the caption.

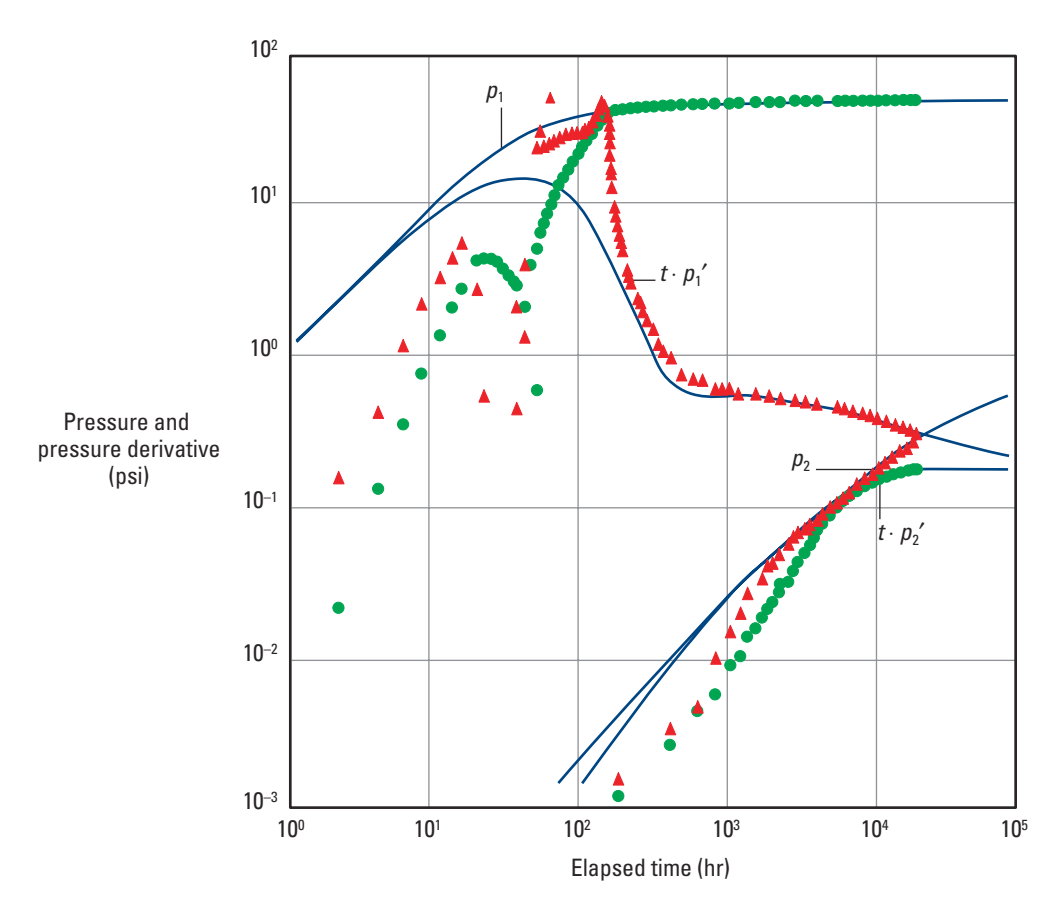


Figure 59. Vertical interference type-curve match for a two-layer carbonate reservoir divided by a tight streak, with $k_1 = 806 \text{ mD}$, $s_1 = 36$, $k_2 = 2120 \text{ mD}$, $k_V = 3.7 \text{ mD}$, permeability ratio = 0.33, and storativity ratio = 0.56 (Ehlig-Economides and Ayoub, 1986).

Measurements while perforating

Combined perforating and testing operations have become popular with oil companies throughout the world. The ability to perform these two tasks simultaneously has not only brought major savings in rig time and improvements in wellsite safety but has also opened up new possibilities in well testing.

Although the range of tool configurations for measurements-while-perforating jobs is wide, there are two types of combined systems—tubing-conveyed perforating (TCP) using a DST string and through-tubing perforation (TTP). Both methods can be used with either real-time monitoring or downhole recording (Fig. 60).

The combined approach has inherent advantages over separate testing and perforating techniques. The TCP-DST configuration saves rig time and improves wellsite safety because it requires fewer trips into the well. TTP using a measurements-while-perforating tool (MWPT) makes the testing of low-energy wells possible.

The transient data are analyzed using the theory for simultaneous measurement of flow rate and pressure. This method is particularly necessary for data from intermediate-energy reservoirs where changes in wellbore storage are expected. The flow rate can be measured directly using a production logging flowmeter. Alternatively, flow estimates can be derived by simultaneously measuring the downhole and wellhead pressures— provided that corrections are made for friction and inertial losses in the tubing string. For low- or high-energy reservoirs, the flow rate can be inferred from the pressure data using a constant wellbore storage model of rising liquid level or compressing wellbore fluids, respectively.

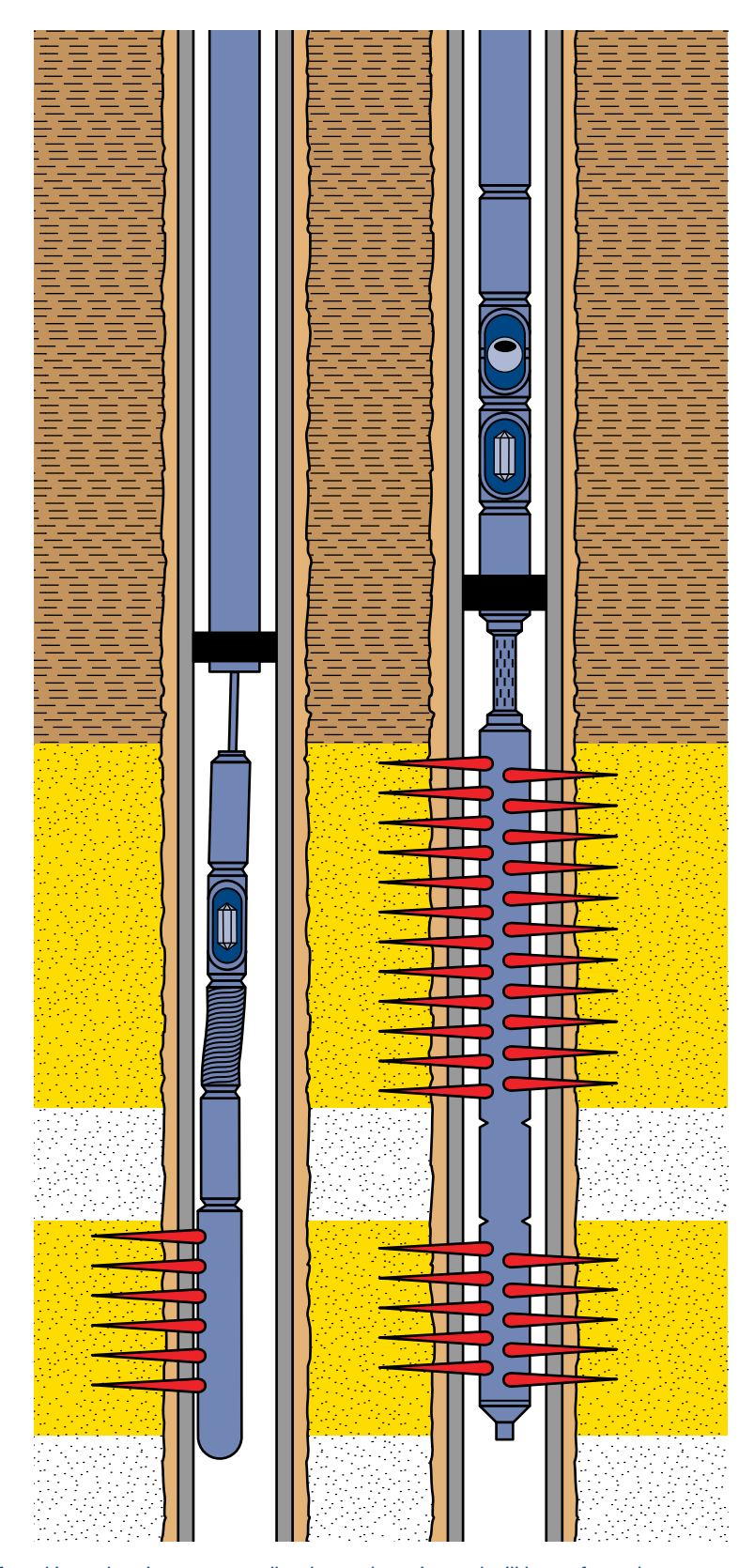


Figure 60. TCP (right) is preferred in exploration or new wells where a large interval will be perforated. TTP (left) is usually more economical for small jobs and is commonly used to perforate producing wells.

Figure 61 shows the sandface rate-convolution plot for a slug test conducted in a well that had insufficient energy to flow naturally and produced using a gas lift system. A 20-ft interval had to be perforated underbalanced, so the operator also recorded the resulting pressure transient data to get a first estimate of reservoir parameters, which could be used in the design of a subsequent major well test.

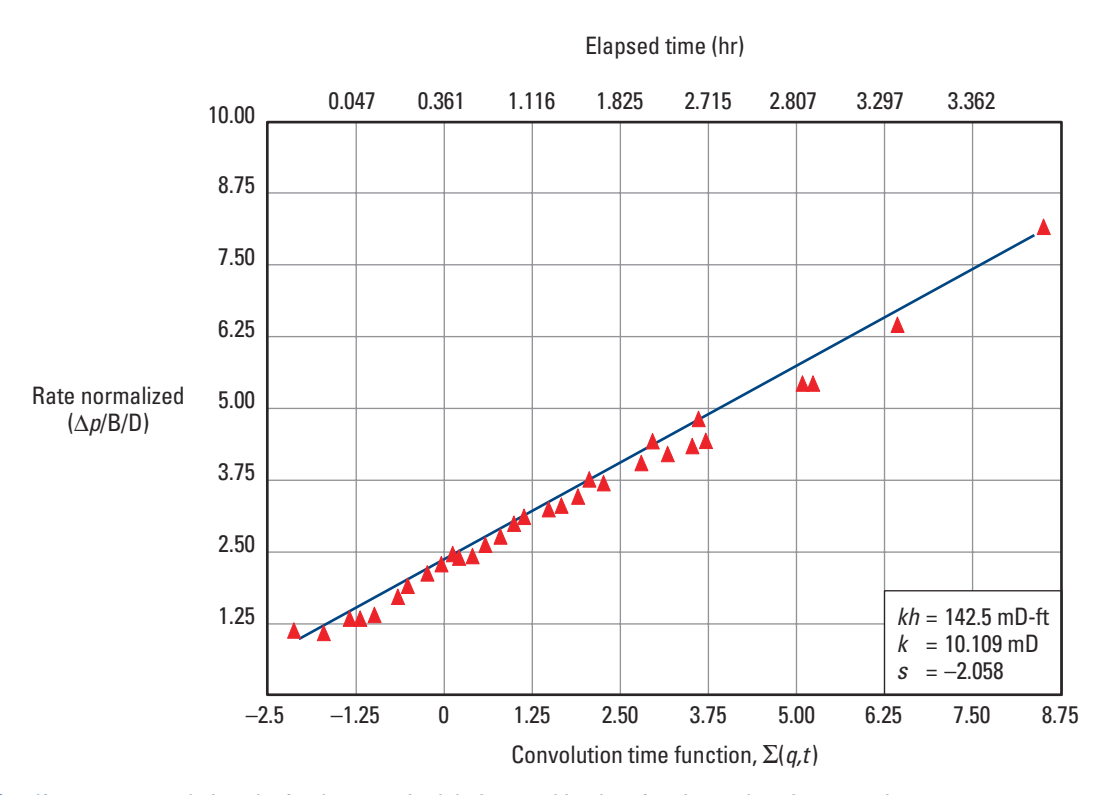


Figure 61. Sandface rate-convolution plot for data acquired during combined perforating and testing operations in a low-energy well.

Impulse testing

Quick and simple, impulse testing is particularly useful for wells that do not flow to the surface, wells in which extended flow may not be desirable (e.g., because of sanding problems) and extremely tight or vuggy formations where wireline formation testers fail to perform. The technique requires knowledge of the initial reservoir pressure, and the resulting estimated parameters include kh and s. Impulse testing can also be used to detect and evaluate nearwellbore heterogeneity in the reservoir.

The impulse testing procedure is an easy and extremely quick form of well testing. The well is first put on production or injection for 3 to 4 min. before being shut in for a period of 6 to 20 times the length of the production or injection period.

Only a small amount of fluid is removed from or injected into the formation during the short impulse period of production or injection, so the associated pressure disturbances are small. Therefore, high-resolution pressure gauges are required to accurately study the small changes in the reservoir's pressure response during the shut-in period.

The depth of investigation of an impulse test is relatively small in comparison with conventional well tests. This is due to the short duration of both the impulse and shut-in periods as well as the small pressure changes developed during the test. Therefore, impulse testing is most appropriately used for the detection of near-well features.

Impulse test theory assumes that a unit volume of fluid is instantly removed from or injected into the formation during the impulse period. Theory shows that the resulting pressure changes in the reservoir are proportional to the derivative of the drawdown pressure response of the reservoir.

Figure 62 shows the simulated pressure response to a short impulse in a double-porosity reservoir on both Cartesian and log-log scales. In practice, the impulse period is not instantaneous because the removal or injection of a unit volume of fluid takes a finite period of time. The pressure changes in the reservoir produced by this change in fluid volume initially do not follow the theory and do not match the pressure derivative curve. Fortunately, these effects dissipate quickly, and generally the pressure response matches the pressure derivative curve once the shut-in time exceeds 3 times the impulse time.

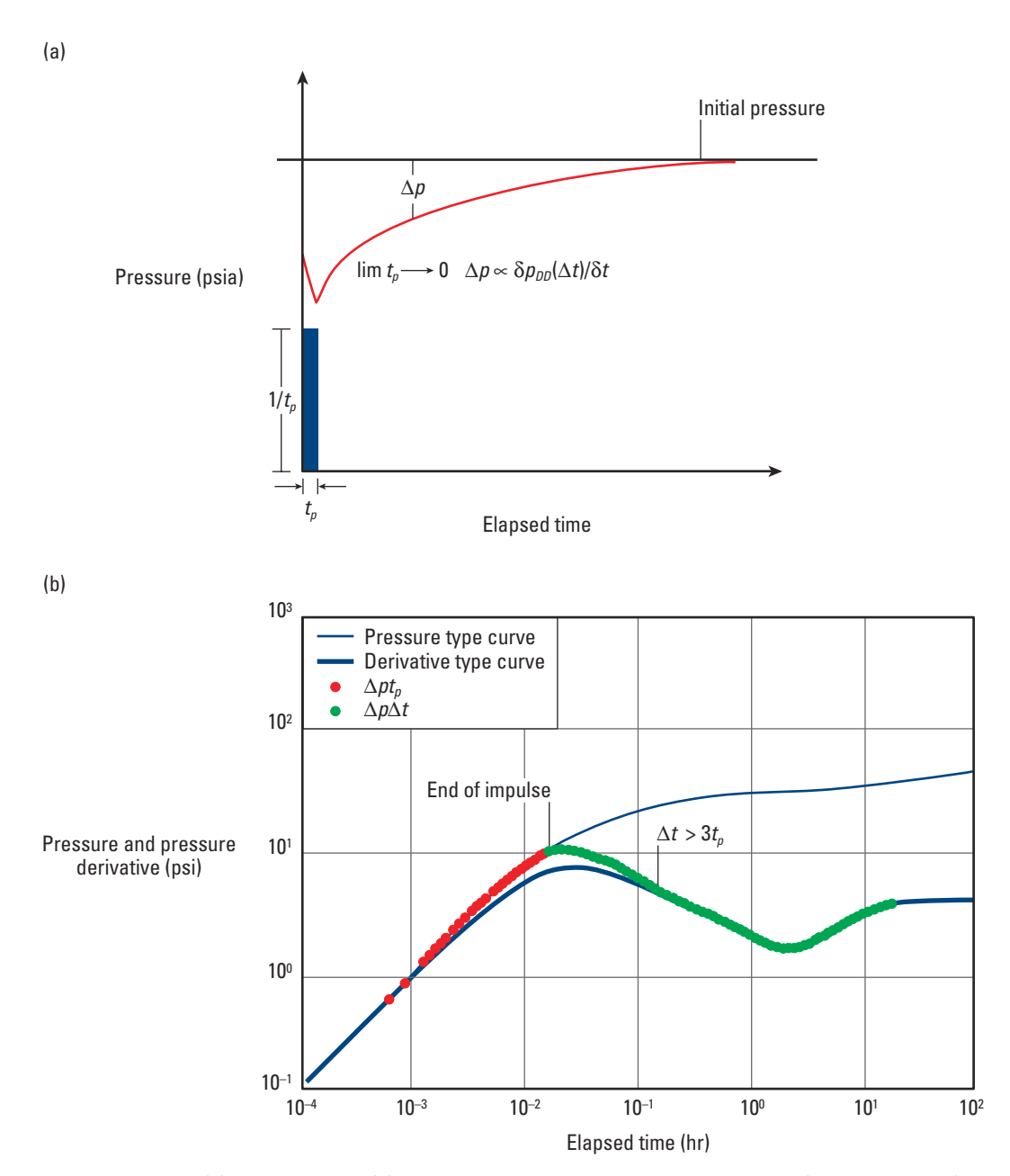


Figure 62. Pressure response plot (a) and impulse plot (b) of a simulated test in a double-porosity reservoir (Ayoub *et al.*, 1988). p_{DD} is the drawdown pressure in the same well.

The analysis of impulse test data requires accurate measurement of the quantity of fluid removed or injected and modification of the measured pressure response so it can be matched directly with published type curves. The data are modified by multiplying the observed pressure change during the shut-in period by the elapsed time since the end of the impulse period. In addition, pressure changes during the impulse period are multiplied by the duration of this period. A log-log plot of the transformed pressure data versus the shut-in time is matched with selected drawdown type curves to obtain the reservoir parameters. Figure 63 shows the impulse technique applied to data acquired in an exploration well.

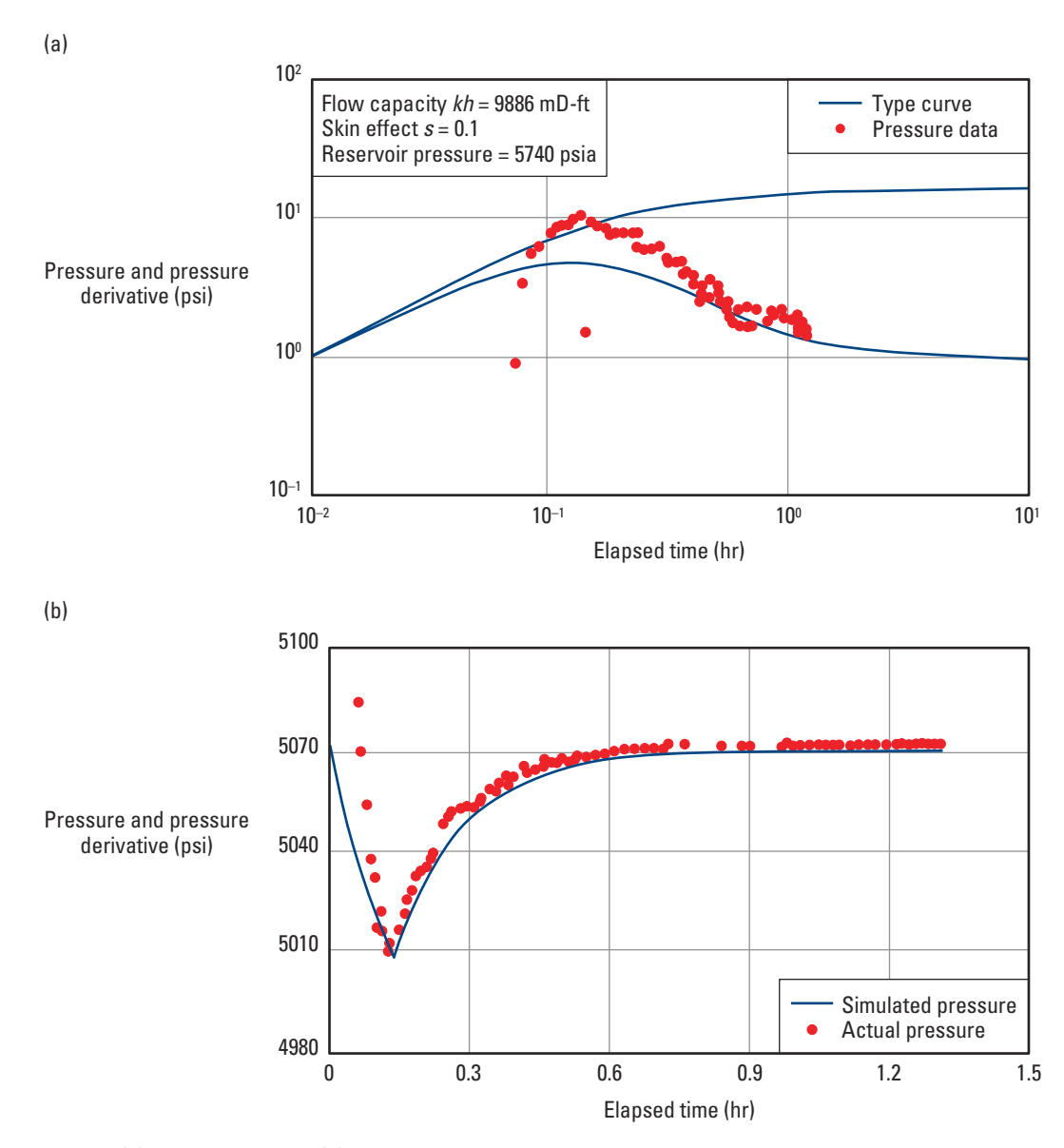


Figure 63. Impulse plot (a) and simulation plot (b) for data acquired in an exploration well.

Closed-chamber DST

In exploration, a priori well test design may be complicated by a lack of data. However, the closed-chamber test can provide an early assessment for determining safe wellsite procedures and acquiring analyzable data while optimizing rig time. This technique is usually applied to the preflow period of a DST job, and the resulting information is used to design (or fine-tune) subsequent test stages. Closed-chamber tests are also suitable when surface flow rates are undesirable or unattainable—hydrogen sulfide (H_2S) gas, night testing, low-energy and low-productivity wells, etc.—because the formation fluid type and flow rate can be determined without surface flow.

Closed-chamber DSTs differ from conventional DSTs in that all surface valves are closed during the flow periods (Fig. 64). When the test tool is opened downhole, formation fluids or drilling fluids enter the DST string, displacing the fluids that initially occupied the internal drill-stem volume. Because the surface valves are closed, the pressure rises in the closed chamber. The pressure rise continues until formation fluids cease to flow (shut-in period commences), at which point the pressure begins to stabilize. Once stabilization has been reached, the drillstem pressure is released following a controlled bleedoff period. The recording of the pressure increase during the closed-chamber flow period and the pressure decrease together with the gas rate during the bleedoff period are used to identify the type of produced fluids and to estimate the fluid entry rate and liquid recovery.

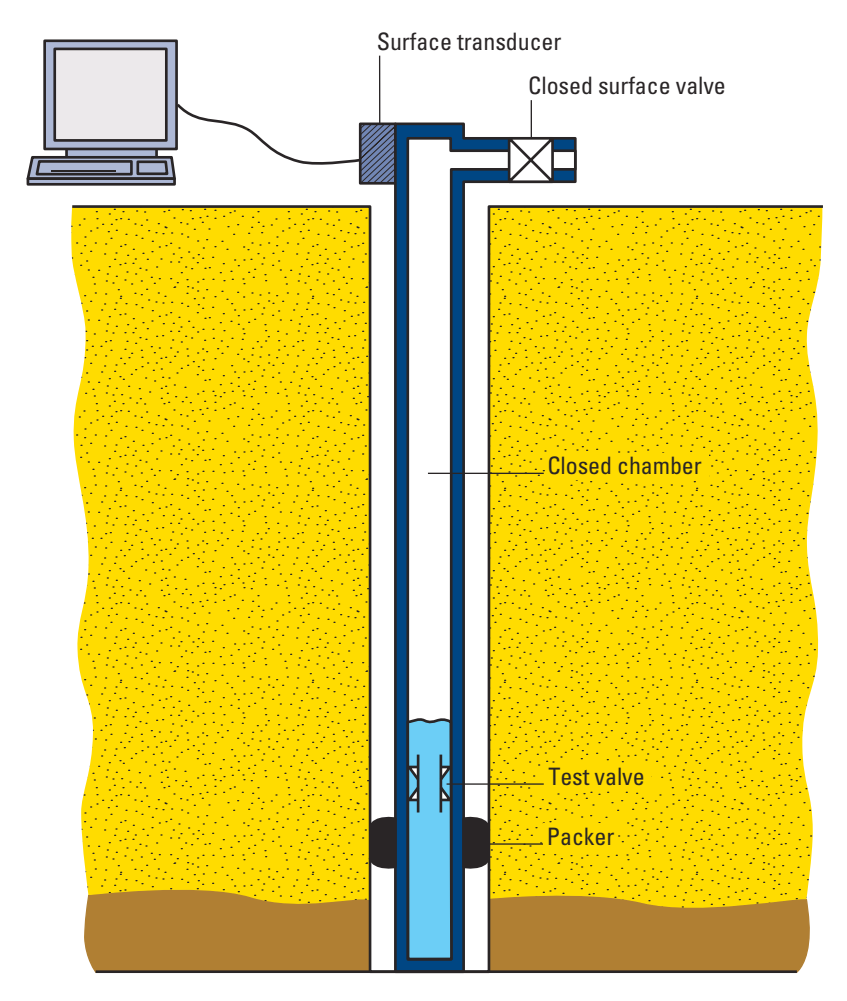


Figure 64. Equipment schematic for closed-chamber testing.

The increase in surface pressure during a closed-chamber DST flow period is caused by

- increase in the mass of gas contained in the chamber (pure gas entry)
- decrease in the gas-filled portion of the string (pure liquid entry)
- combined gas and liquid entry.

The pressure increase can be translated into approximate flow rates using the principle of conservation of mass and the real gas law. The general mass-balance equation (Alexander, 1976) used to relate flow rates to changes in pressure and volume is

$$q_{in} \quad q_{out} = \frac{286V}{Tz} \quad \frac{dp}{dt} + \frac{286p}{Tz} \quad \frac{dV}{dt} ,$$
 (14)

where

 q_{in} and q_{out} = flow in and out, respectively, of a closed chamber

V = volume

T = temperature.

This equation can easily be adapted for the most commonly used combinations of cushion fluids in the field.

The calculation of fluid recovery requires the initial and final gas-filled volumes. The initial gas-filled volume is computed from the DST string capacity and the level of the liquid cushion. The final gas-filled volume can be determined either from the real gas law (for pure liquid entry) or by measuring the gas rate and the rate of decrease of the average closed-chamber pressure during the bleedoff period (for pure gas entry and for gas and liquid entry). The liquid recovery is simply the difference between the initial and final gas-filled DST string volumes.

Because the initial and final gas-filled volumes can be determined, the gas content of the DST string before and after the test can be calculated using the real gas law. The difference in the DST gas content divided by the actual liquid recovery provides an estimate of the average produced gas/liquid ratio.

The fluid-type entry can be estimated by calculating the maximum rates of pressure change that would be observed if pure gas, pure liquid or gas-saturated water was produced at the maximum rate allowed by the tool string configuration (Fig. 64). Estimates of the bottomhole temperature and pressure, formation gas gravity and approximate gas/liquid ratio are required to compute the slopes of these lines. The value of kh can be obtained using the techniques previously described for the simultaneous measurement of flow rate and pressure.

Figure 65 shows the surface pressure record from a closed-chamber test. The rate of increase of the surface pressure indicates gas entry because pure liquid entry at the maximum possible rate could not produce such a rapid increase. The continuous increase in surface pressure during shut-in is an indication of phase segregation, suggesting the entry of gas and liquid during the flow period. The subsequent bleedoff test confirmed this interpretation.

Knowledge of the formation fluid type and flow rate prior to the initiation of subsequent flow periods enables optimizing the remainder of the test. Considerable rig time was saved during the test plotted in Fig. 65 as a result of the early determination of the average produced gas/oil ratio, which indicated that surface flow was improbable.

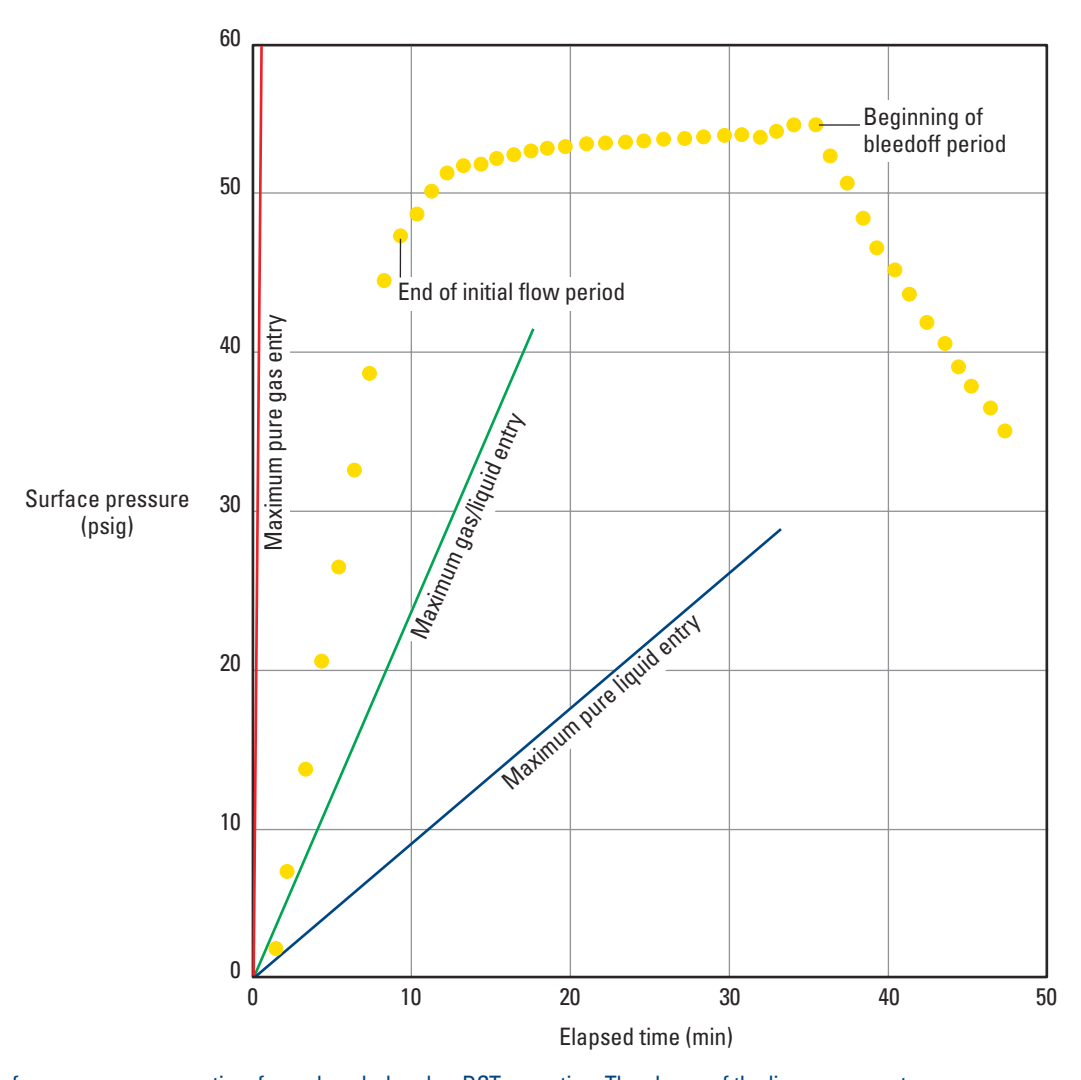


Figure 65. Surface pressure versus time for a closed-chamber DST operation. The slopes of the lines represent the maximum rates of change in pressure that would occur if pure gas, pure liquid or gas-saturated water entered the DST string at the maximum possible rates allowed by the test tool (Erdle *et al.*, 1977).

Water injection wells

Waterflooding is used throughout the world to increase oil recovery. The success of waterflooding projects depends largely on adequate prediction of the reservoir response. Pressure transient testing—usually in the form of falloff or injectivity tests—is conducted to obtain parameters for modeling injection schemes. In addition to these same parameters as obtained with conventional well testing, the pressure transient tests also provide information for monitoring parameters that change with time in a waterflood (i.e., location of the water front, well injectivity and average interwell reservoir pressure).

The pressure transient response in a reservoir under waterflooding differs from single-phase flow behavior because of differences in the properties of oil and water. Soon after injection begins, a saturation gradient is established in the reservoir. This forms a region of high water saturation around the wellbore, termed the water bank. Outside this region is the transition bank, in which water saturation decreases away from the wellbore until the flood front is reached. The region located ahead of the injection front—with the initial water saturation—is called the oil bank. A system that consists of regions with different properties is called a composite reservoir (Fig. 66a). The composite system is modeled assuming that the fluid properties are constant within each bank but change sharply at an interface. A simplified version is the two-bank model shown in Fig. 66b.

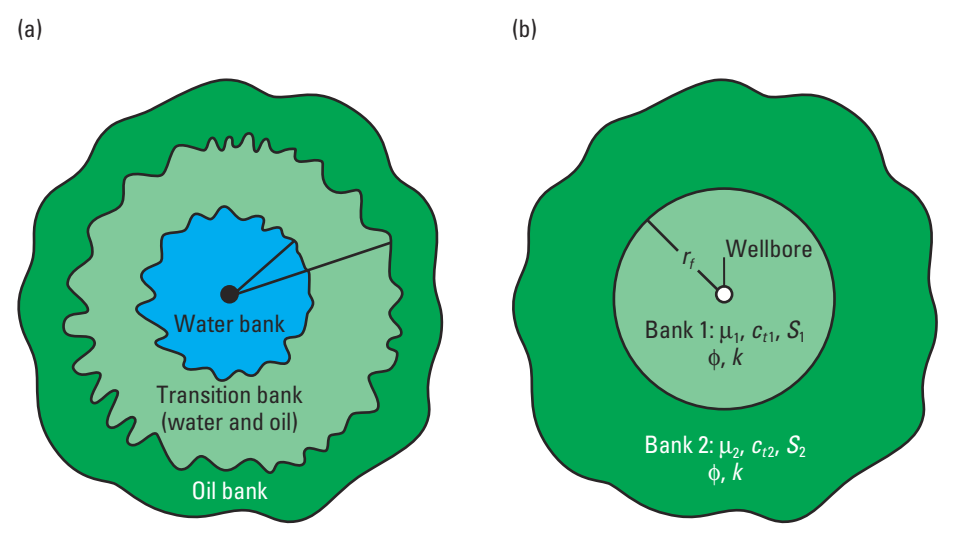


Figure 66. Composite system of a waterflooded reservoir: (a) multibank and (b) two-bank models. S = saturation, $r_f =$ radial distance to the fluid front.

In a water injection well test, three main features can be identified after the wellbore storage effects have disappeared. Initially, the pressure response is identical to single-phase flow and is governed by the rock and fluid properties of the water bank. This is displayed as a horizontal line in the derivative curve (Fig. 67a). The second identifiable response occurs when the transient travels through the transition bank. This period is characterized by the saturation distribution within the transition bank and the corresponding displacement mobility ratio M. The derivative curve shows a hump for M > 1 and a dip for M < 1. The duration of the transition period depends on the storativity ratio of the banks. The third feature is observed as the transient penetrates deeper into the reservoir and the flow becomes controlled by the properties of the oil bank. This period exhibits a second horizontal line in the derivative curve. The level of stabilization of this second plateau is related to the mobility of the oil bank.

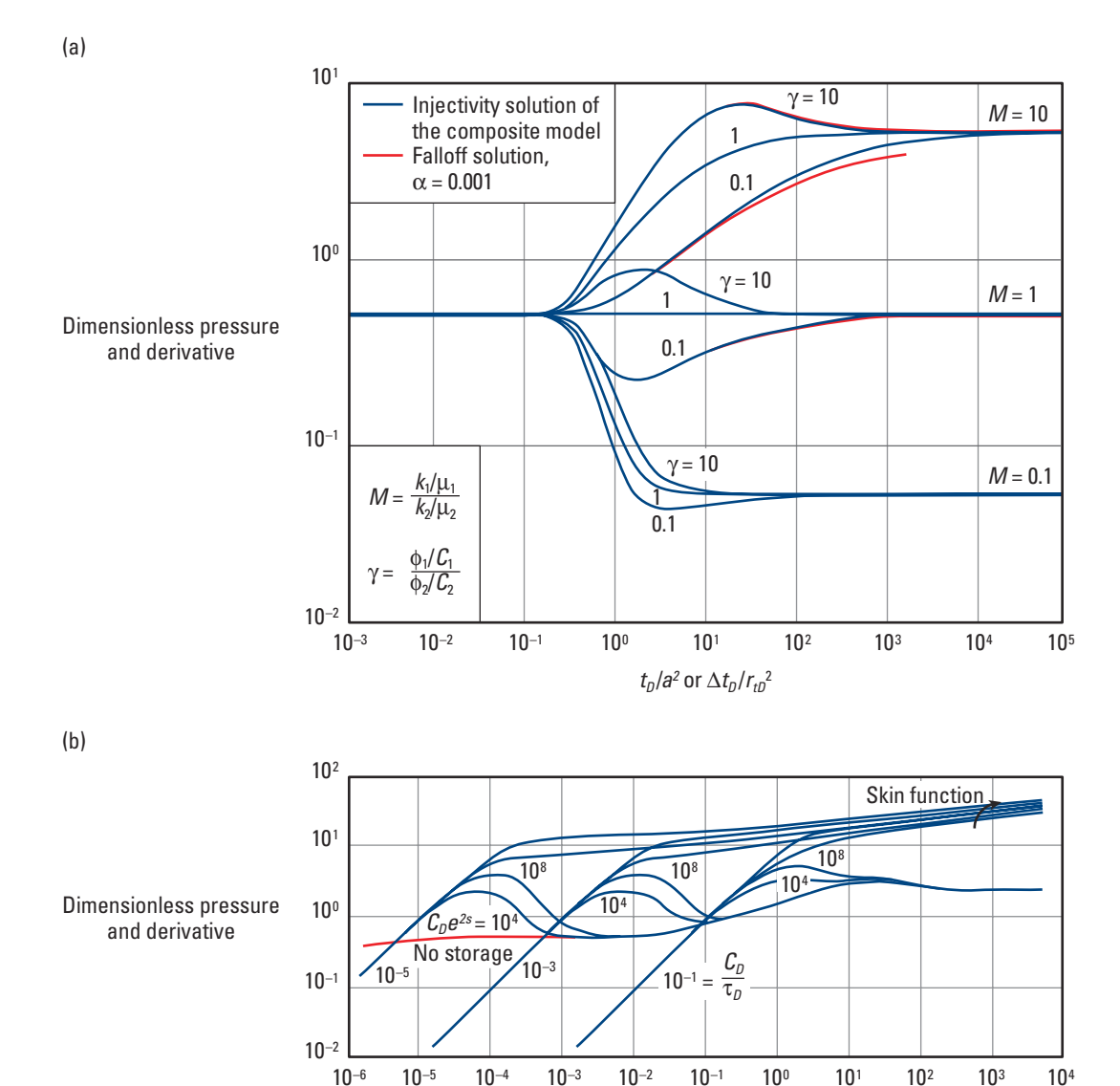


Figure 67. Two-bank model ($C_D = 0$) match to pressure and derivative type curves (a) and multibank model customized falloff type curves (b), which include wellbore storage, skin effects and relative permeability (Abbaszadeh and Kamal, 1989). a = 1 location of discontinuity in the composite reservoir, a = 1 compressibility ratio in the two-bank system.

Dimensionless falloff time

The match of field data with the type curves yields all the parameters of the system. The first radial flow regime gives the mechanical skin factor and the mobility of the water bank. The time match provides the water front location (intermediate-flow period). The late-time radial flow regime supplies the mobility of the oil bank.

For a pressure transient test to contain all features of a waterflood and therefore provide a unique solution, the test should be conducted during the early stage of injection. It should also be sufficiently long to detect the reservoir response in the oil zone, but interference from nearby wells can hamper the capture of all three features. Consequently, the performance of tests early in the life of the injector well is recommended.

The interpretation of pressure transient tests in water injection wells can be refined through use of the multibank model (Fig. 66a). This model incorporates the saturation distribution within the transition bank, which makes it particularly useful when the various banks exhibit substantial storativity contrasts. These customized type curves are constructed on computers and require the relative permeability and individual rock and fluid compressibility values. Therefore, the type curves are field dependent. The type curves shown in Fig. 67b were developed for a water-oil system for which the relative permeability and total mobility curves are shown in Fig. 68.

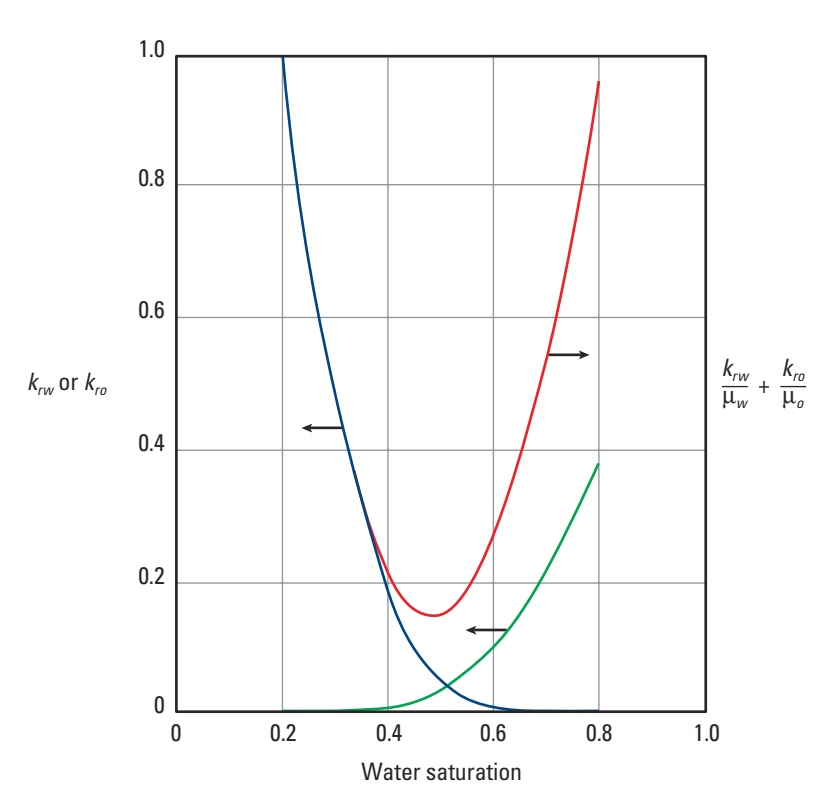


Figure 68. Relative permeability and total mobility curves for the customized type curves in Fig. 67b. $k_{\Gamma W}$ = relative permeability to water, $k_{\Gamma O}$ = relative permeability to oil, $k_{\Gamma W}$ = water viscosity. $k_{\Gamma O}$ = oil viscosity.

Figure 69 shows the comparison between a falloff data set and the theoretical response of the multibank model. The data are from a 24-hour falloff test conducted two months after injection began. The type curve that assumes no wellbore storage is also shown. Although wellbore storage masks the response from the water bank and part of the transition zone in the data, analysis was possible because the test was sufficiently long to detect the total reservoir response. The pressure match yielded the permeability to water at residual oil saturation. The time match provided the location of the water front. A second test performed four months later found that the water front had moved 300 ft farther away. This example clearly shows how using falloff tests as monitoring tools assists operators in the management of waterflooding projects.

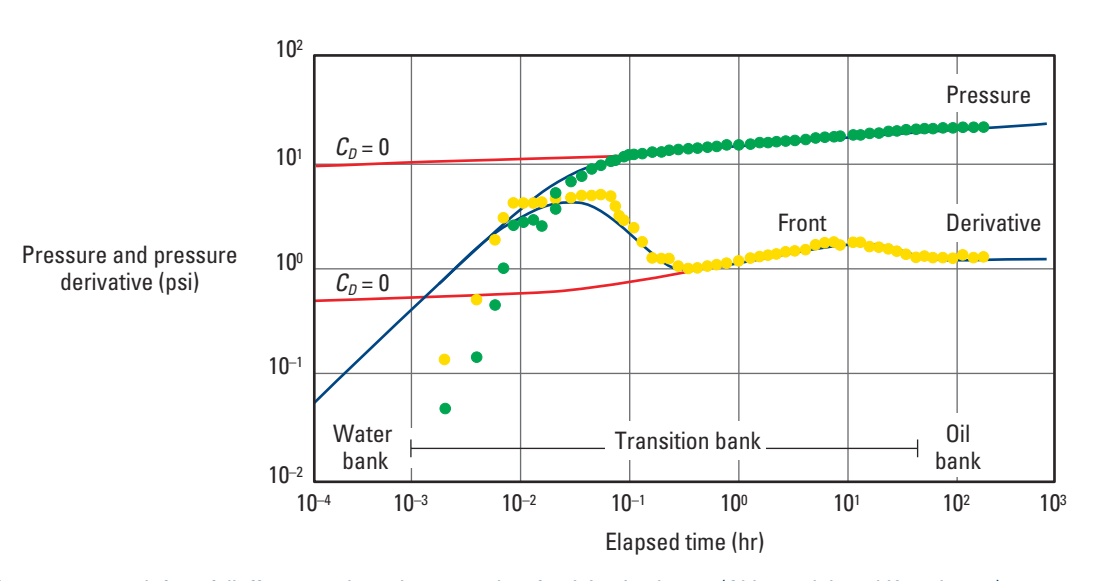


Figure 69. Type-curve match for a falloff test conducted two months after injection began (Abbaszadeh and Kamal, 1989).

Pumping wells

Sucker-rod pumping wells present special well testing problems. The first difficulty relates to mechanical constraints resulting from the presence of the rods inside the tubing string (Fig. 70). This configuration precludes the running in hole of pressure gauges— unless the rods and pump are pulled out of the hole or there is enough room in the annular space for a gauge. The second problem is associated with the long duration of the wellbore storage period during shut-in. The low reservoir energy and low productivity associated with pumping wells, compounded by high fluid compressibility in the wellbore, cause these long periods. Both problems, however, can be overcome.

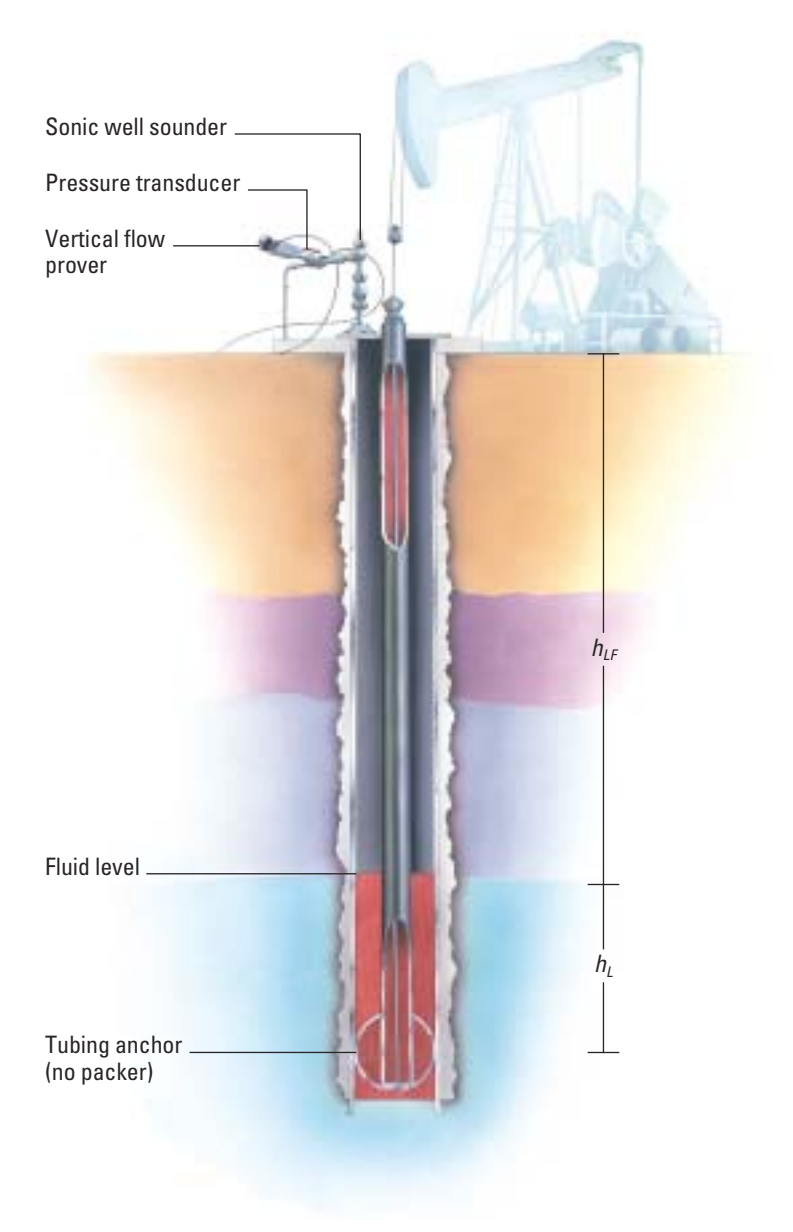


Figure 70. Sucker-rod pumping well configuration.

Testing pumping wells by removing the pump from the hole is quite expensive. Workover or pulling rigs are needed twice— to extract the pump and rods and then to rerun them after the test is completed. Furthermore, the bottomhole flowing pressure before shut-in and the early-time data cannot be recorded in these tests because of the nature of the operation, which leaves the values of s and the productivity index undetermined.

A cost-effective alternative is to compute the bottomhole pressure and flow rate from indirect measurements: casing head pressure p_c and the height of the gas/liquid interface h_L of the rising liquid column in the annulus. The first measurement is acquired with conventional pressure transducers, and the second is determined by acoustic well-sounding techniques.

The conversion of these indirect measurements to downhole pressure and rate requires an accurate determination of the changing liquid gradient in the well annulus. The controlling parameter is the gas void fraction f_g of the annular liquid column, which can be derived using a hydrodynamic model or from empirical correlation. Once the position of h_L and the value of f_g are known, the bottomhole pressure can be estimated using the following relation (Hasan and Kabir, 1985):

$$p_{ws} = p_c + h_{LF} g + h_L \left[\begin{pmatrix} 1 & f_g \end{pmatrix}_L + f_g g \right], \tag{15}$$

where

L = pressure gradient of the liquid

g = pressure gradient of the gas

 h_{LF} = height of the gas column in the annulus.

The rate of change in the liquid level dh_L/dt is used to obtain the flow rate:

$$q = a \left(d_c^2 - d_t^2 \right) \frac{d}{dt} - \frac{p_{ws} - p_c}{dt} \tag{16}$$

$$q = a \begin{pmatrix} d_c^2 & d_t^2 \end{pmatrix} \frac{d}{dt} \quad \frac{h_L + h_{FL-g}}{\begin{pmatrix} 1 & f_g \end{pmatrix}_L + f_{g-g}} , \qquad (17)$$

where

 $\alpha = constant$

 d_c = diameter of the casing

 d_t = diameter of the tubing.

The use of a hydrodynamic model— which requires the values of d_c and d_t , gas and liquid densities and surface tension— is preferred to empirical correlation. This is because the prediction of f_g is crucial for the afterflow period, during which gas continues to bubble through the liquid column. Afterflow normally dominates buildup tests in pumping wells, and in most cases radial flow is seldom reached. Moreover, this period exhibits a variable value of C, which complicates type-curve matching that uses pressure only. In such cases, reliable interpretation of afterflow-dominated tests uses both downhole pressure and rate transient data.

Figure 71 shows downhole pressure and flow rate data obtained following the indirect measurement technique. Conventional data analysis is performed for the simultaneous measurement of downhole pressure and rate—rate-normalization, convolution and convolution type curves. Figure 72 shows the data match to a convolution type curve based on step rate change for a well intersected by a finite-conductivity fracture. Although the data do not exhibit sufficient character for a unique solution, the model selection is justified because the well was hydraulically fractured. The acceptable match between the measured and simulated data provides confidence in the results.

Application of the technique in several wells has shown that estimating the bottomhole pressure is more reliable than flow rate computation. Consequently, the best results are obtained when pumping well tests are sufficiently long to allow radial flow to develop.

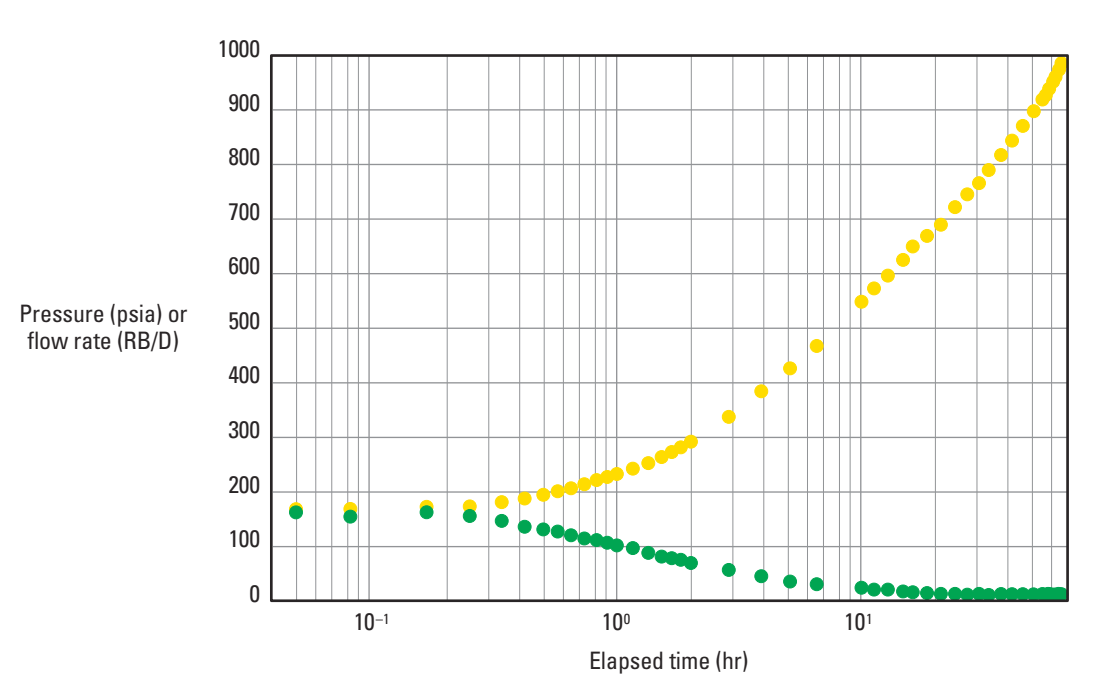


Figure 71. Pressure and flow rate variations derived from casing wellhead pressure and the rising liquid level in the annulus (Kabir *et al.*, 1988).

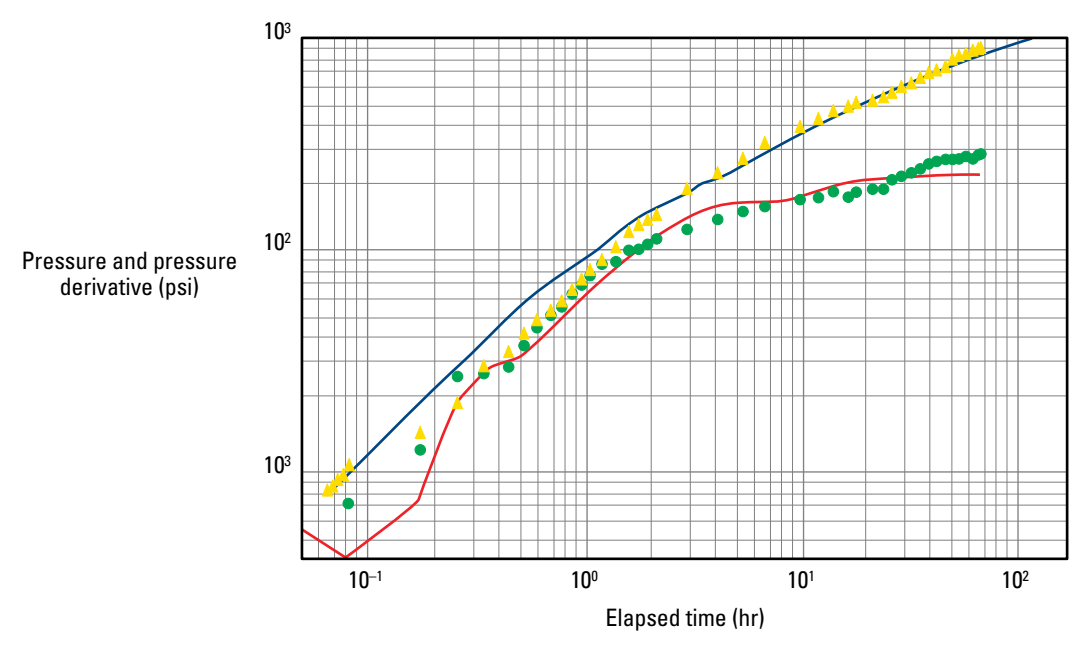


Figure 72. Convolution type-curve match for pumping well data (Kabir et al., 1988).

Permanent monitoring

More wells are being instrumented with permanent pressure gauges, and multiphase flow metering technology is being introduced in intelligent well completions. The rationale for these devices is not just passive monitoring to enable better reservoir characterization. Typically they are accompanied by flow control components that are intended to avoid expensive or even technically impossible well interventions by building flexibility into the well completion. In turn, this flexibility enables well and reservoir flow optimization.

The combined presence of permanent gauges and remotely activated downhole controls enables new well test configurations that will provoke new attention to test design. Likewise, the continual data stream acquired from permanent monitoring poses new interpretation challenges.

Pressure Transient and System Analysis

In general, system analysis helps determine the cost effectiveness of treatments under consideration and assists in completion decisions, such as a hydraulically fractured vertical well versus a horizontal well. The critical parameters for system analysis can be determined from transient tests.

NODAL* system analysis is a methodical approach to optimizing oil and gas well deliverability. This thorough evaluation of the complete producing system establishes the flow rate versus pressure drop relation for each component of the producing system— reservoir, near-wellbore completion configuration, wellbore strings and surface facilities. The major source of restriction for flow in the system is then identified. If the major pressure drop is associated with a component that can be modified, a sensitivity study is performed to determine options for removing the flow restriction; this assessment provides reliable guidelines for optimizing the well performance.

The following example illustrates the application of NODAL analysis to an offshore oil well that had a level of performance far below that of the neighboring wells. Production was about 25% of the average production for other wells in the reservoir. Formation damage was the suspected cause of the low productivity, and the well was tested. Interpretation of the pressure transient data identified a severely damaged well with s = 210 (Fig. 73). NODAL analysis was used to study the effect of damage removal on IPR. Figure 74 shows the reservoir performance curves for three values of s plotted with the tubing intake for the required wellhead pressure. The plot shows that the flow rate could be increased by a factor of about 5 at the same wellhead pressure if the impeding damage around the wellbore was removed. This could be achieved by an acid treatment without jeopardizing the integrity of the gravel pack. The well was treated with a specially designed acid injection program, and a post-acidizing well test was conducted to evaluate the effectiveness of the acid job. The interpretation results of the post-acidizing well test (Fig. 75) show that s was reduced to 15 from its preacidizing value of 210. The final stabilized rate of the well agreed with the post-acidizing predictions made by NODAL analysis (4300 STB/D, as indicated by the intersection of the tubing intake curve and the reservoir performance curve for s = 15).

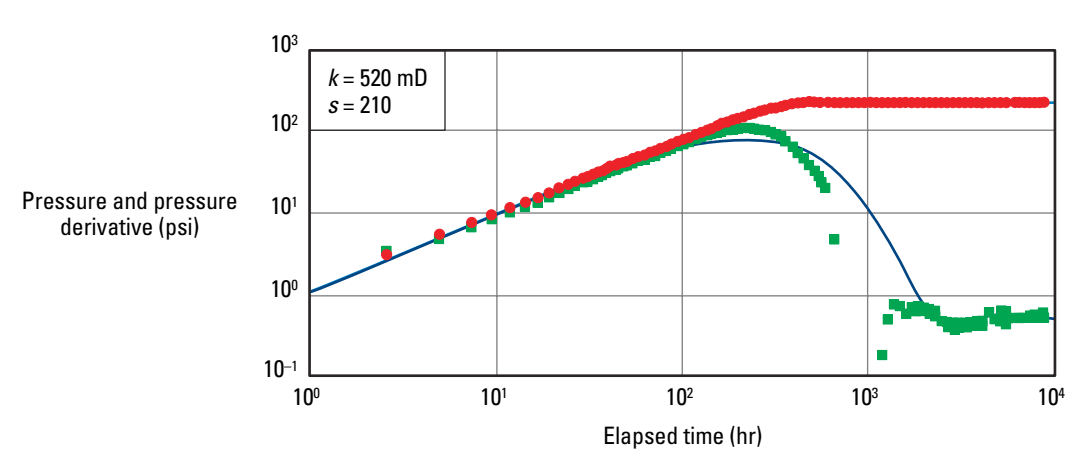


Figure 73. Pressure transient analysis using type-curve matching.

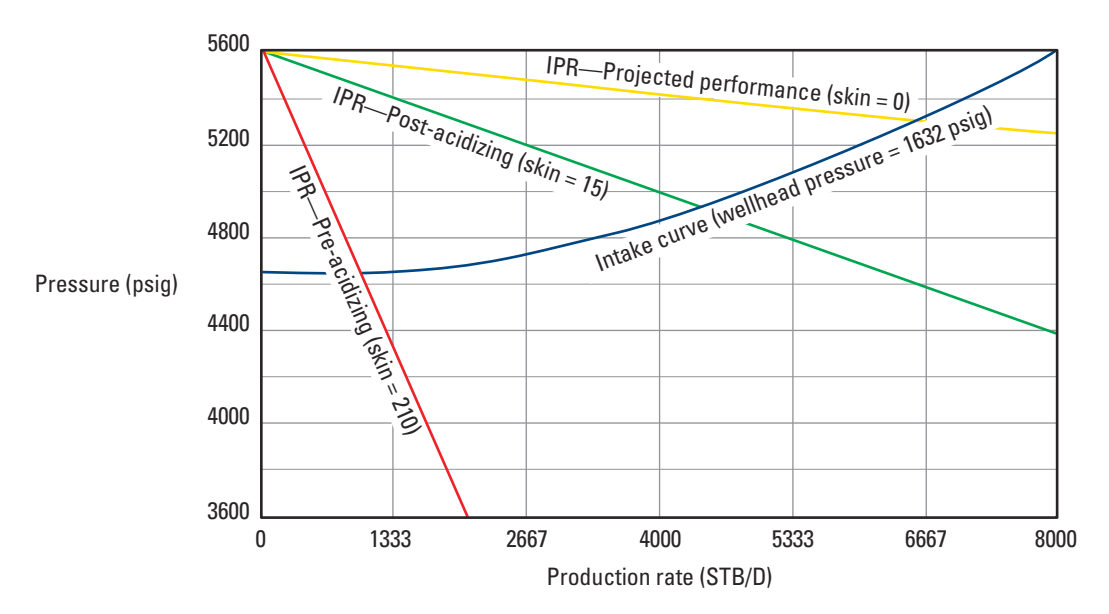


Figure 74. NODAL analysis of pressure transient data.

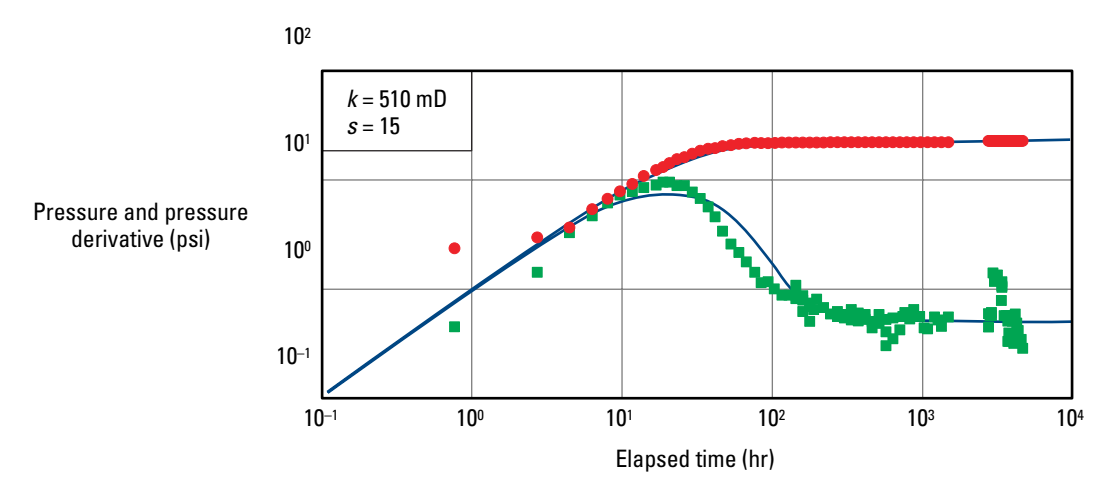


Figure 75. Post-acidizing well test.

Appendix: Type Curve Library

In general, conducting the interpretation of transient tests preceded by a variable rate history requires computer processing. A customized type curve must be constructed for each well test, except for the analysis of pressure buildup tests of wells that have undergone a lengthy drawdown period before the test. In this situation, it is possible to construct a generalized set of type curves using the theory described on pages 7 and 8. The resulting curves, presented in dimensionless form, can then be universally applied to wells with conditions that fit the reservoir models used to generate the type curves.

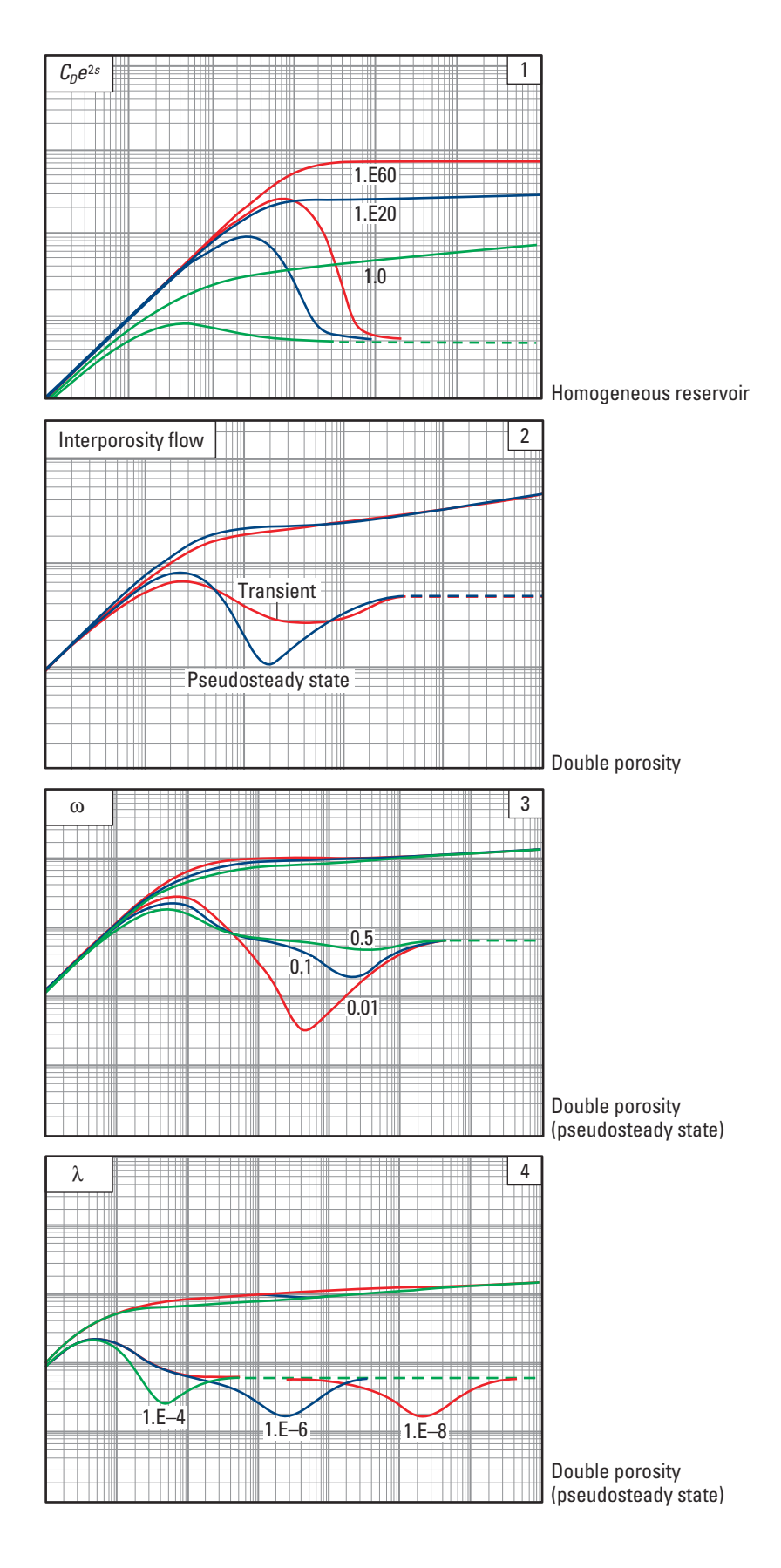
The Appendix to this book is a library of published type curves along with the reservoir models that exhibit the pressure responses. The curves were derived for a step rate change and assume constant wellbore storage. Each log-log plot consists of several sets of pressure and pressure derivative curves differentiated by color. Identified flow regimes described previously in this chapter are differentiated by symbols: dashes (radial), dots (linear), triangles (spherical) and squares (closed system).

The type curves can be applied directly to drawdown periods at a constant flow rate or buildup tests performed with downhole shut-in devices and preceded by a long drawdown period. However, with appropriate plotting techniques, as explained later, this library may be extremely useful for the model identification stage of the interpretation process of any type of transient test. Care must be taken when dealing with closed systems because the late-time portion exhibits different features for drawdown than for shut-in periods.

In practice, drawdowns are short or exhibit widely varying flow rates before shut-in. Also, buildup tests are often conducted with surface shut-in, exhibiting variable wellbore storage. These situations undermine the assumptions on which published type curves are based, impairing their direct usage. The weaknesses inherent in analysis using published type curves can be avoided by constructing curves that account for the effects of flow changes that occur before and during the test. Improved computing techniques have facilitated the development of custom curves, resulting in a major advance in well test interpretation. Analysts are also able to develop type curves that incorporate the potential effects of complex reservoir geometries on the pressure response of the reservoir. The computer-generated type curves are displayed simultaneously with the data and carefully matched to produce precise values for the reservoir parameters.

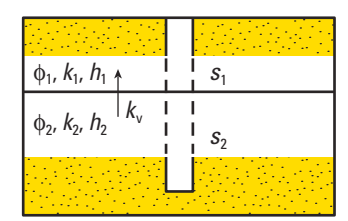
Type curves 1–4

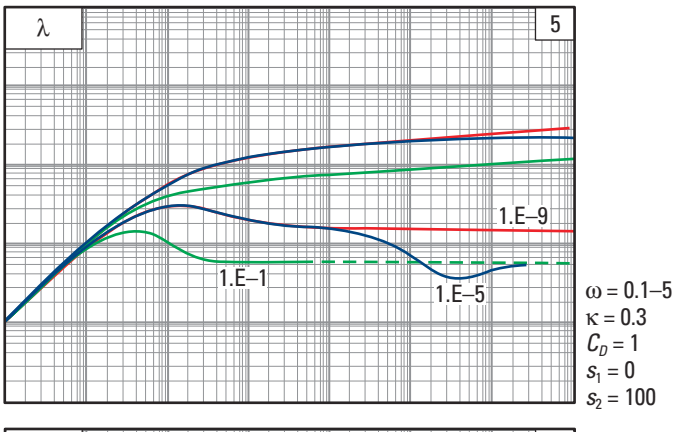
Infinite-acting radial flow model

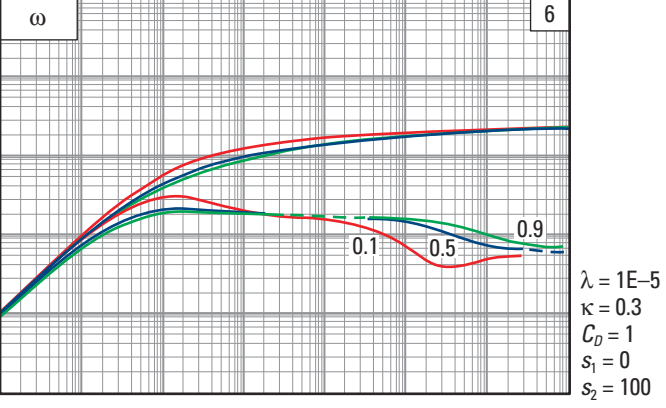


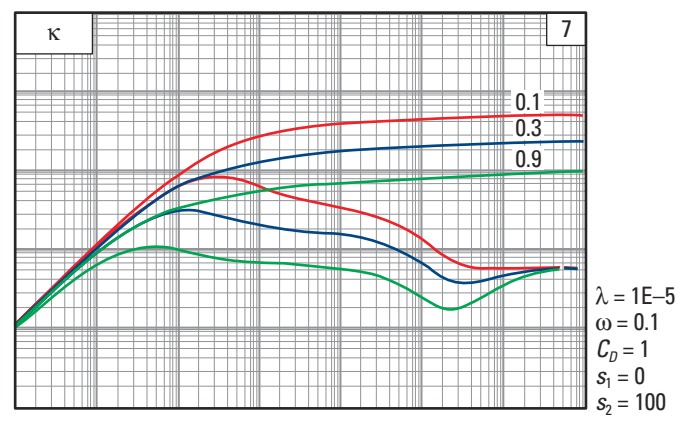
Type curves 5–8

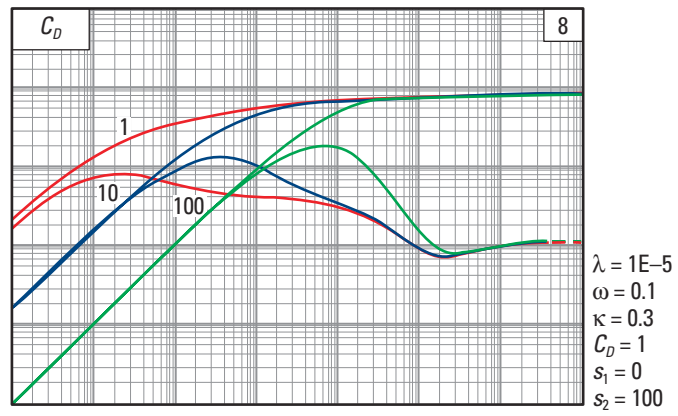
Infinite-acting doublepermeability model



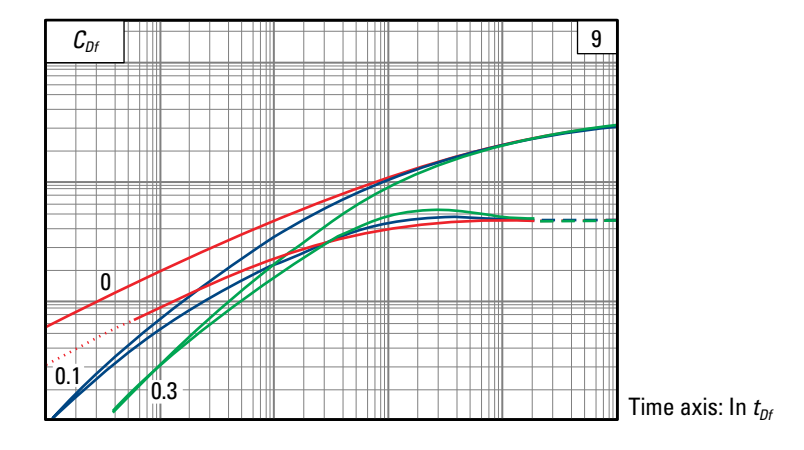






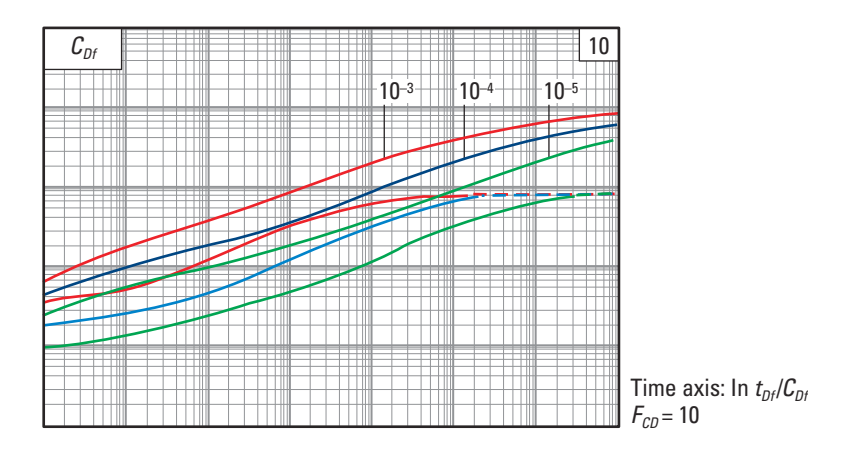


Infinite-conductivity vertical fracture in homogeneous reservoir



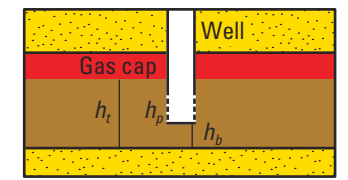
Type curve 10

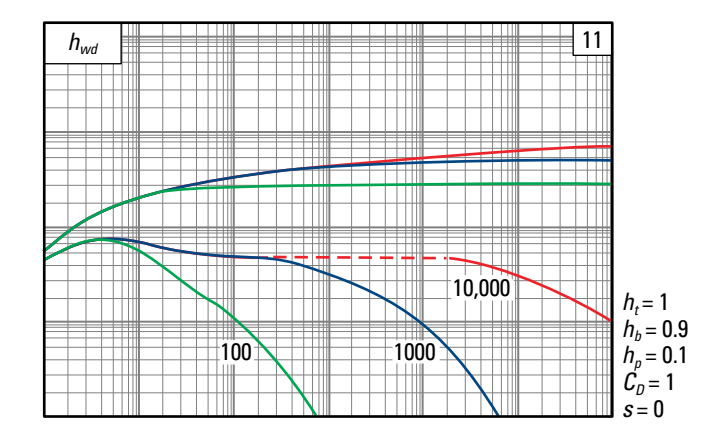
Finite-conductivity vertical fracture in homogeneous reservoir

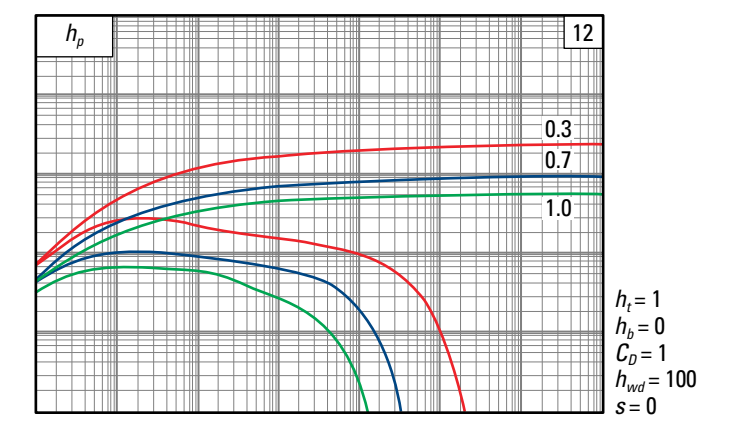


Type curves 11–12

Partial completion near gas cap

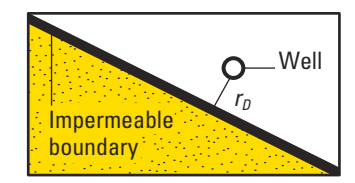


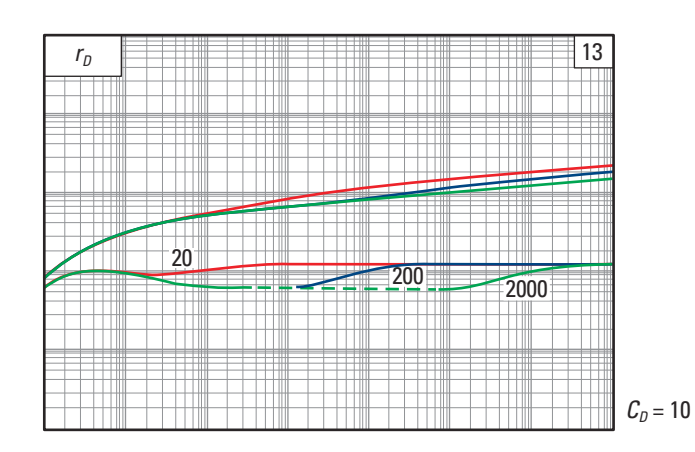


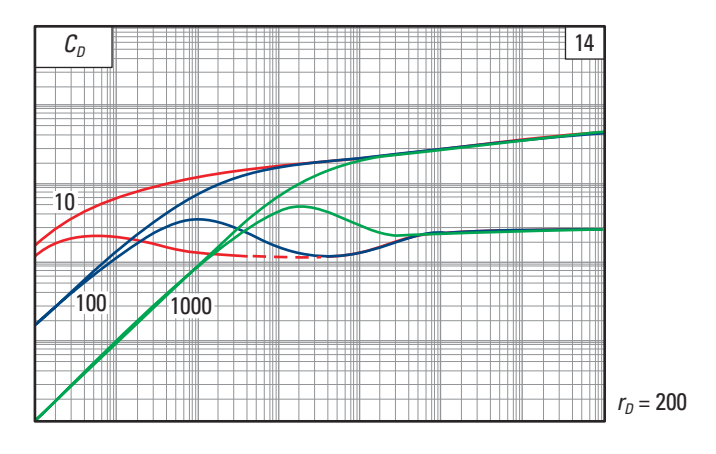


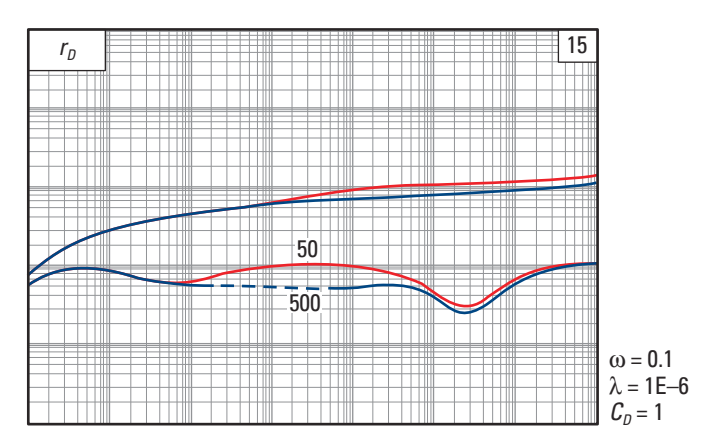
Type curves 13-15

Well near impermeable boundary





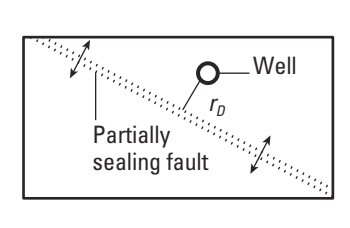


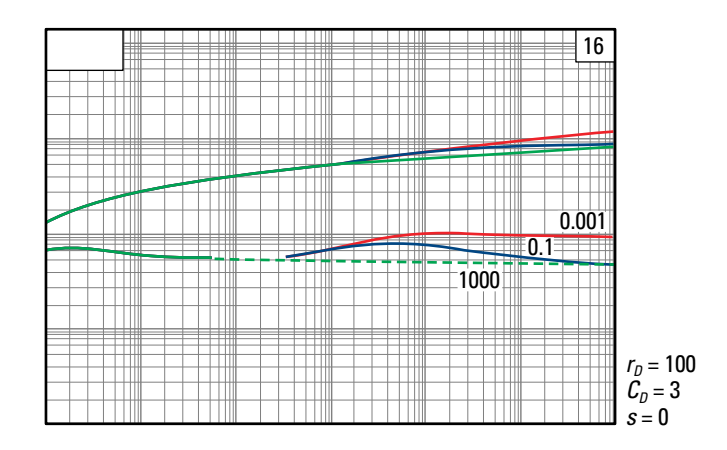


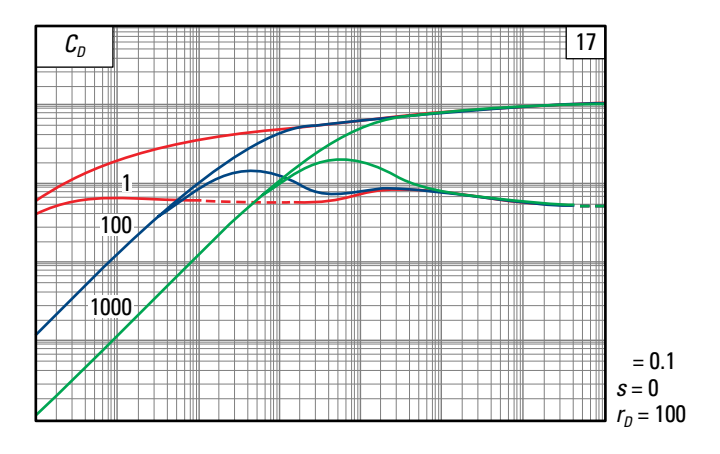
Schlumberger Schlumberger

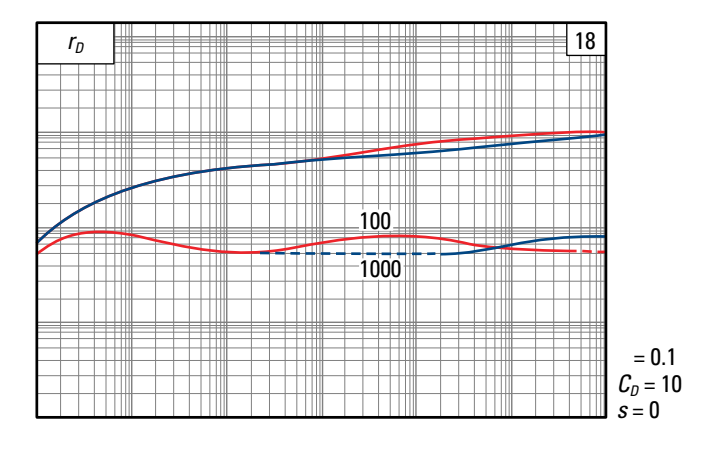
Type curves 16-18

Well near partially sealing fault



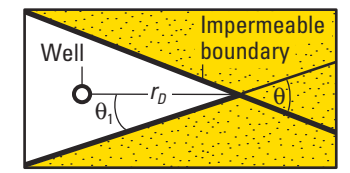


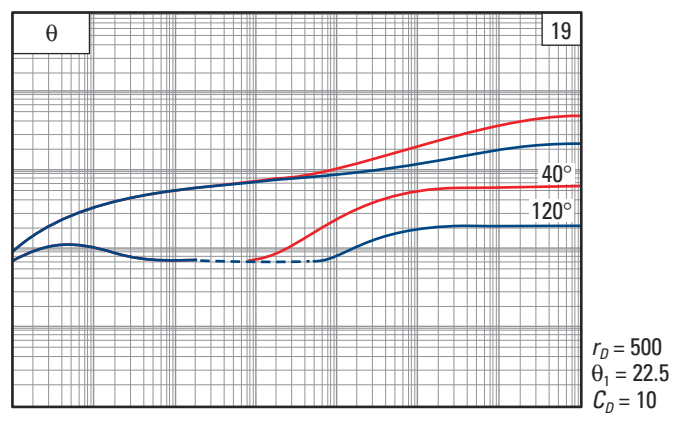


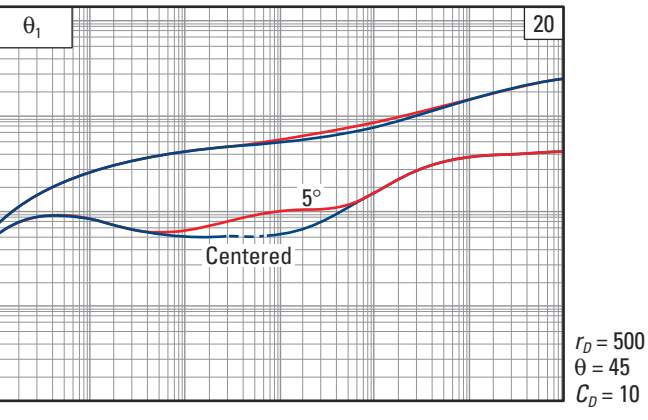


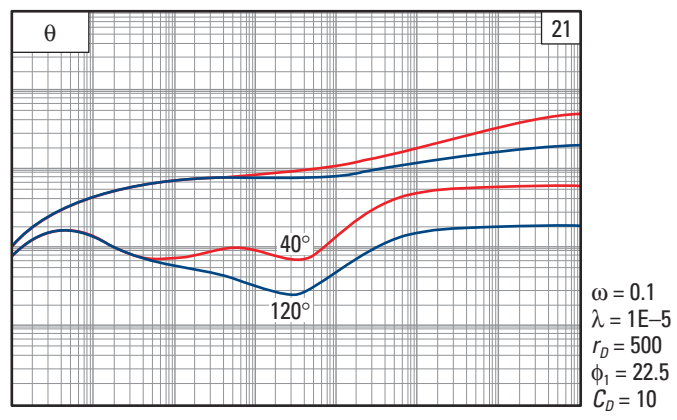
Type curves 19-22

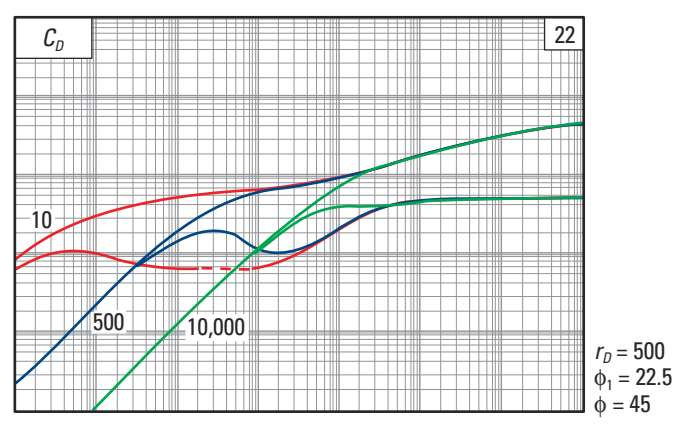
Well between two intersecting impermeable boundaries





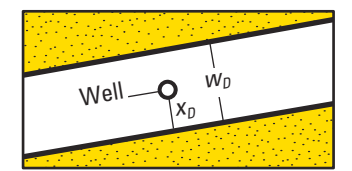


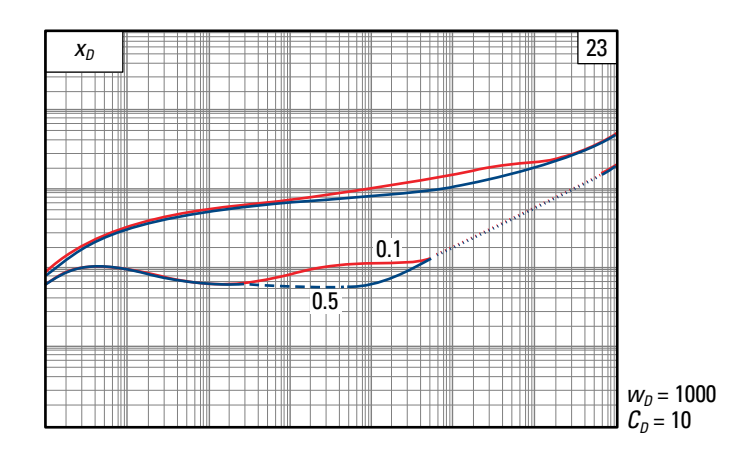


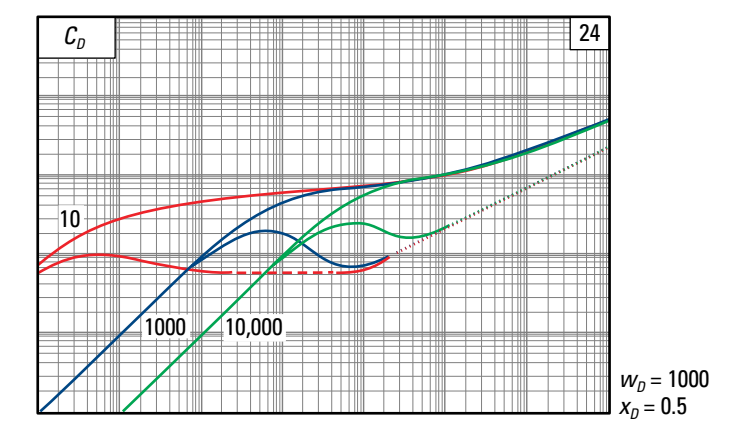


Type curves 23-24

Well between two parallel impermeable boundaries

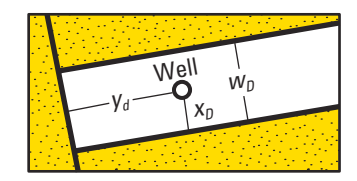


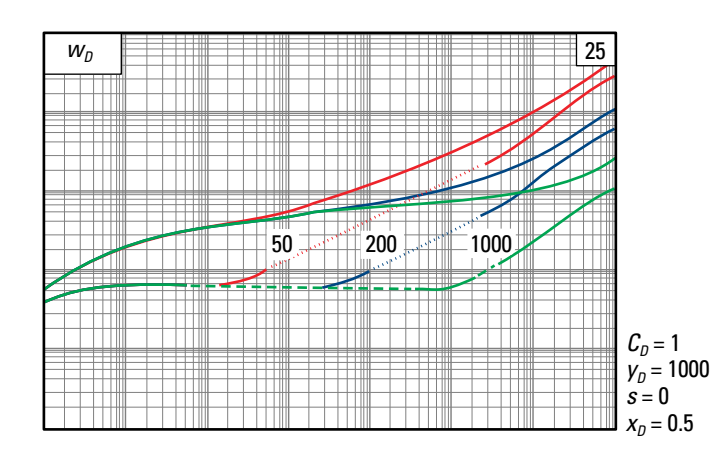


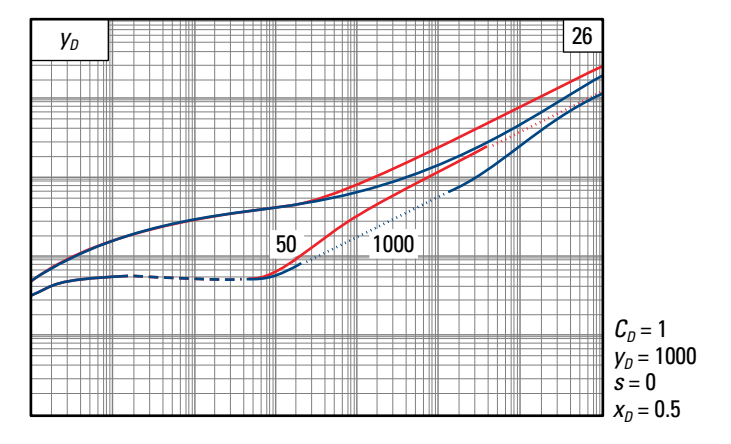


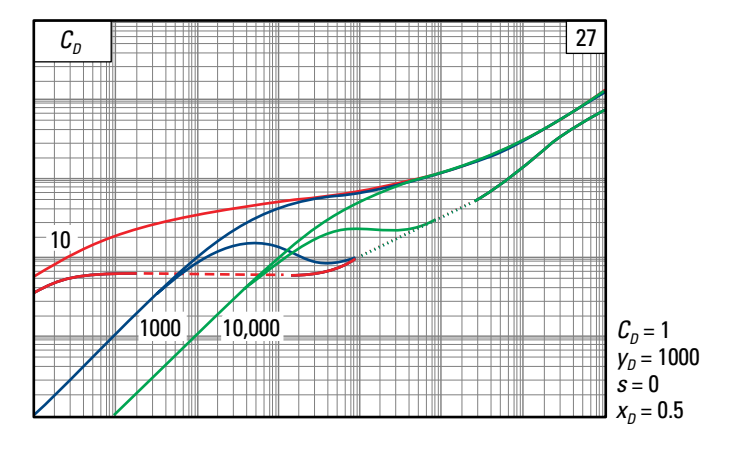
Type curves 25-27

Well in truncated channel

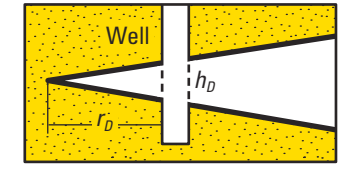


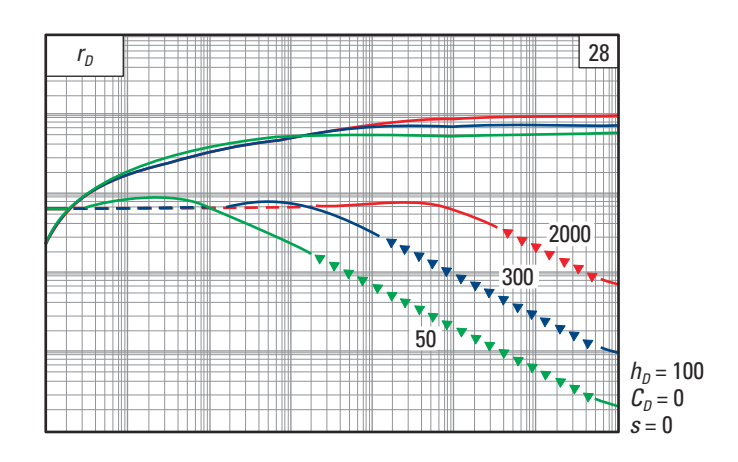






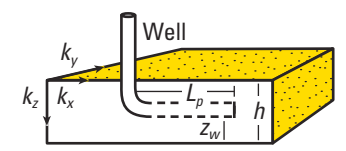
Well in pinchout

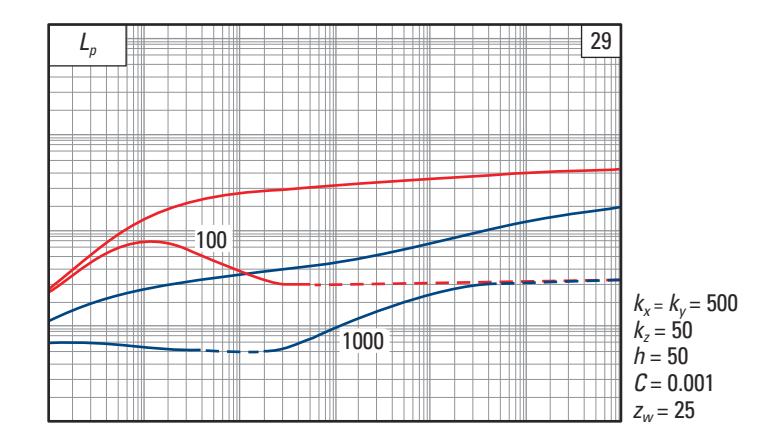


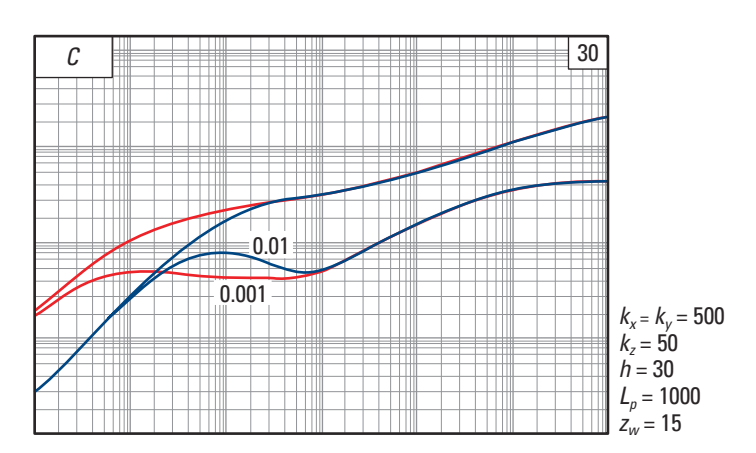


Type curves 29-30

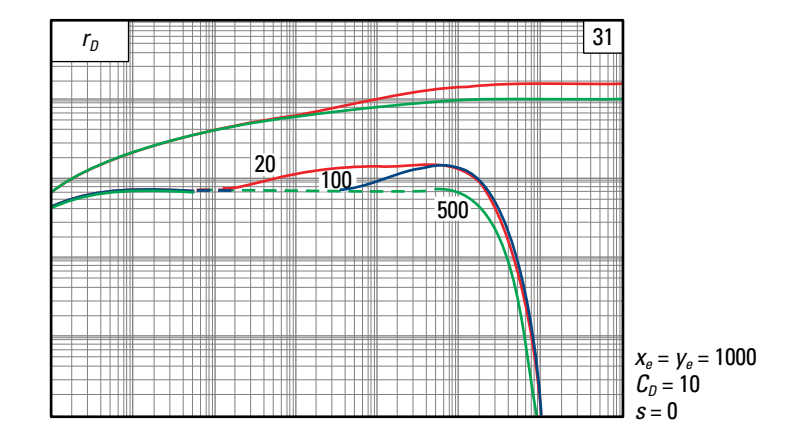
Horizontal well





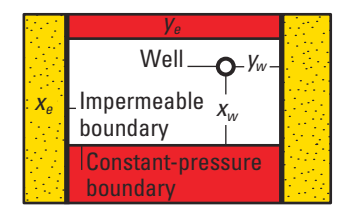


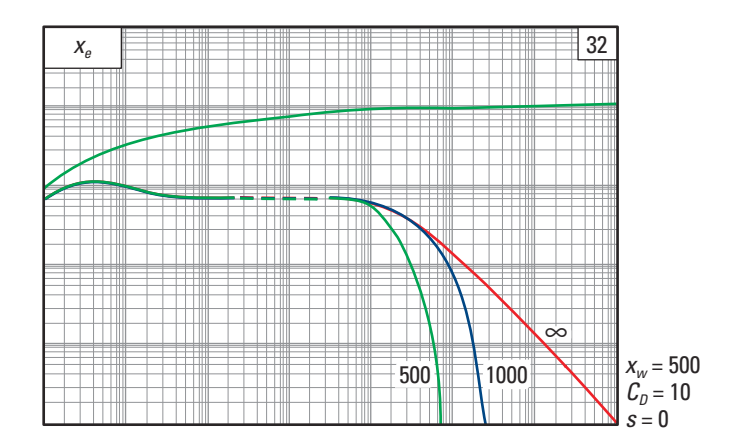
Well in rectangular reservoir with one impermeable and three constant-pressure boundaries $(r_D = \text{distance to impermeable boundary})$

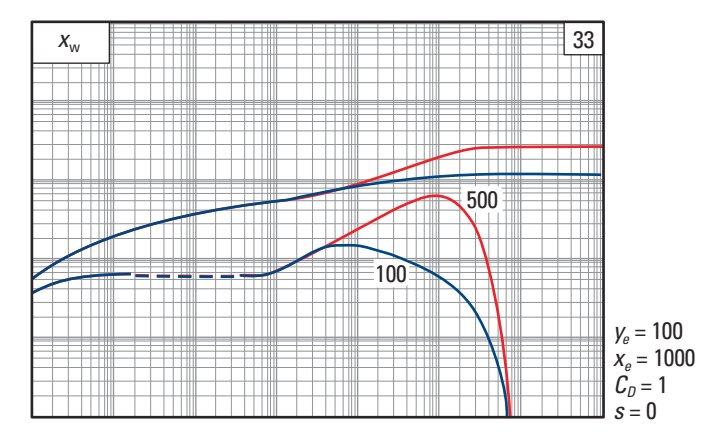


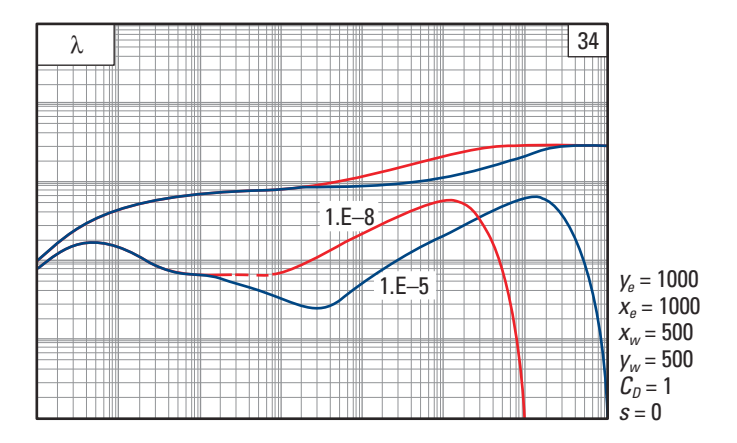
Type curves 32-34

Well in rectangle between two constant-pressure boundaries



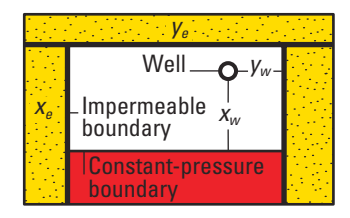


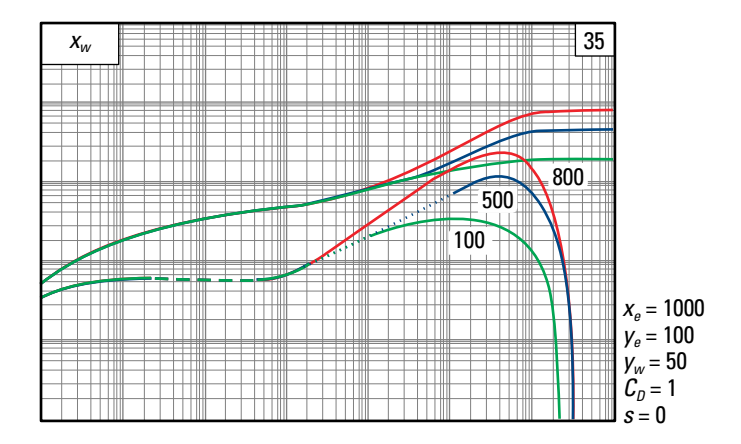


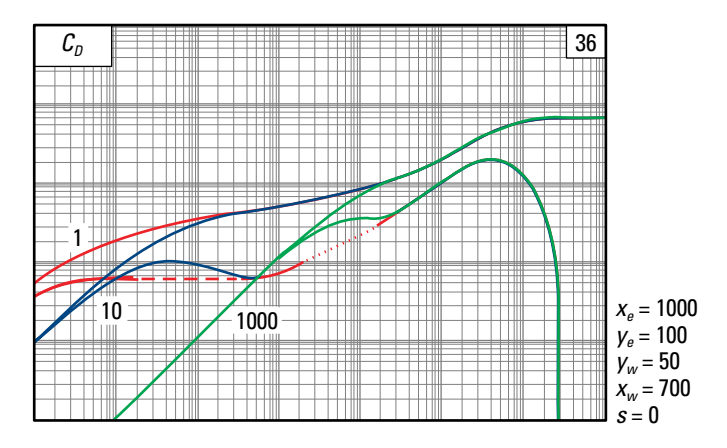


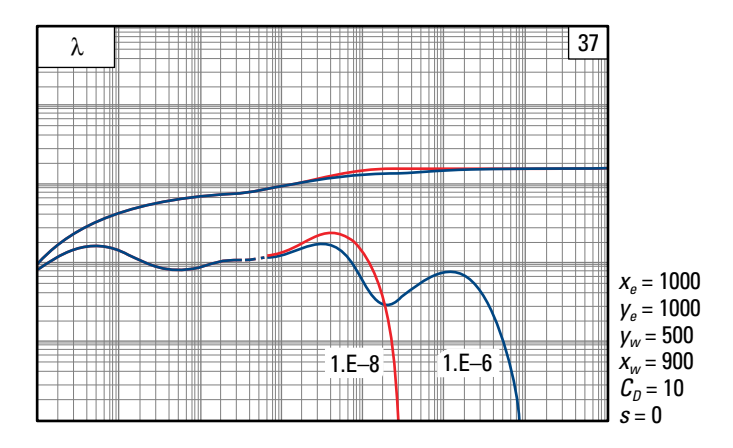
Type curves 35-37

Well in rectangle near constantpressure boundary



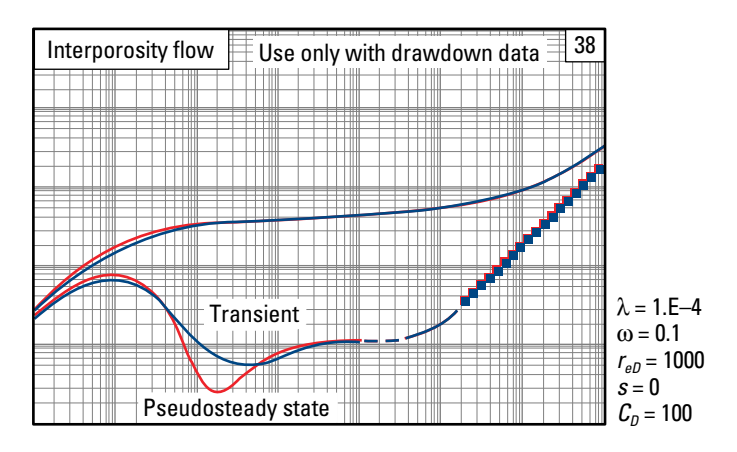






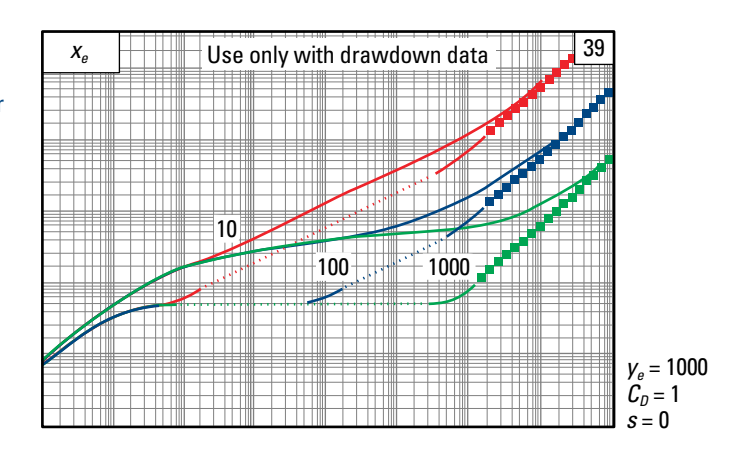
120 Schlumberger

Well in closed circular reservoir



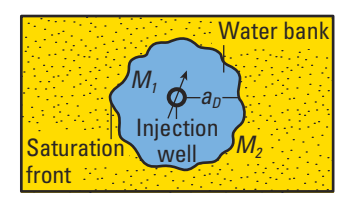
Type curve 39

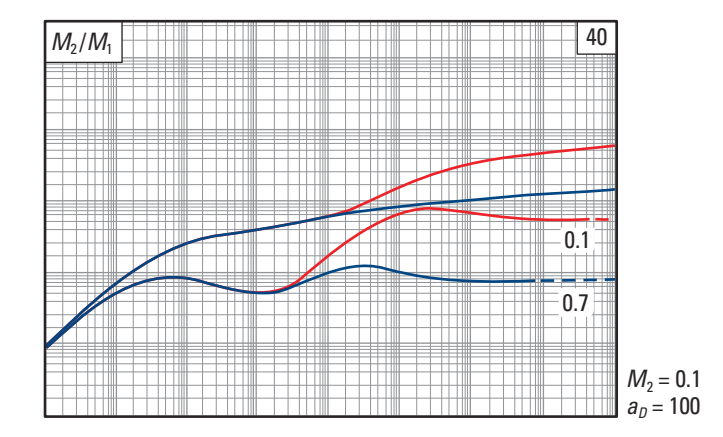
Well centered in closed rectangular reservoir



Type curve 40

Injection well





References

Abbaszadeh M and Kamal MM: "Pressure Transient Testing of Water-Injection Wells," SPE Reservoir Engineering 4 (February 1989): 115–124.

Agarwal RG: "Real Gas Pseudo-Time: A New Function for Pressure Buildup Analysis of MHF Gas Wells," paper SPE 8279, presented at the 54th SPE Annual Technical Conference and Exhibition, Las Vegas, Nevada, September 23–26, 1979.

Alexander LG: "Theory and Practice of the Closed-Chamber Drillstem Test Method," paper SPE 6024, presented at the 51st SPE Annual Technical Conference and Exhibition, New Orleans, Louisiana, October 3–6, 1976.

Al-Hussainy R, Ramey HJ Jr and Crawford PB: "The Flow of Real Gases Through Porous Media," *Journal of Petroleum Technology* 18 (May 1966): 624–636.

Ayestaran L, Minhas HN and Kuchuk FJ: "The Use of Convolution Type Curves for the Analysis of Drawdown and Buildup Tests," paper SPE 18535, presented at the SPE Eastern Regional Meeting, Charleston, West Virginia, November 1–4, 1988.

Ayoub JA, Bourdet DP and Chauvel YL: "Impulse Testing," *SPE Formation Engineering* 3 (September 1988): 534–554.

Bourdet D, Ayoub JA and Pirard YM: "Use of Pressure Derivative in Well Test Interpretation," paper SPE 12777, presented at the SPE California Regional Meeting, Long Beach, California, April 11–13, 1984.

Bourdet D, Whittle TM, Douglas AA and Pirard YM: "A New Set of Type Curves Simplifies Well Test Analysis," World Oil 196, no. 6 (May 1983): 95–106.

Ehlig-Economides C and Ayoub JA: "Vertical Interference Testing Across a Low-Permeability Zone," SPE Formation Engineering 1 (October 1986): 497–510.

Ehlig-Economides CA, Hegeman P and Vik S: "Guidelines Simplify Well Test Interpretation," Oil and Gas Journal (July 18, 1994).

Ehlig-Economides CA, Joseph JA, Ambrose RW Jr and Norwood C.: "A Modern Approach to Reservoir Testing," *Journal of Petroleum Technology* 42 (December 1990): 1554–1563.

Erdle JC, Upchurch JM and Warren DA: "Early-Fluid Entry Determination; Key to Safe, Optimum Drill Stem Testing," paper SPE 6884, presented at the 52nd SPE Annual Technical Conference and Exhibition, Denver, Colorado, October 9–12, 1977.

Gringarten AC, Bourdet DP, Landel PA and Kniazeff VJ: "A Comparison Between Different Skin and Wellbore Storage Type Curves for Early-Time Transient Analysis," paper SPE 8205, presented at the 54th SPE Annual Technical Conference and Exhibition, Las Vegas, Nevada, September 23–26, 1979.

Hasan AR and Kabir CS: "Determining Bottomhole Pressures in Pumping Wells," *SPE Journal* 25 (December 1985): 823–838.

Hegeman PS, Hallford DL and Joseph JA: "Well-Test Analysis With Changing Wellbore Storage," *SPE Formation Engineering* 8 (September 1993): 201–207.

Joseph J and Ehlig-Economides CA: "The Role of Downhole Flow and Pressure Measurements in Reservoir Testing," paper SPE 18379, presented at the SPE European Petroleum Conference, London, England, October 18–19, 1988.

Kabir CS, Kuchuk FJ and Hasan AR: "Transient Analysis of Acoustically Derived Pressure and Rate Data," *SPE Formation Engineering* 3 (September 1988): 607–616.

Mahmoud ML, Torre AJ and Ayan C: "Pulse Test Interpretation for Badri Field," paper SPE 25632, presented at the SPE Middle East Oil Technical Conference and Exhibition, Bahrain, April 3–6, 1993.

Shah PC, Gupta DK, Singh L and Deruyck BG: "A Field Application of the Methodology for Interpretation of Horizontal Well Transient Tests," paper SPE 20611, presented at the 65th SPE Annual Technical Conference and Exhibition, New Orleans, Louisiana, September 23–26, 1990.

Some portions of this document were extracted from the "Reservoir Testing Supplement" of the *Middle East Well Evaluation Review* published by Schlumberger Technical Services, Dubai, UAE, and the Schlumberger *Oilfield Review* April 1992 issue.